12-2017

Trace Plutonium Geochemistry in Hydrogeological Systems Containing Natural Organic Matter

Nathan Alec Conroy
Clemson University

TRACE PLUTONIUM GEOCHEMISTRY IN HYDROGEOLOGICAL SYSTEMS CONTAINING NATURAL ORGANIC MATTER

A Dissertation
Presented to
the Graduate School of
Clemson University

In Partial Fulfillment
of the Requirements for the Degree
Doctor of Philosophy
Environmental Engineering & Earth Science

---

by
Nathan Alec Conroy
December 2017

Accepted by:
Brian A. Powell, Committee Chair
Mark A. Schlautman
Lindsay Shuller-Nickles
Apparao M. Rao
Mavrik Zavarin

ABSTRACT

Plutonium (Pu) mobility through the subsurface is dependent on the chemical composition of the source-term and biogeochemical conditions that impact its speciation. Regardless of future decision making, existing stockpiles of Pu need to be isolated from the biosphere. Therefore, understanding the speciation of trace Pu is essential for assessing and mitigating any risk of Pu transport from the source-term to a human or environmental receptor. After a brief introduction (Chapter One) and statement of research objectives (Chapter Two), this dissertation investigated Pu speciation under saturated conditions and in the presence of natural organic matter (NOM) and pure synthesized mineral phases. Batch sorption experiments, infrared spectroscopy, and diffuse-layer modeling were used to better understand Pu speciation in the presence of NOM and mineral surfaces. In addition, new tools were developed for preparing Pu(V) stock solutions for experimental use (Chapter Five), and for simultaneously quantifying Pu and NOM in ternary batch sorption experiments (Chapter Three). In Chapter Three, the effects of citric acid (CA), Desferrioxamine B (DFOB), fulvic acid (FA), and humic acid (HA) on Pu sorption to goethite were studied as a function of organic carbon concentration and pH. Between pH 5 and 7, all of these organic ligands reduced Pu sorption to goethite relative to a ligand-free experiment. At pH 3 however, CA, FA, and HA all increased Pu sorption relative to a ligand-free experiment. The formation of ternary goethite-NOM-Pu complexes were attributed to the increase in Pu sorption at pH 3. Possible sorption mechanisms for ternary complexes were investigated using Fourier-transform infrared spectroscopy, and a hybrid

empirical/diffuse-layer surface complexation model was used to predict Pu sorption to goethite in the presence of CA, HA, and DFOB. In Chapter Four, that hybrid model was refined by narrowing the scope to CA, and studying Pu and CA sorption to goethite and gibbsite from pH 2 – 10. An entirely diffuse-layer model was used to describe Pu and CA sorption to goethite and gibbsite. Ternary mineral-citrate-Pu(IV) surface complexes were necessary to describe plutonium sorption to both minerals from pH 2 – 4.

DEDICATION

I have been fortunate to have had several extraordinary mentors in my life, and this work is dedicated to them. In particular, I would like to thank the following people: **Brian Powell** for his mentorship and patience as I postponed graduate school for other pursuits, only to return months later; **Tim DeVol** for his academic guidance, and also for his role as a sounding board and life-coach over the past few years; **Frank Dunnivant** for helping me find a niche in earth science as an undergraduate, and for encouraging me to get my "union card"; **Gary D'Agostino** for teaching me how to probe complex problems with logic, scientific method, and abstract thought (I apply your philosophy of triage and common sense almost daily); **Mike Timony** for instilling in me both a strong work ethic and the importance of work-life balance; **Zach Conroy** for paving the way most of my life, you were a tough act to follow; and **Patrick Conroy** for showing me at a young age that if I didn't know the answer, I was fully capable of figuring it out.

ACKNOWLEDGMENTS

This work was funded by the Subsurface Biogeochemical Research Program of the U.S. Department of Energy's Office of Biological and Environmental Research and the Office of Basic Energy Sciences of the U.S. Department of Energy as part of the Heavy Element Chemistry Program.

TABLE OF CONTENTS

Page

Page

Page

Page

LIST OF TABLES

Page

LIST OF FIGURES

CHAPTER ONE

INTRODUCTION

Background

Plutonium Releases to the Environment

Plutonium (Pu) has been introduced into the environment from numerous sources including nuclear weapons manufacturing and testing, nuclear power plant accidents, nuclear fuel reprocessing discharges, and an incident when a Pu-powered satellite failed to achieve orbit. Atmospheric releases, which have resulted in worldwide Pu distribution, have not been of insignificant quantity. The *Treaty Banning Nuclear Weapon Tests in the Atmosphere, in Outer Space and Under Water*, ratified in 1963 and signed by 136 countries including the United States and former Soviet Union, was largely motivated out of concern for increasing concentrations of radionuclides in the atmosphere and fear of nuclear fall-out.[1] After the ban on atmospheric testing, weapons testing shifted to underground tunnels, where the products of nuclear detonations would be retained by the surrounding geomedia. While the transition to underground testing meant that Pu and fission products were largely contained and off-site contamination mitigated, large quantities of those isotopes remain in the subsurface to this day.[2] Weapons materials production and fabrication sites also have released significant quantities of Pu through fires and inadequate waste management practices. Plutonium purification for weapons, typically accomplished using the Plutonium Uranium Reduction Extraction (PUREX) Process, produced vast quantities of highly radioactive waste. Largely out of haste, wastes were not always isolated from the

environment, and the at-that-time unknown reactivity and pyrophoricity of Pu contributed to accidental releases Pu at manufacturing and fabrication sites.

Plutonium has been globally dispersed from multiple sources of atmospheric releases, both purposeful and accidental. In the United States, the Nevada National Security Site (NNSS) was the location of 86 atmospheric weapons tests conducted from 1951 to 1962.[1] Collectively, the United States, former Soviet Union, France, China, and the UK have conducted 541 atmospheric nuclear weapons tests, resulting in a total yield of 440 megatons of TNT.[3,4] Excluding local fall-out, the estimated $^{239\text{-}241}$Pu activity dispersed from those tests was 4×10^{6} Ci, equaling 3392 kg of $^{239\text{-}241}$Pu.[4]

Non-weapons related accidents, though far fewer than weapons tests, have also released an appreciable amount of Pu into Earth's atmosphere. A single incident in April 1964 released 1.7×10^{4} Ci of ^{238}Pu into the stratosphere when a United States satellite failed to achieve orbit, breaking apart and burning the ^{238}Pu-powered radioisotope thermoelectric generator upon reentry.[5] Additionally, fires and meltdowns at commercial power reactors, such as those at Chernobyl in Ukraine in 1986 (estimated 7.2×10^{4} Ci $^{238\text{-}241}$Pu released)[6] and Fukushima in Japan in 2011 (estimated 3.0 – 7.1 Ci $^{238\text{-}241}$Pu released)[7], have released Pu as well as other actinides and fission products into the atmosphere, and deposited Pu bearing particulate matter in the regions surrounding those reactors. Despite the considerable quantity of Pu dispersed throughout the atmosphere, concentrations are sufficiently dilute not to pose a major health concern to either humans or the environment. In fact, recent studies have determined that tropospheric Pu concentrations are largely controlled by resuspension of Pu bearing particulate from land.[8] These particles are

removed by fall-out or rain-out, but have a mean residence time of weeks to months.[8] By contrast, stratospheric Pu, bound to significantly smaller particles and aerosols, is more refractory and can have residence times of several years.[8]

Underground weapons testing and subsurface disposal of weapons legacy wastes typically do not release significant quantities of Pu into the atmosphere, but high concentrations do remain localized in the subsurface. The NNSS was the site of 828 underground weapons tests from 1951 to 1992, approximately one-third of which were detonated below the standing water table.[2,9] Conducting weapons tests below the static water level is of environmental concern, as groundwater can provide a transport vector should the Pu be present in a readily soluble or water-mobile (colloidal) form. Fortunately, the majority of the estimated 461,500 Ci of $^{238\text{-}242}$Pu remaining in the subsurface of the NNSS (decay corrected to September 30th, 2016) is projected to be associated with refractory melt glass at the bottom of test cavities.[10–12] Unfortunately, kilometer-scale transport of Pu has been observed at the NNSS. Kersting *et al.*[2] found that Pu transport was being facilitated by mobile clay and zeolite colloids which had associated Pu. Colloid-facilitated Pu transport, also kilometer-scale but associated with iron oxide colloids, was also observed at Lake Karachay, a site in the former Soviet Union.[13] It should be noted that risk to the public remains miniscule at the NNSS, as the site is a massive 1375 square miles, and no subsurface Pu has come close to migrating off-site. The observed colloidal transport mechanism however, could pose concerns at smaller sites, or on significantly longer time scales.

Weapons testing sites are not the only highly contaminated weapons legacy sites, and weapons production has also resulted in accidental Pu releases. In 1957, a fire in the graphite-moderated reactor at Windscale Works, which produced Pu for the United Kingdom nuclear weapons program, was estimated to have released 0.08 – 2.7 Ci of ^{239}Pu into the atmosphere.[14] Just 11 days earlier, a chemical explosion in a waste tank at the Mayak Production Association in the former Soviet Union released an estimated 2.7 Ci of ^{239,240}Pu that was eventually deposited across three provinces.[15] Mayak was also the location of Lake Karachay, a 110 acre natural lake with no surface outlet that served as the containment for diluted high-level wastes from the facility. In 1967, drought dried a portion of the lake and dust from the lake bed was dispersed by wind and contaminated an area of 1800 – 2700 km^2 to a level of 0.1 Ci·km^{-1} with ^{90}Sr.[16] Traces of Pu were also dispersed.[15]

The United States was not immune to nuclear incidents. It has had numerous weapons production-related releases and continues to cope with complex and hazardous wastes generated decades ago. Waste management at sites where irradiated nuclear fuel was processed to extract Pu and create weapons components was grossly inadequate, either by haste, naivety, or in some cases negligence. The Hanford Reservation, a Department of Energy (DOE) site in Washington State that produced and processed Pu for bomb production, stores 53 million of gallons of highly chemically toxic and radioactive waste.[17] The site is adjacent to the Columbia River, the largest river in the Pacific Northwest United States, and a vital waterway for drinking water, transportation, and power. The vast quantities of waste, largely byproducts from separations processes, was dumped into unlined trenches, injected into wells, or stored in massive carbon steel tanks.[18] There is

currently an estimated 210,000 Ci of Pu stored in the 177 tanks at the Hanford Site, 67 of those tanks are believed to have developed leaks.[19,20] An additional 11,800 Ci of ^{239}Pu was applied to the vadose zone as liquid waste.[18] Some tank waste has been transferred from known leaking tanks and is currently distributed amongst 149 single-shell tanks and 28 double-shell tanks.[19,20] The tank wastes are radiologically and thermally very hot, tank sludge is known to exceed the boiling temperature of water, and is chemically complex and heterogeneous.[20] The chemical conditions are extreme: pH exceeds 12 in some tanks, the high ionic strength solutions are fully saturated resulting in a precipitated salt layer called "salt cake," and a sludge with the consistency of peanut butter lines the bottom of the tanks and contains the majority of the actinides.[21] The heterogeneity of the wastes and limited access to the tanks through relatively small portals makes the wastes extremely difficult to characterize and remove, and therefore, to produce acceptable long-term waste forms.[20]

The Savannah River Site (SRS), located in South Carolina, also produced and purified Pu for weapons. That site has an additional 51 underground storage tanks, 12 of which have a history of leaks, though no leaks are considered "active". The SRS tanks received 160 million gallons of radioactive waste starting in 1954.[22–24] Similar to Hanford, the waste in the SRS tanks is stratified into supernatant, salt cake, and sludge layers, of which the actinides have predominantly partitioned into the sludge phase.[20,22,24] Fortunately, purification methodology had advanced by the time SRS started producing Pu, and the wastes were largely derived only from the PUREX process and a modified version of the PUREX process.[23,24] The wastes generated at SRS were therefore, significantly less varied than those at Hanford. Final waste disposal at SRS has also progressed substantially further

than at Hanford. At SRS, evaporation followed by grouting of low level waste and vitrification of high level waste has reduced the volume of waste awaiting disposal to 36 million gallons.[25]

Following the production and purification of Pu, the Pu metal needed to be fabricated into usable weapons components. This task was completed at the Rocky Flats Plant, just northwest of Denver, Colorado. The Rocky Flats Plant was a bomb parts production facility that specialized in producing the Pu pits used in thermonuclear weapons. At the plant, Pu metal was melted, cast, pressed, and precisely machined into weapons components. Many of these tasks were completed within gloveboxes, and buildings at the plant were filled with of an elaborate connected system of such boxes. While Pu production and purification at Hanford and SRS produced vast quantities of waste, machining the metallic Pu at Rocky Flats produced novel radioactive waste forms such as Pu laden cutting oils. It was at Rocky Flats that workers discovered Pu was pyrophoric, especially so as the metal filings common to machining operations, and Pu fires became routine. The Rocky Flats Fire department responded to thirty-one Pu fires between 1966 and 1969, and numerous others were put out without being reported to the fire department.[26] When Pu filings ignited spontaneously, workers would drop them into machining oil to put out the flames. Two major Pu fires occurred at Rocky Flats. In 1957, Pu within gloveboxes of Building 771 caught fire during the night, and in 1969 Pu laden oil caught fire in Building 776. Both fires were exacerbated by flammable materials used in construction of the gloveboxes and lack of water-based fire suppression systems, purposefully excluded out of

criticality concerns.[26] Releases from the 1957 fire in Building 771 were estimated at 50 mCi of Pu, and those of the 1969 fire in Building 776 were 2.8 mCi.[27,28]

Plutonium fires were not the most significant Pu release at the Rocky Flats Plant. The largest release came from the accidental but negligent dispersal of machining oils contaminated with Pu that were being stored in steel drums in a field near building 903. Plant engineers were hopeful that the valuable Pu from this waste oil could be recovered and reintroduced into pit production. Never intended for long-term storage however, the steel drums corroded in the harsh Colorado weather. Officials would later estimate that 5000 gallons of machining oil containing approximately 86 grams of Pu had likely leaked onto the soil.[29] Wind then dispersed soil particles with sorbed Pu across Rocky Flats. Mongan *et al.*[30] used the Fugitive Dust Model and surface Pu-deposition data to estimate that the total Pu released from the 903 pad was 25 Ci. Of that total, an estimated 11 Ci was redeposited on the pad, 8 Ci traveled beyond the plant security fence, and 7 Ci had been carried beyond the uninhabited buffer zone surrounding the plant. Plutonium fires and poor waste management practices resulted in widespread Pu distribution on surface soil and water at Rocky Flats. In 1995, DOE estimated the cleanup of Rocky Flats would take approximately 65 years and cost more than $37 billion. By October of 2005 however, DOE and its contractor completed the cleanup at a cost of only $7 billion.

Safe disposal of current and future nuclear wastes will require a comprehensive understanding of Pu mobility in biogeochemical systems. Nuclear arms agreements and a general trend towards blending down weapons-grade Pu for disposal or use in commercial reactors (for electricity production) suggests that that worldwide inventories of weapons-

grade Pu are unlikely to grow.[31] Nevertheless, 70 – 90 tons of Pu are produced incidentally in commercial power reactors annually.[32] Existing Pu stockpiles, either as weapons, tank waste, or a component of spent nuclear fuel, will also need to be properly isolated from the biosphere in a permanent storage facility that exploits the host geology to limit transport in the event engineered barriers deteriorate or are breached. Congruently, the backend of the nuclear fuel cycle is the major impedance to a particularly clean and plentiful energy source.

Plutonium Fate & Transport

The mobility of any contaminant, including Pu, depends on the chemical composition of its source-term and the biogeochemical conditions it encounters that impact its chemical speciation. Oxidation state plays a significant role in reactivity, and Pu has particularly dynamic redox chemistry. While Pu can exist in four oxidation states in natural waters (III, IV, V, and VI), and all four can even be present simultaneously under certain conditions, Pu(IV) and Pu(V) are the dominant oxidation states in most natural waters (Figure 1.1).

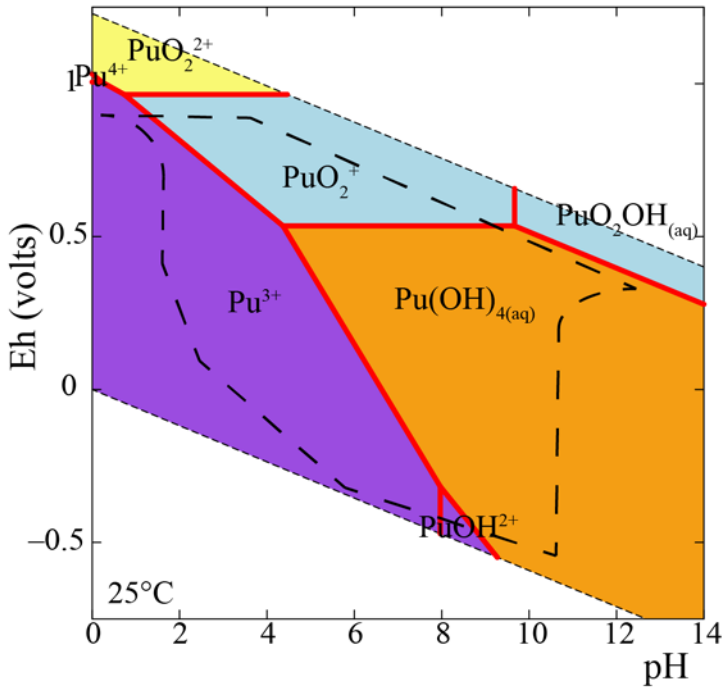

Figure 1.1. Pourbaix diagram of Pu (10^{-9} M) dominate species with respect to Eh and pH at equilibrium in a carbonate-free 0.01 M NaCl solution. Dashed line represents distribution of Eh-pH measurements of natural waters studied by Baas Becking et al.[33] Dominate Pu species are listed and oxidation is given by color: Pu^{3+} (purple); Pu^{4+} (orange); PuO_2^{+} (light blue), PuO_2^{2+} (yellow).

Pentavalent Pu is the dominate oxidation state in ocean water and many oxidizing surface waters.[34–36] Pentavalent Pu is somewhat soluble and stable in aquatic environments. The environmental mobility of Pu(V) however, is hindered by surface-mediated reduction, which has been demonstrated by several mineral surfaces, to the significantly less soluble form Pu(IV).[35,37–40] The prevalence of Pu(V) in the aqueous phase, with Pu(IV) on the mineral surface, under oxic conditions was recently observed on kaolinite clay.[41] Marsac

et al.[41] found that the stability field of Pu(IV), with respect to E_H and pH, was effectively extended by the thermodynamic stability of Pu(IV) surface complexes. Meanwhile, Pu(V) remained as a stable aqueous actinyl cation in solution. The dynamic redox chemistry of Pu can therefore, be the predominate mechanism controlling its mobility. In fact, oxidation of sorbed Pu(IV) to Pu(V) was found to be controlling Pu mobility in the vadose zone of SRS.[42]

Plutonium mobility in water is also constrained by the limited solubility of Pu. Tetravalent Pu is only scarcely soluble and will precipitate at concentrations greater than approximately 10^{-10} M in water without any complexing ligands. The solubility product of $Pu(OH)_{4(s)}$ is $\log K_{sp} = -58.7 \pm 0.9$.[43] Even at concentrations that do not exceed its solubility limit, Pu(IV) tends to either sorb, hydrolyze, or form complexes at pH > 0. Pentavalent Pu is only sparingly soluble, however it is significantly more soluble than Pu(IV); concentrations can reach 10^{-8} to 10^{-6} M before precipitating.[44] The solubility product of the Np(V) precipitate, $NpO_2OH_{(s)}$, is $\log K_{sp} = -8.76$, and the solubility product of the Pu(V) precipitate, $PuO_2OH_{(s)}$, can be expected to be similar.[45] Pentavalent Pu solubility however, is generally limited by reduction to Pu(IV). Despite the stability of Pu(V) in aqueous systems, numerous studies have demonstrated surface-mediated reduction of Pu(V) to Pu(IV) even in the presence of mineral surfaces that are considered non-redox reactive or oxidizing.[35,38,39,46–48] Meanwhile, Pu complexed by organic ligands is most stable in the 4+ oxidation state, so much so that other oxidation states are rapidly oxidized/reduced in the presence of significant complexing organic acids.[49] Therefore, trace Pu in the presence of either NOM or mineral surfaces is expected to be driven toward Pu(IV). Nevertheless,

given the propensity for transport of Pu(V), a comprehensive understanding of both Pu(IV) and Pu(V) speciation in the environment will be crucial to assessing the total fate and transport of Pu.

Natural Organic Matter

Natural organic matter (NOM) is ubiquitous in surface waters and shallow groundwater, and is comprised of a wide range of molecules with both defined and nonspecific structures. While NOM inherently refers to the entire organic molecule, included oxygen, nitrogen, and hydrogen, "matter" is difficult to quantify in practice and the preferred normalizing element is carbon. Typically, carbon accounts for about half the mass of NOM. Organic carbon can be present as dissolved organic carbon (DOC) or particulate organic carbon (POC), differentiated by the fraction passable and retained by a 0.45 μm glass-fiber filter, respectively.[50] Particulate fractions can be intrinsic or as organic coatings on inorganic surfaces. Natural organic matter is comprised of countless diverse organic molecules, which often share similar molecular building blocks, but may differ in their adjacent structures. Functional moieties therefore, exhibit a broad distribution of reactivity, acid-base chemistry, and complexation affinity.

Dissolved organic carbon concentrations in natural waters range from 0.1 $mg_C \cdot L^{-1}$ in seawater to 60 $mg_C \cdot L^{-1}$ in tea-colored swamp water.[50–52] Rivers and lakes typically contain 2 – 10 $mg_C \cdot L^{-1}$ DOC while swamps and bogs will have 10 – 60 $mg_C \cdot L^{-1}$ DOC.[50] At these concentrations, DOC has a significant buffering capacity. In fact, swamp and bog water chemistry is often buffered to pH 3 – 5,[50] demonstrating that DOC is out-buffering even inorganic carbon. Subsurface DOC concentrations are generally lower than surface waters.

Concentrations in vadose zone interstitial water range from 0.1 $mg_C \cdot L^{-1}$ to 30 $mg_C \cdot L^{-1}$.[50] These concentrations typically decrease with depth through biological decay and adsorption processes. Dissolved organic carbon in groundwater ranges from 0.1 to 20 $mg_C \cdot L^{-1}$, though 0.7 $mg_C \cdot L^{-1}$ is typical.[50,53] Higher concentrations can be observed, however, in shallow groundwater that experiences more frequent surface water recharge or in groundwater associated with coal or petroleum deposits.

Particulate organic carbon constitutes a smaller fraction of the total organic carbon than DOC in most natural waters. Notable exceptions would include turbid river water at times of high flow. Seawater and lakes will contain POC, mostly derived from algal detritus, at average concentrations of 0.01 – 0.1 $mg_C \cdot L^{-1}$ and 0.1 – 1.0 $mg_C \cdot L^{-1}$, respectively.[50] Vadose zone interstitial water and groundwater will not contain considerable amounts of POC. While the differentiation between DOC and POC is helpful in understanding the behavior of the two fractions, it is important to recognize that the 0.45 µm filter size is arbitrary and that properties of DOC and POC are a continuum rather than distinct.

Natural organic matter is derived from the decomposition of plant and animal matter and is broadly comprised of many recognizable molecules such as amino acids, fatty acids, phenols, sterols, natural sugars, hydrocarbons, urea, and porphyrins.[50] Organic acids released by plants and microorganisms to perform some function are also NOM. Siderophores, for example, are organic acids released by microorganisms to scavenge Fe^{3+} from mineral phases for biological use. In addition to molecularly defined organic acids and biological building blocks, NOM consists of a conglomerate of organic acids many without distinct origin, called humic substances. Humic substances are thought to form

from the random polymerization of organic carbon monomers, which are derived from the breakdown of biopolymers.[54] Humic substances account for 40 - 80 % of the DOC and POC in natural waters, and are the largest fraction of NOM present in soils and sediments.[50,52,54] Metals will associate with both DOC and POC, and there is not a clear distinction between the two with regards to metal complexation. Lamar *et al.*[55] demonstrated that both forms of organic carbon in natural waters, whether DOC or POC, were equivalently associated with iron.

Humic substances do not have defined molecular structures and instead are operationally divided into three fractions based on their solubility in acidic and alkaline solutions: 1) humin is insoluble at any pH; 2) humic acid is soluble in alkaline solution but will precipitate in acid; and 3) fulvic acid is the fraction that remains soluble when humic acid is precipitated in acid. Operationally definitions vary somewhat depending on the origin of the humic substance, and therefore, the method of extraction and isolation. Humic substances from soil are extracted using sodium hydroxide, and then acidified to fractionate humic and fuvic acids.[50] Aquatic humic substances by contrast, are first isolated from water by adsorption onto XAD resin. Once eluted from the resin with sodium hydroxide, the humic and fulvic acid fractions are isolated by acidification, similar to the soil humic substances.[56] Of the three humic substance fractions fulvic acid tends to be most abundant in natural waters, though not always by a huge margin. In a review of available literature values, Boggs *et al.*[52] found that fulvic acid accounted for 60 – 97 % of the humic substances in five groundwaters, and 62 – 98 % of marine humic substances. Due to their operational definitions, humin would always be considered POC, intrinsic fulvic acid

would always be considered DOC under natural water conditions, and intrinsic humic acid could have both DOC and POC fractions. Predicting the concentrations or chemical natural of these fractions is non-trivial, but the trend is toward greater coagulation at lower pH values and higher ionic strengths. For these reasons, NOM mobility in the environment is highly variable.

Natural organic matter is not strictly soluble or intrinsically precipitated (insoluble) in hydrogeological systems, as it will also exhibit some sorption affinity for subsurface solids and be subject to microbial oxidation.[50,57] Sorption to minerals will reduce aqueous NOM concentrations and produce surface sites which have the capacity to behave like complexing ligands. Natural organic matter coatings on mineral colloids can yield species with intermediate behavior, with some NOM character and some mineral colloid character. Natural organic matter coatings on colloids also tends to increase colloid mobility, increasing stability by keeping colloids from aggregating. Intrinsic NOM colloids may also precipitate under certain conditions, particularly at low pH and high ionic strength. Intrinsic colloid formation will likely retard transport with respect to the dissolved organic ligand, but may enhance transport compared to sorbed NOM. Natural organic matter mobility can therefore be both chemically and physically driven, and predicting those processes is, at least quantitatively, non-trivial.

The Influence of Minerals and NOM on Plutonium Mobility

Plutonium mobility through a natural hydrogeological environment is dynamic, with several competing processes, ultimately controlled by the speciation of the Pu. Natural organic matter introduces several additional processes that can change the speciation of Pu

and thus affect its mobility. Most straightforwardly, in sufficient concentrations organic ligands are known to form thermodynamically stable complexes with Pu.[58] If those complexes are sufficiently stable, they may inhibit Pu hydrolysis and sorption to mineral surfaces. This process will increase the Pu transport potential by shifting Pu speciation towards more soluble species. This was observed inside the U12n and U12t tunnel complexes at the NNSS, where >65 % of Pu was found dissolved.[2] This is in sharp contrast to the <10 % found dissolved in groundwater from other parts of the site. The difference was the concentrations of DOC. The water in the tunnels contained 15 – 19 $mg_C \cdot L^{-1}$ DOC, while the spring water contained only 0.2 $mg_C \cdot L^{-1}$ DOC.[59] Diesel and construction debris are believed to be responsible for the elevated DOC concentrations in the tunnel water.[2]

Natural organic matter has also been shown to sorb to inorganic surfaces and, through sorption processes, could facilitate formation of ternary mineral-NOM-Pu complexes.[60–65] Given their size and complexity, it is easy to conceive how a NOM molecule could sorb in one region of the molecule, while another region could continue to behave as a complexant. While ternary sorption would generally be considered an immobilizing process, that would not be the case if the inorganic surface were a mobile inorganic colloid. Therefore, ternary mineral-NOM-Pu complexes could increase or decrease the mobility of Pu depending on the mobility of the inorganic surface. Concurrently, NOM coatings can influence the fate of mineral colloids by changing their surface potential. Coatings that increase the absolute surface potential will stabilize colloids and conversely, coatings that decrease the absolute surface potential will destabilize colloids, resulting in aggregation. Depending on the nature of the NOM, it may also form intrinsic aggregates, effectively transitioning from

DOC to POC depending on solution conditions. The POC will provide an additional surface for Pu sorption, and depending on how dynamic the NOM physical state is, POC could effectively sequester Pu and shield it from outside chemical influence. Natural organic matter has the possibility to influence Pu speciation through several possible mechanisms, both direct and indirect, those mechanisms could enhance or reduce the mobility of Pu depending on the physical and chemical natural of the NOM and the solutions conditions. The processes by which NOM could influence Pu mobility are thus summarized:

Directly,

1. Formation of soluble Pu-NOM complexes that reduce Pu hydrolysis and compete with Pu sorption to geomedia.
2. Formation of intrinsic NOM aggregates that incorporate Pu, either by adsorption or absorption.
3. Formation of coatings on inorganic surfaces that enhance or reduce the affinity of those surfaces for Pu.
4. Formation of coatings on inorganic surfaces that previously adsorbed Pu, shielding Pu from changing solution conditions.

Indirectly,

1. Natural organic matter, in sufficient concentrations, will hold Pu in the 4+ oxidation state.
2. Natural organic matter coatings will affect the fate of inorganic colloids which have associated Pu.

3. Natural organic matter coatings will affect the fate of intrinsic Pu colloids.

References

(1) Fehner, T.; Gosling, F. G. *Battlefi eld of the Cold War The Nevada Test Site Volume I Atmospheric Nuclear Weapons Testing*; DOE/MA-0003; US Department of Energy, 2006.

(2) Kersting, A. B.; Efurd, D. W.; Finnegan, D. .; Rokop, D. J.; Smith, D. K.; Thompson, J. L. Migraion of plutonium in ground water at the Nevada Test Site. *Nature* **1999**, *397*, 56–59.

(3) *The chemistry of the actinide and transactinide elements*, 3rd ed.; Morss, L. R., Edelstein, N. M., Fuger, J., Katz, J. J., Eds.; Springer: Dordrecht, 2006.

(4) Abel, G. Radioactive Resisude of the Cold War Period: A Radiological Legacy. *IAEA Bull.* **1998**, *40* (4).

(5) *PLUTONIUM AND OTHER TRANSURANIUM ELEMENTS: Sources, Environmental Distribution And Biomedical Effects*; WASH-1359; US Atomic Energy Commission, 1974.

(6) *The Fukushima Daiichi accident*; Internationale Atomenergie-Organisation, Ed.; International Atomic Energy Agency: Vienna, 2015.

(7) Zheng, J.; Tagami, K.; Watanabe, Y.; Uchida, S.; Aono, T.; Ishii, N.; Yoshida, S.; Kubota, Y.; Fuma, S.; Ihara, S. Isotopic evidence of plutonium release into the environment from the Fukushima DNPP accident. *Sci. Rep.* **2012**, *2* (1).

(8) Alvarado, J. A. C.; Steinmann, P.; Estier, S.; Bochud, F.; Haldimann, M.; Froidevaux, P. Anthropogenic radionuclides in atmospheric air over Switzerland during the last few decades. *Nat. Commun.* **2014**, *5*.

(9) *United States Nuclear Tests July 1945 through September 1992*; DOE/NV-209, Rev. 16; US Department of Energy, 2015.

(10) Finnegan, D. L.; Bowen, S. M.; Thompson, J. L.; Miller, C. M.; Baca, P. L.; Olivas, L. F.; Geoffrion, C. G.; Smith, D. K.; Goishi, W.; Esser, B. K.; et al. *Nevada National Security Site Underground Radionuclide Inventory, 1951-1992: Accounting for Radionuclide Decay through September 30, 2012*; LA-UR--16-21749; US Department of Energy, 2016.

(11) Smith, D.; Finnegan, D. .; Bowen, S. . An inventory of long-lived radionuclides residual from underground nuclear testing at the Nevada test site, 1951–1992. *J. Environ. Radioact.* **2003**, *67* (1), 35–51.

(12) Kersting, A. B.; Zavarin, M. Colloid-Facilitated Transport of Plutonium at the Nevada Test Site, NV, USA. In *Actinide Nanoparticle Research*; Kalmykov, S. N., Denecke, M. A., Eds.; Springer Berlin Heidelberg: Berlin, Heidelberg, 2011; pp 399–412.

(13) Novikov, A. P.; Kalmykov, S. N.; Utsunomiya, S.; Ewing, R. C.; Horreard, F.; Merkulov, A.; Clark, S. B.; Tkachev, V. V.; Myasoedov, B. F. Colloid transport of plutonium in the far-field of the Mayak Production Association, Russia. *Science* **2006**, *314* (5799), 638–641.

(14) Gallagher, D.; McGee, E. J.; Mitchell, P. I.; Alfimov, V.; Aldahan, A.; Possnert, G. Retrospective Search for Evidence of the 1957 Windscale Fire in NE Ireland Using 129 I and Other Long-Lived Nuclides. *Environ. Sci. Technol.* **2005**, *39* (9), 2927–2935.

(15) Aarkrog, A.; Dahlgaard, H.; Nielsen, S. P.; Trapeznikov, A. V.; Molchanova, I. V.; Pozolotina, V. N.; Karavaeva, E. N.; Yushkov, P. I.; Polikarpov, G. G. Radioactive inventories from the Kyshtym and Karachay accidents: estimates based on soil samples collected in the South Urals (1990–1995). *Sci. Total Environ.* **1997**, *201* (2), 137–154.

(16) Cochran, T. B.; Norris, R. S.; Suokko, K. L. Radioactive Contamination at Chelyabinsk-65, Russia. *Annu. Rev. Energy Environ.* **1993**, *18*, 507–528.

(17) *Hanford Tank Vapor Assessment Report*; SNNL-RP-2014-00791; US Department of Energy, 2014.

(18) Cantrell, K. J. *Transuranic contamination in sediment and groundwater at the US DOE Hanford site*; Pacific Northwest National Laboratory Richland, WA, 2009.

(19) Tank Farms (accessed Sep 5, 2017).

(20) Zachara, J. M.; Serne, J.; Freshley, M.; Mann, F.; Anderson, F.; Wood, M.; Jones, T.; Myers, D. Geochemical Processes Controlling Migration of Tank Wastes in Hanford's Vadose Zone. *Vadose Zone J.* **2007**, *6* (4), 985.

(21) Field, J.; Fort, L. A.; Shrum, A.; Wood, M. I. *Hanford 241-S Farm Leak Assessment Report*; RPP-RPT-48589; washington river protection solutions, 2011.

(22) Radioactive Liquid Waste Facilities. Savannah River Remediation LLC.

(23) Adu-Wusu, K.; Barnes, M. J.; Bibler, N. E.; Cantrell, J. R.; Fondeur, F. R.; Hamm, B. A.; Herman, C. C.; Hobbs, D. T.; Singleton, M.; Stallings, M. E.; et al. *Waste Tank Heel Chemical Cleaning Summary*; WSRC-TR-2003-00401; Savannah River Site, 2003.

(24) *Liquid Waste System Plan*; SRR-LWP-2009-00001; Savannah River Remediation LLC, 2016.

(25) Radioactive Liquid Waste: Operational Closure of Tanks http://www.srs.gov/general/news/factsheets/srr_tank_closure.pdf.

(26) *Rocky Flats Plant – Site Description*; Oak Ridge Associated Universities, 2007.

(27) Mongan, T. R.; Ripple, S. R.; Brorby, G. P.; diTommaso, D. G. Plutonium Releases from the 1957 Fire at Rocky Flats: *Health Phys.* **1996**, *71* (4), 510–521.

(28) Ripple, S. R.; Widner, T. E.; Mongan, T. R. Past Radionuclide Releases from Routine Operations at Rocky Flats: *Health Phys.* **1996**, *71* (4), 502–509.

(29) Ackland, L. *Making a real killing: Rocky Flats and the nuclear West*, 1st ed.; University of New Mexico Press: Albuquerque, 1999.

(30) Mongan, T. R.; Ripple, S. R.; Winges, K. D. Plutonium Release from the 903 Pad at Rocky Flats: *Health Phys.* **1996**, *71* (4), 522–531.

(31) Plutonium Down-blend Process at SRS http://www.srs.gov/general/news/factsheets/srs_plutonium_blend_down.pdf.

(32) Kersting, A. B. Plutonium Transport in the Environment. *Inorg. Chem.* **2013**, *52* (7), 3533–3546.

(33) Baas Becking, L. G. .; Kaplan, I. R.; Moore, D. Limits of the Natural Environment in Terms of pH and Oxidation-Reduction Potentials. *J. Geol.* **1960**, *68* (3), 243–284.

(34) Orlandini, K. A.; Penrose, W. R.; Nelson, D. M. Pu(V) as the stable form of oxidized plutonium in natural waters. *Mar. Chem.* **1986**, *18* (1), 49–57.

(35) Keeney-Kennicutt, W. L.; Morse, J. W. The redox chemistry of Pu(V)O2+ interaction with common mineral surfaces in dilute solutions and seawater. *Geochim. Cosmochim. Acta* **1985**, *49*, 2577–2588.

(36) Morse, J.; Choppin, G. The Chemistry of Transuranic Elements in Natural Waters. *Rev. Aquat. Sci.* **1991**, *4* (1), 1–22.

(37) Powell, B. A.; Fjeld, R. A.; Kaplan, D. I.; Coates, J. T.; Serkiz, S. M. Pu (V) O2+ adsorption and reduction by synthetic magnetite (Fe3O4). *Environ. Sci. Technol.* **2004**, *38* (22), 6016–6024.

(38) Powell, B. A.; Fjeld, R. A.; Kaplan, D. I.; Coates, J. T.; Serkiz, S. M. $Pu(V)O_2^+$ Adsorption and Reduction by Synthetic Hematite and Goethite. *Environ. Sci. Technol.* **2005**, *39* (7), 2107–2114.

(39) Sanchez, A. L.; Murray, J. W.; Sibley, T. H. The adsorption of plutonium IV and V on goethite. *Radiochim. Acta* **1985**, *49*, 2297–2307.

(40) Romanchuk, A. Y.; Kalmykov, S. N.; Aliev, R. A. Plutonium sorption onto hematite colloids at femto- and nanomolar concentrations. *Radiochim. Acta* **2011**, *99* (3), 137–144.

(41) Marsac, R.; Banik, N. L.; Lützenkirchen, J.; Buda, R. A.; Kratz, J. V.; Marquardt, C. M. Modeling plutonium sorption to kaolinite: Accounting for redox equilibria and the stability of surface species. *Chem. Geol.* **2015**, *400*, 1–10.

(42) Kaplan, D. I.; Powell, B. A.; Demirkanli, D. I.; Fjeld, R. A.; Molz, F. J.; Serkiz, S. M.; Coates, J. T. Influence of oxidation states on plutonium mobility during long-term transport through an unsaturated subsurface environment. *Environ. Sci. Technol.* **2004**, *38* (19), 5053–5058.

(43) Neck, V.; Kim, J. I. Solubility and hydrolysis of tetravalent actinides. *Radiochim. Acta* **2001**, *89*, 1–16.

(44) Choppin, G. R. Actinide speciation in the environment. *J. Radioanal. Nucl. Chem.* **2007**, *273* (3), 695–703.

(45) Neck, V.; Kim, J. I.; Kanellakopulos, B. Solubility and Hydrolysis Behaviour of Neptunium(V). *Radiochim. Acta* **1992**, *56*, 25–30.

(46) Powell, B. A.; Duff, M. C.; Kaplan, D. I.; Fjeld, R. A.; Newville, M.; Hunter, D. B.; Bertsch, P. M.; Coates, J. T.; Eng, P.; Rivers, M. L. Plutonium oxidation and subsequent reduction by Mn (IV) minerals in Yucca Mountain tuff. *Environ. Sci. Technol.* **2006**, *40* (11), 3508–3514.

(47) Hixon, A. E.; Arai, Y.; Powell, B. A. Examination of the effect of alpha radiolysis on plutonium(V) sorption to quartz using multiple plutonium isotopes. *J. Colloid Interface Sci.* **2013**, *403*, 105–112.

(48) Romanchuk, A. Y.; Kalmykov, S. N.; Aliev, R. A. Plutonium sorption onto hematite colloids at femto- and nanomolar concentrations. *Radiochim. Acta* **2011**, *99* (3), 137–144.

(49) Clark, D. L.; Hecker, S. S.; Jarvinen, G. D.; Neu, M. P. Plutonium. In *The Chemistry of the Actinide and Transactinide Elements*; Springer: The Netherlands; Vol. 2, p 1176.

(50) Thurman, E. M. *Organic geochemistry of natural waters*; Developments in biogeochemistry; M. Nijhoff ; Distributors for the U.S. and Canada, Kluwer Academic: Dordrecht ; Boston : Hingham, MA, USA, 1985.

(51) Stumm, W.; Morgan, J. J. *Aquatic chemistry: chemical equilibria and rates in natural waters*, 3rd ed.; Environmental science and technology; Wiley: New York, 1996.

(52) Boggs, S.; Livermore, D.; Seitz, M. *Humic Substances in Natural Waters and Their Complexation with Trace Metals and Radionuclides: A Review*; ANL-84-78; Aregonne National Lab, 1985.

(53) Zhou, P.; Yan, H.; Gu, B. Competitive complexation of metal ions with humic substances. *Chemosphere* **2005**, *58* (10), 1327–1337.

(54) Reuter, J.; Perdue, E. . Importance of heavy metal-organic matter interactions in natural waters. *Geochim. Cosmochim. Acta* **1977**, *41* (2), 325–334.

(55) Lamar, W. Evaluation of Organic Color and Iron in Natural Surface Waters. *Geol. Surv. Prof. Pap.* **1968**, D24–D29.

(56) Thurman, E. M.; Malcolm, R. L. Preparative isolation of aquatic humic substances. *Environ. Sci. Technol.* **1981**, *15* (4), 463–466.

(57) Petteys, M. P.; Schimpf, M. E. Characterization of hematite and its interaction with humic material using flow field-flow fractionation. *J. Chromatogr. A* **1998**, *816* (2), 145–158.

(58) Bryan, N. D.; Abrahamsen, L.; Evans, N.; Warwick, P.; Buckau, G.; Weng, L.; Van Riemsdijk, W. H. The effects of humic substances on the transport of radionuclides: Recent improvements in the prediction of behaviour and the understanding of mechanisms. *Appl. Geochem.* **2012**, *27* (2), 378–389.

(59) Zhao, P.; Zavarin, M.; Leif, R. N.; Powell, B. A.; Singleton, M. J.; Lindvall, R. E.; Kersting, A. B. Mobilization of actinides by dissolved organic compounds at the Nevada Test Site. *Appl. Geochem.* **2011**, *26* (3), 308–318.

(60) Gu, B.; Schmitt, J.; Chen, Z.; Liang, L.; McCarthy, J. F. Adsorption and desorption of natural organic matter on iron oxide: mechanisms and models. *Environ. Sci. Technol.* **1994**, *28* (1), 38–46.

(61) Weng; Van Riemsdijk, W. H.; Koopal, L. K.; Hiemstra, T. Adsorption of Humic Substances on Goethite: Comparison between Humic Acids and Fulvic Acids †. *Environ. Sci. Technol.* **2006**, *40* (24), 7494–7500.

(62) Ghosh, S.; Wang, Z.-Y.; Kang, S.; Bhowmik, P. C.; Xing, B. S. Sorption and fractionation of a peat derived humic acid by kaolinite, montmorillonite, and goethite. *Pedosphere* **2009**, *19* (1), 21–30.

(63) Kang, S.; Xing, B. Humic Acid Fractionation upon Sequential Adsorption onto Goethite. *Langmuir* **2008**, *24* (6), 2525–2531.

(64) Wang, L.; Chin, Y.-P.; Traina, S. J. Adsorption of (poly) maleic acid and an aquatic fulvic acid by geothite. *Geochim. Cosmochim. Acta* **1997**, *61* (24), 5313–5324.

(65) Weng, L.; Van Riemsdijk, W. H.; Hiemstra, T. Adsorption of humic acids onto goethite: Effects of molar mass, pH and ionic strength. *J. Colloid Interface Sci.* **2007**, *314* (1), 107–118.

(66) Gevantman, L. H.; Kraus, K. A. *Chemistry of Plutonium(V) Stability, Spectrophotometry*; National Nuclear Energy Service Div IV 14B, 1949; pp 500–518.

(67) Haschke, J. M.; Oversby, V. M. Plutonium chemistry: a synthesis of experimental data and a quantitative model for plutonium oxide solubility. *J. Nucl. Mater.* **2002**, *305* (2), 187–201.

(68) Choppin, G.; Bond, A.; Hromadka, P. Redox speciation of plutonium. *J. Radioanal. Nucl. Chem.* **1997**, *219* (2), 203–210.

(69) Nebel, D. Potentiometrische Untersuchungen des Gleichgewichtes Pu(IV)-Citrat in wäβriger Lösung. *Z Phys Chem* **1966**, *232*, 368–376.

(70) Metivier, H.; Guillaumont, R. Complexes Citriques Du Plutonium Tetravalent. *Radiochem Radional Lett.* **1972**, *10* (4), 239–250.

CHATPER TWO

OBJECTIVES

The overall goal of this work was to deepen fundamental understanding of the sorption, complexation, and aggregation processes that govern Pu transport in hydrogeological environments containing NOM. In order to achieve that goal, several ancillary experimental methods needed to be developed or refined. While not the primary objective of this work, the novel methods presented here for tritium labeling NOM (Chapter Three) or for preparing clean solutions of PuO_2^+ (Chapter Five) supported the goals of this work and will support future endeavors within the field. Following an assessment of the need to include ternary mineral-NOM-Pu species to describe Pu(IV) sorption to goethite in the presence of NOM (Chapter Three), it was decided to narrow the scope to only citrate when developing diffuse-layer models to describe ternary sorption data. The choice to study only the citrate system in greater detail was one of feasibility. Humic and fulvic acids are operationally defined by solubility in acidic and alkaline solutions. Due to a highly variable configuration of functional groups, the acid-base chemistry of humic and fulvic acids is effectively a smear of reactivity across a range of pH values, without discrete pK_a values. In addition, the ionic strength dependent aggregation behavior of humic and fulvic acids is not fully understood and would make modeling efforts significantly more complex. Meanwhile, while the siderophore Deferoxamine-B (DFOB) has well defined acid-base chemistry, it exhibited nearly insignificant sorption to goethite, making it a poor choice for study of ternary surface complexes. The well-defined chemistry of citrate, coupled with

strong Pu(IV) complexation and known sorption to minerals, made it an ideal NOM for study of mineral-NOM-Pu ternary surface species thermodynamic behavior (Chapter Four).

More specifically, the objectives of this work were to:

1. Develop methods to radiolabel humic and fulvic acids to reduce their detection limits whilst providing a means to quantify Pu and NOM concentrations simultaneously using the α/β discriminator function liquid scintillation counters. (Chapter Three)
2. Examine the effect of humic acid, fulvic acid, citric acid and DFOB on Pu(IV) sorption to goethite. (Chapter Three)
3. Use a hybrid empirical/thermodynamic surface complexation modeling approach to qualitatively appraise the significance of ternary mineral-NOM-Pu(IV) complexes on Pu sorption to goethite in the presence of humic acid, fulvic acid, citric acid and DFOB. (Chapter Three)
4. Develop a ternary surface complexation model for simultaneous sorption of Pu(IV) and citrate to gibbsite and goethite, and compare the role of the ternary complex in Pu(IV) sorption to both minerals. (Chapter Four)
5. Use competitive complexation with AnaLig-Pu02 resin to determine Pu(IV)-citrate thermodynamic behavior at alkaline pH. (Chapter Four)
6. Develop a less burdensome method for preparing Pu in the +5 oxidation state for use in future work. (Chapter Five)

CHAPTER THREE

THE EFFECT OF NATURAL ORGANIC MATTER ON PLUTONIUM SORPTION TO GOETHITE

Accepted November 21, 2016 to Environmental Science & Technology:

Conroy, N. A.; Zavarin, M.; Kersting, A. B.; Powell, B. A. Effect of Natural Organic Matter on Plutonium Sorption to Goethite. *Environ. Sci. Technol.* **2017**.

DOI: 10.1021/acs.est.6b03587

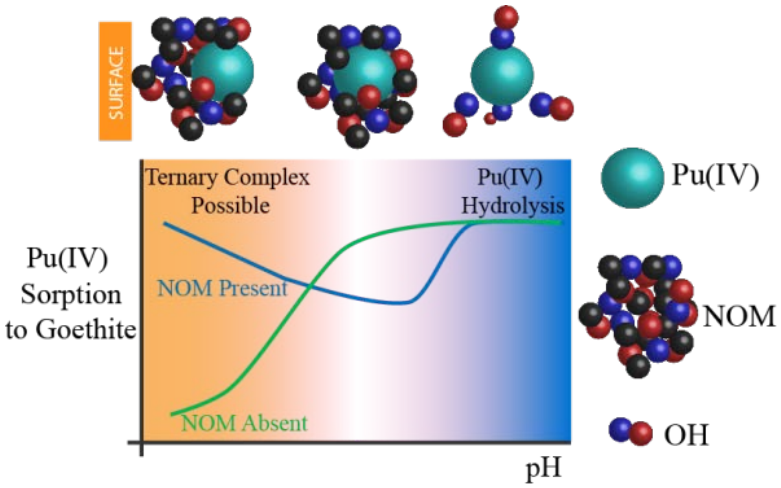

Figure 3.1 Schematic of the pH dependent effect of natural organic matter on Pu(IV) sorption goethite; ternary complexes possible at acidic pH, decreased sorption at intermediate pH, little effect at alkaline pH (abstract art).

Abstract

The effect of citric acid (CA), Desferrioxamine B (DFOB), fulvic acid (FA), and humic acid (HA) on plutonium (Pu) sorption to goethite was studied as a function of organic carbon concentration and pH using batch sorption experiments at 5 $mg_C \cdot L^{-1}$ and 50 $mg_C \cdot L^{-1}$ natural organic matter (NOM), 10^{-9} - 10^{-10} M ^{238}Pu, and 0.1 $g \cdot L^{-1}$ goethite concentrations, at pH 3, 5, 7, and 9. Low sorption of ligands coupled with strong Pu complexation decreased Pu sorption at pH 5 and 7, relative to a ligand-free system. Conversely, CA, FA, and HA increased Pu sorption to goethite at pH 3, suggesting ternary complex formation or, in the case of humic acid, incorporation into HA aggregates. Mechanisms for ternary complex formation were characterized by Fourier transform infrared spectroscopy in the absence of Pu. CA and FA demonstrated clear surface interactions at pH 3, HA appeared unchanged suggesting HA aggregates had formed, and no DFOB interactions were observed. Plutonium sorption decreased in the presence of DFOB (relative to a ligand free system) at all pH values examined. Thus, DFOB does not appear to facilitate formation of ternary Pu-DFOB-goethite complexes. At pH 9, Pu sorption in the presence of all NOM increased relative to pH 5 and 7; speciation models attributed this to Pu(IV) hydrolysis competing with ligand complexation, increasing sorption. The results indicate that in simple Pu-NOM-goethite ternary batch systems, NOM will decrease Pu sorption to goethite at all but particularly low pH conditions.

Introduction

Plutonium (Pu) has been dispersed into the global environment as a result of atmospheric nuclear weapons testing, nuclear power plant accidents, and reentry of satellites and, in limited environments, via underground nuclear testing and accidental releases.[1] While

detectable Pu is found all over the world from nuclear fallout, these trace concentrations are insufficient to pose a major health risk. However, this may not be the case in the local environments surrounding nuclear weapons manufacturing and testing sites. In the United States the major production and testing sites are the Hanford (Washington) and Savannah River Sites (SRS, South Carolina) where Pu was produced and processed, the Rocky Flats Environmental Technology Site (RFETS, Colorado) where bomb parts were cast and finished, and the Nevada National Security Site (NNSS, Nevada) where nuclear weapons were tested above and below ground. Both the Hanford and SRS sites store thousands of curies of Pu in various chemical forms awaiting final disposal.[2,3] At the former Rocky Flats Plant, Pu fires and inadequate waste management resulted in widespread Pu contamination of the vadose zone and surface waters at what is now the RFETS.[4,5] The NNSS was the location of 86 atmospheric weapons tests from 1951 to 1962[6] and 828 underground nuclear tests from 1951 to 1992[7]. There is an estimated 793,800 Ci of $^{238\text{-}242}$Pu in the subsurface at the NNSS, the majority of which is projected to be associated with the melt glass at the bottom of test cavities.[1,8] Approximately one third of the underground nuclear tests were detonated below the standing water table. Each of these sites has the potential for surface water or groundwater Pu contamination.[9] Thus, understanding Pu mobility through subsurface hydrogeochemical systems is essential for remediation efforts and to ensure protection of human and environmental health.

Due to strong sorption and low solubility of Pu(IV), and surface mediated reduction of the more mobile Pu(V) and Pu(VI) species to Pu(IV), Pu exhibits low mobility at environmentally relevant pH and in the absence of strong inorganic or organic

complexants. For example, the sorption edge of Pu(IV) to numerous minerals, including goethite, occurs at pH 3 – 5.[10–13] The sorption edge of Pu(V) on goethite is near pH 7, but a gradual shift in the Pu(V) sorption edge over time has been attributed to reduction of Pu(V) to Pu(IV).[10] This surface mediated reduction has since been experimentally confirmed for goethite[10,14]; hematite[12]; magnetite[15,16]. Pu(IV) will therefore be the dominant oxidation state under the majority of environmentally relevant conditions.

Despite expected low mobility, far-field transport of Pu has been observed at several nuclear weapons legacy sites. In such cases, sorption to mobile colloids has been implicated in the mobility of these strongly sorbing species. Kersting *et al.*[7] found that Pu had migrated over 1.3 km from its source at the NNSS and that greater than 99% of the mobile Pu was associated with inorganic colloids, which were primarily clays and zeolites.[7] Colloid facilitated transport was also observed in the far-field of the Mayak Production Association in Russia, where Pu was detected 4 km from Lake Karachai, the discharge site for reprocessing wastes.[17] Novikov *et al.*[17] found that the distribution of Pu between aqueous species and those sorbed to colloids was nearly constant within 2.15 km of the source, regardless of Pu concentration, and that the Pu distribution shifted to greater colloid-sorbed fractions at distances >2.5 km. While both of these studies implicated inorganic colloids for the observed Pu transport, other studies have found that dissolved natural organic matter can also influence Pu transport.[5,7,8,18]

Natural organic matter (NOM) has been shown to profoundly affect Pu mobility. Complexation of Pu by dissolved or suspended NOM in solution can increase the total amount of Pu available for transport.[11] Inside the U12n and U12t tunnel complexes (Rainer

Mesa, NNSS), >65 % of Pu was dissolved and not associated with colloidal matter. Instead, it was associated with dissolved organic matter (DOM).[8] This is in sharp contrast to the <10 % found dissolved in groundwater from other parts of the NNSS, where typically >90 % of mobile Pu was associated with inorganic colloid fractions (>20 nm).[7,8] DOM concentrations reach 15 – 19 $mg_C \cdot L^{-1}$ in the Rainer Mesa tunnel system compared with 0.2 $mg_C \cdot L^{-1}$ in the local spring water.[18] Organic material released during construction of the Rainer Mesa tunnel system is believed to be responsible for the high concentrations of DOM in the tunnel water (pH 8.3 – 8.8).[8] NOM was also implicated in a study of Pu mobilization in surface water at the RFETS where Pu was associated with colloids (3 kDa - 0.45 µm, 10 - 60%) and larger particulates (≥0.45 µm, 40 – 90%).[5] The Pu bound colloid fractions were primarily 10 – 15 kDa organic macromolecules.[5] The pH of these surface waters ranged from 7.5 – 9.9, thus imparting a negative surface charge on the colloids. Colloidal Pu was in the tetravalent oxidation state and largely not associated with the inorganic clay or iron oxide colloids abundant at the site.[5] Therefore, field data suggest that Pu-NOM complexes (<20 nm) may be the dominant Pu species at high NOM concentrations.

NOM has demonstrated high affinity for natural and anthropogenic metal ions[19] and has also been shown to sorb significantly to iron oxide minerals[20–25]. Studies examining the effect of NOM on Pu sorption to minerals however are lacking. NOM sorption to a mineral colloid could alter the surface characteristics of the colloid and enhance its environmental mobility.[26] Furthermore, NOM contains a multitude of reactive functional groups such that it could sorb to a mineral surface and complex with metals simultaneously (i.e. form ternary

mineral-NOM-metal complexes).[26–29] This could lead to the formation of mobile ternary Pu complexes in environmental systems. In addition, NOM may form intrinsic colloids which could sequester Pu.[5,18] NOM therefore has the possibility of influencing Pu mobility through 1) formation of dissolved Pu-ligand complexes, 2) formation of ternary Pu-NOM-surface complexes on immobile surfaces, 3) formation of ternary complexes on mobile inorganic colloids and/or, 4) Pu sequestration/sorption to aggregated NOM colloids. This study examines the effects of NOM on Pu sorption to goethite with respect to NOM concentration and solution pH, in an effort to understand NOMs influence on Pu mobility. Goethite was selected as a model mineral surface due to the high abundance of iron minerals in most environments and for comparison with previous studies also examining Pu interactions with goethite. The NOM used in this study (Citric acid (CA), desferrioxamine B (DFOB), fulvic acid (FA), and humic acid (HA)) were chosen to represent a range of molecular weights, hydrophobicity, and functionality.

Materials and Methods

NOM Stock Preparation

Carbon-14 labeled CA (50 – 60 $mCi \cdot mmol^{-1}$) was purchased from American Radiolabeled Chemicals, Inc. FA (Suwannee River II Standard) and HA (Leonardite Standard) were purchased from the International Humic Substance Society. FA and HA were radiolabeled with ^{3}H using a method adapted from a previous study.[30] Procedure details and adaptations are provided in the Supporting Information (SI). Radiolabeling lowers the detection limit of aqueous NOM and allows for simultaneous quantification of aqueous Pu and NOM by liquid scintillation counting (LSC). DFOB experiments were performed without a radiotracer, due to lack of commercial availability and inability to be

labeled by the method used for FA and HA. For convenience CA, DFOB, FA, and HA are referred to below as NOM when discussing organic matter as a group.

Citric acid monohydrate (BDH ACS Grade), DFOB mesylate salt (Sigma Aldrich, ≥ 92.5 %), FA, and HA solutions were prepared in 0.01 M NaCl at concentrations of 5 $mg_C \cdot L^{-1}$ and 50 $mg_C \cdot L^{-1}$. Radiotracers were spiked into these solutions to reach activities of approximately 125,000 $Bq \cdot L^{-1}$ in ^{3}H systems and 700,000 $Bq \cdot L^{-1}$ in ^{14}C systems. Given the relatively high specific activities of ^{3}H and ^{14}C, these tracers did not add significant mass to the system. The exact NOM concentrations of the batch sorption experiments are given in Table 1; (molarities of HA and FA were calculated from titration data available from IHSS; 7.46 $meq \cdot g_C^{-1}$ and 11.17 $meq \cdot g_C^{-1}$, respectively).

Table 3.1. Concentrations of NOM, goethite, and Pu used in batch sorption

Experimental Analyte*	NOM	NOM	NOM	Pu	Goethit	Detection Method	Target Isotope
		$mg_C \cdot L^{-1}$	-----	$mol \cdot L^{-1}$ -----	$g \cdot L^{-1}$		
^{238}Pu	–	–	–	9.4×10^{-10}	0.104	LSC (α)	^{238}Pu
^{238}Pu/CA	CA	5.00	6.93×	5.6×10^{-10}	0.095	LSC (α/β)	^{238}Pu /^{14}C
^{238}Pu/CA	CA	50.0	6.93×	6.5×10^{-10}	0.092	LSC (α/β)	^{238}Pu /^{14}C
^{238}Pu	DFO	4.93	1.6×1	2.5×10^{-9}	0.097	LSC (α)	^{238}Pu
^{238}Pu	DFO	50.6	1.7×1	2.5×10^{-9}	0.097	LSC (α)	^{238}Pu
DFOB	DFO	5.02	1.7×1	–	0.11	TOC	$^{12\text{-}14}C$
DFOB	DFO	50.2	1.7×1	–	0.11	TOC	$^{12\text{-}14}C$
^{238}Pu/HA	HA	5.08	3.9×1	8.5×10^{-10}	0.096	LSC (α/β)	^{238}Pu /^{3}H
^{238}Pu/HA	HA	50.3	3.8×1	8.5×10^{-10}	0.097	LSC (α/β)	^{238}Pu /^{3}H
^{238}Pu/FA	FA	5.05	5.6×1	9.7×10^{-10}	0.097	LSC (α/β)	^{238}Pu /^{3}H
^{238}Pu/FA	FA	49.9	5.6×1	9.7×10^{-10}	0.097	LSC (α/β)	^{238}Pu /^{3}H

*Targeted analyte(s) for sorption data

Goethite Stock Preparation

Goethite was synthesized using the procedure described by Schwertmann *et al.* (1991) and confirmed by power X-ray diffraction (Bruker D8 X-ray diffractometer). The average

surface area was 38.8 $m^2 \cdot g^{-1}$ measured by N_2(g) adsorption (Quadrasorb SI surface area analyzer with QuadraWin™ v.5.02 software, Quantachrome Instruments); and the point of zero charge (pzc) was 8.3, measured by mass titration (Figure A14). Goethite stock suspensions were prepared by adding 0.02 g of dry goethite to 200 mL of each NOM solution.

Pu Stock Preparation

Pu(IV) solutions were prepared by pipetting 0.8 mL of a 3.9×10^{-8} M (0.16 $\mu Ci \cdot mL^{-1}$) ^{238}Pu stock solution in 4 M HNO_3 (Eckert and Zeigler) into a Teflon® vial and evaporating off the liquid at low temperature. The Pu was reconstituted into 15 mL of each NOM solution. This evaporative step has been shown to produce high purity Pu(IV) solutions at low Pu concentrations.[31] The final Pu stock concentrations ranged from 1.7×10^{-8} M to 9.7×10^{-8} M. There was a drastic excess of NOM relative to Pu in all experiments, NOM:Pu molar ratios were approximately $10^3 - 10^5$. Given the starting oxidation state of Pu in this work (91% ±0.15% Pu(IV); 3.4% ±0.02% Pu(V); 5.4% ±0.04% Pu(VI)) determined by solvent extraction[32], and previous observations that Pu(IV) is the dominant Pu oxidation state in the presence of NOM [27,33–37], nearly all the Pu in these experiments is anticipated to be Pu(IV).

Batch Sorption Experiments

Samples were prepared in clear centrifuge tubes (polypropylene, VWR) by mixing NOM-goethite and NOM-Pu solutions; final concentrations listed in Table 1. Eight samples were prepared for each ligand and concentration, and duplicates were adjusted to pH 3, 5, 7, and 9. The pH of each sample was measured and adjusted periodically using

small additions of 0.01 M NaOH or 0.01 M HCl. Samples were mixed on an end-over-end rotator at approximately 8 RPM. Sampling occurred 1, 7, 14, and 30 days after the goethite suspensions and Pu solutions were initially mixed; an additional sampling occurred for CA after 45 days. During each sampling event, a 1.3 mL aliquot of the Pu-NOM-goethite suspension was removed and centrifuged (Beckman Coulter Allegra X22R) for 20 minutes at 8000 RPM (6596 RCF) using a Beckman 2402 rotor. A 1 mL aliquot of the supernatant was removed and mixed with 5 mL of Hi Safe 3 (Perkin Elmer) liquid scintillation cocktail and counted for the radiolabel and Pu using a Tri-Carb Liquid Scintillation Analyzer or Hidex 300SL. DFOB sorption was determined in a separate, Pu-free, experiment where supernatant DFOB concentrations were measured by TOC (Shimadzu TOC-V TOC Analyzer). DFOB sorption was quantified in a Pu free system to prevent contamination of the TOC analyzer.

The data are presented below using a surface area normalized solid-water distribution ratio (K_a) (Equation 1).

$$K_a(L \cdot m^{-2}) = \frac{[C]_{total} - [C]_{aq}}{[C]_{aq}} \times \frac{1}{[SS]} \times \frac{1}{SA} \qquad \text{Equation 1}$$

where $[C]_{total}$ and $[C]_{aq}$ are the total and aqueous molar concentrations, respectively, of either Pu or NOM, [SS] is the concentration of goethite ($kg \cdot L^{-1}$), and SA is the average surface area of the goethite ($m^2 \cdot kg^{-1}$). Data are presented as surface area normalized distributions ratios to facilitate comparison with other studies.

A minimum detectable activity (MDA) can be calculated from LSC data using counting statistics as defined by Currie[38] and subsequently used to determine a maximum detectable

K_a. In practice, the MDA of NOM could be lowered by increasing the amount of tracer NOM used. In these experiments the tracer molecules accounted for <1% of the total carbon present in each experiment. For the given experimental conditions, measured background count rates, and counting times of 30 minutes, the approximate maximum detectable K_a was 19,000 $L \cdot m^{-2}$ for the ^{14}C experiments, 500 $L \cdot m^{-2}$ for the FA and 50 $mg_C \cdot L^{-1}$ HA experiments, and 800 $L \cdot m^{-2}$ for the 5 $mg_C \cdot L^{-1}$ HA experiments. Detailed descriptions of the equations used to determine the MDA and maximum K_a values are in the SI. DFOB sorption was quantified using TOC to determine the total carbon remaining in the aqueous fraction. The TOC instrumentation has a detection limit near 1 $mg_C \cdot L^{-1}$, which resulted in a maximum detectable K_a of approximately 9 and 111 $L \cdot m^{-2}$ in the 5 and 50 $mg_C \cdot L^{-1}$ DFOB sorption experiments, respectively. Use of the radiolabeled NOM tracers therefore provided significant reductions in detection limits; all K_a values reported in this study were determined based on aqueous concentrations above the limit of detection.

We found that significant Pu can be removed from solution in the absence of goethite when HA is present, presumably through HA aggregation. To study Pu aggregation with HA, similar batch sorption experiments were performed without goethite and with 6 $mg_C \cdot L^{-1}$ and 64 $mg_C \cdot L^{-1}$ HA. In the presence of goethite, vial walls are a small contributor to the total surface area in the experimental system. This is not the case in a goethite-free system, therefore, Pu sorption to vial walls could contribute to Pu removal from solution. To account for this, prior to centrifugation 1mL of the solution was counted by LSC to determine total aqueous (dissolved and suspended) Pu and compared with the total Pu added to each vial, which was carefully tracked gravimetrically.

Attenuated Total Reflectance – Fourier Transform Infrared Spectroscopy (ATR-FTIR)

NOM interaction mechanisms with goethite were characterized using ATR-FTIR (Thermo Scientific 6700; Smart iTR diamond ATR crystal; mercury cadmium telluride narrow band detector). Samples were prepared by suspending 25 $g \cdot L^{-1}$ goethite in 10 mL of 2.5 $g_C \cdot L^{-1}$ NOM and 0.01 M NaCl. Suspensions were mixed for 3 days, the pH adjusted to 3 regularly before centrifuging to separate the "free" supernatant and sorbed NOM fractions. The supernatant and sorbed fractions were lyophilized to desiccation and ATR-FTIR spectra taken of the solids. Spectroscopy was used to validate that the HA and FA used in this study behaved similarly to other NOMs in previous spectroscopic studies. Inferring sorption mechanisms through FTIR is normally accomplished by observing differences between spectra of surface complexed and "free" sorbate in the bulk solution. Previous studies of metal carboxylate complexes have found that the change in $\Delta\nu$ (where $\Delta\nu = \nu_{as} - \nu_s$ of the carboxylate ion) between the free and sorbed carboxylate species, can be used to infer the sorption mechanism (discussed in SI).[39-42] The spectra presented include the "free" NOM (supernatant) and "goethite subtracted" sorbed NOM, in which the overtone bands of goethite (1662 cm^{-1} and 1788 cm^{-1}) have been subtracted for clarity. Raw spectra are available in the SI (Figures A10 – A13).

Particle Size & Zeta Potential Measurements

Humic acid aggregation behavior was studied using zeta potential analysis and dynamic light scattering particle size analysis. HA solutions were prepared at 6 $mg_C \cdot L^{-1}$ and 46 $mg_C \cdot L^{-1}$, some with 0.1 $g \cdot L^{-1}$ goethite suspended, and pH adjusted from 3 – 7. Surface charge of HA solutions with goethite suspended was determined by a Malvern Instruments

Zetasizer Nano Series Zeta Potential Analyzer. Effective particle size of the HA in goethite free solutions was determined by a Brookhaven 90Plus Nanoparticle Size Analyzer.

Results & Discussion

The ligands selected for this work range in molecular weight, functionality, and hydrophobicity; from small, hydrophilic molecules (CA and DFOB) to more complex, high molecular weight ligands (FA and HA). The sorption data presented were collected after 30 days of mixing (45 days for the Pu-citrate system). Data from 1, 7, and 14 days are presented in the SI (Figures A2-A6). With the exception of CA, minimal Pu and NOM sorption changes occurred between 14 and 30 days (Figures A7 and A8, respectively), indicating 30 days is sufficiently close to equilibrium to warrant discussion. The Pu-CA system was equilibrated for 45 days because slight changes were observed between 14 and 30 days. As discussed in detail below, NOM sorption onto goethite generally increased with decreasing pH (Figure 3.2); this observation is least evident for DFOB due to high pK_as ($pKa_{1\text{-}3}$ = 8.35; 8.97; 9.71)[43], and therefore, minimal sorption at any pH. NOM sorption is consistent with the presence of anionic forms of the NOM which interact with the positively charged goethite surface below the pzc near pH 8.3. This effect is evident in Figure 3.6, right, where the zeta potential of goethite suspensions is shown to be negative in the presence of 6 and 46 $mg_C \cdot L^{-1}$ HA, and corroborates Pu sorption to goethite in the presence of NOM through ternary complexes.

NOM Sorption to Goethite

CA is a triprotic acid whose sorption to goethite (Figure 3.2) was dependent on the charge of the citrate species and the goethite surface with respect to pH. Below the lowest acid

dissociation constant (pK_a = 3.13)[44] of CA, the majority of CA present is a neutral, fully protonated species. Sorption increases from pH 3 to 5 as the CA deprotonates and becomes increasingly negatively charged based on the pK_a values where half the CA species are doubly charged ions at pH 4.78[44] and half are triply charged at pH 6.36[44]. At pH 3, ATR-FTIR data (Figure 3.3) indicate bridging-bidentate interactions between CA and goethite at both terminal carboxyl groups. Upon sorption, the C=O peak near 1724 cm^{-1} decreases significantly relative to the $\nu_{as(COO-)}$ and $\nu_{s(COO-)}$ peaks found at 1577 cm^{-1} and 1401 cm^{-1}, respectively. Neither of these peaks shift once sorbed, and the C=O to COO^- peak ratios are disproportionate for pH 2.98, both of which strongly suggest a bridging bidentate sorption complex[43]. Above the pH corresponding to the third pK_a (6.36), sorption decreases as CA persists as a highly charged anion while the goethite surface becomes less positively charged (the pzc of goethite is near pH 8.3).

Batch sorption experiments revealed only slight removal of DFOB from solution by goethite (Figure 3.2). Likewise, there was no spectral evidence of DFOB sorption to goethite (Figure 3.3). None of the numerous DFOB bands were observable in the sorbed fraction. However, the ATR-FTIR spectra of the sorbed fraction revealed peaks not characteristic of goethite. These peaks were attributed to the mesylate salt of the DFOB mesylate salt reagent. Methylsulfonic acid has a very low pKa (-1.9) and will exist in solution as a sulfonate. The bands observed in the DFOB – goethite spectrum are consistent with the presence of mesylate groups.[45]

Due to the complex nature of HA and FA, exact complexation mechanisms are difficult to determine. Suwannee River FA sorption decreased with increasing pH (Figure 3.2). The

approximately linear trend has been well studied, highlighted in a recent review article by Stockdale *et al.*[29], and is typical of FA and HA sorption to several minerals over the entire pH range.[29] A study by Guo *et al.*[46] showed that in the presence of significantly higher concentrations of goethite (5 $g \cdot L^{-1}$), >80% of FA (20 $mg \cdot L^{-1}$) was sorbed from pH 3 – 10, and the linearly decreasing trend with increasing pH was not observed.[46] However, based on >80 % FA sorption and an assumed goethite surface area of 38.8 $m^2 \cdot g^{-1}$, the work by Guo *et al.* results in a $K_a > 0.021$ $m^2 \cdot L^{-1}$ which is in agreement with our results. The ATR-FTIR spectrum of goethite-sorbed FA at pH 3.1 demonstrated significant changes in the carbonyl region that were consistent with observations from previous studies.[20,41] Upon sorption, the asymmetric band shifts 39 cm^{-1} to lower energy and the symmetric band remains at 1394 cm^{-1}, suggesting a bidentate-mononuclear sorption mechanism[41,48]. It is noteworthy however, that a $\Delta\nu$ shift of 39 cm^{-1} is very near the, albeit arbitrary, cutoff previously cited[48] to delineate a bidentate-mononuclear and a bringing-bidentate complex. Therefore, both surface coordination complexes could be contributors to the overall sorption.

Leonardite HA sorption to goethite decreased with increasing pH, similar to our FA and to previous observations for HA sorption to other minerals.[29] In this study, HA sorption was greater than FA at any given pH or concentration. However, due to the hydrophobic character of the HA, formation of aggregates is possible. HA is particularly hydrophobic at low pH where fewer sites are deprotonated and can lead to formation of intrinsic HA colloids and precipitates. Thus, removal of HA at low pH may be due to either sorption or aggregation.

The ATR-FTIR spectrum of goethite-sorbed HA was only marginally different from HA and goethite independently (Figure 3.3), indicating minimal spectroscopically significant interaction between HA and goethite. While much of the $\nu_{as(COO-)}$ and $\nu_{a(COO-)}$ intensity appears unchanged, the maximum intensity of the $\nu_{as(COO-)}$ peak is shifted from 1618 cm^{-1} to 1607 cm^{-1} upon sorption and the maximum intensity of the $\nu_{a(COO-)}$ peak is shifted from 1383 cm^{-1} to 1379 cm^{-1} upon sorption. These shifts result in an overall decrease in the difference between the asymmetric and symmetric peak locations of 7 cm^{-1}, suggesting bridging-bidentate surface interactions. Minimal intensity losses at the free carbonyl peak locations, combined with little observable change in the C=O peak near 1710 cm^{-1} however, suggests minimal spectroscopically significant interaction between HA and goethite. Coagulation of particle sized HA aggregates could result in sufficiently large colloids to be removed by the centrifugation step. Alternatively, previous studies have shown that HA tends to form multiple adsorption layers on hematite surfaces.[49] Driven by hydrophobicity, the formation of relatively thick layers of HA over a surface could shield the evanescent wave from an ATR-FTIR measurement from interacting with functional groups at the goethite – HA interface. In the case of layered HA, since the majority of HA would be aggregated with itself, it would appear spectroscopically similar to aggregated HA. It is worth mentioning that FA tends to form monolayers on the same surfaces.[49] Decreased intensity of the $\nu_{as(COO-)}$ peak with respect to the $\nu_{sym(COO-)}$ peak does not seem to be the result of surface sorption as the same relative decrease is observed in a sample of HA that was hydrated and then freeze dried; this further suggests the observed peaks are the result of HA coagulation rather than surface sorption.

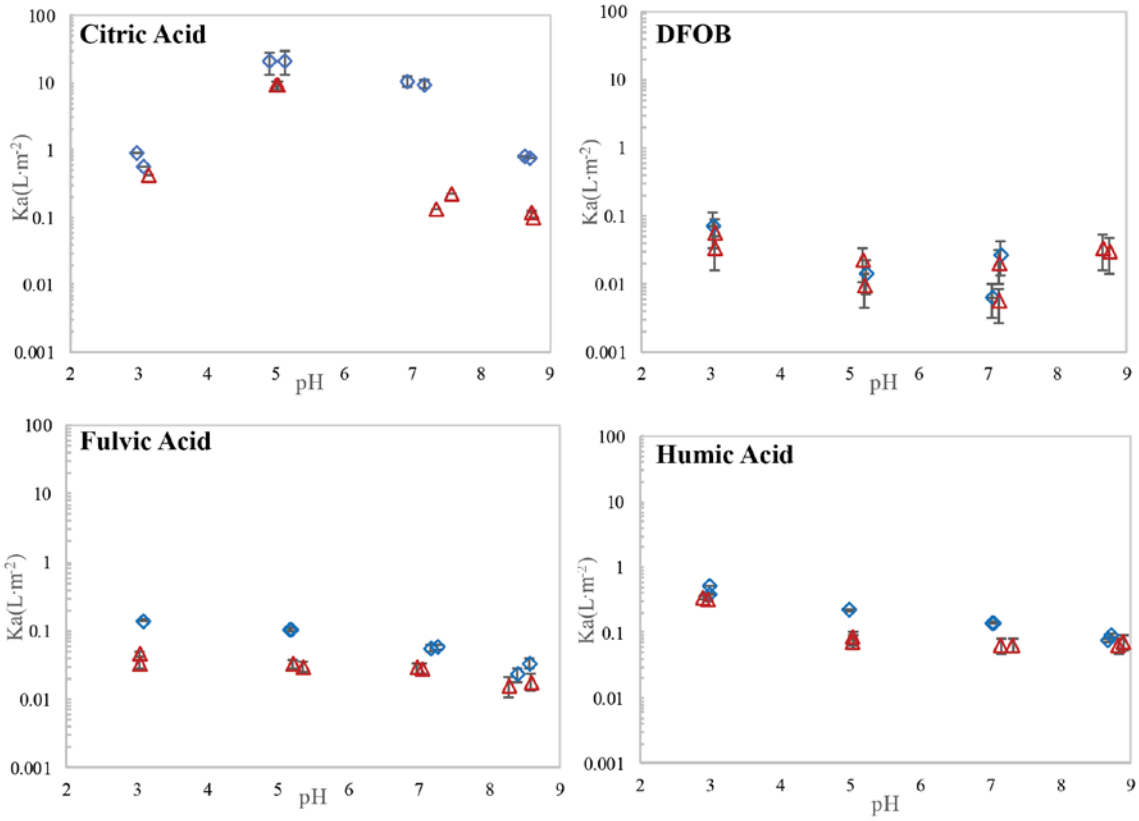

Figure 3.2. NOM sorption to goethite (0.1 $g \cdot L^{-1}$) at 5 $mg_C \cdot L^{-1}$ (blue diamonds) and 50 $mg_C \cdot L^{-1}$ (red triangles) NOM in 0.01 M NaCl after 30 days (CA after 45 days). CA, FA, and HA error bars calculated from counting statistics; DFOB error bars calculated from standard deviation of duplicates.

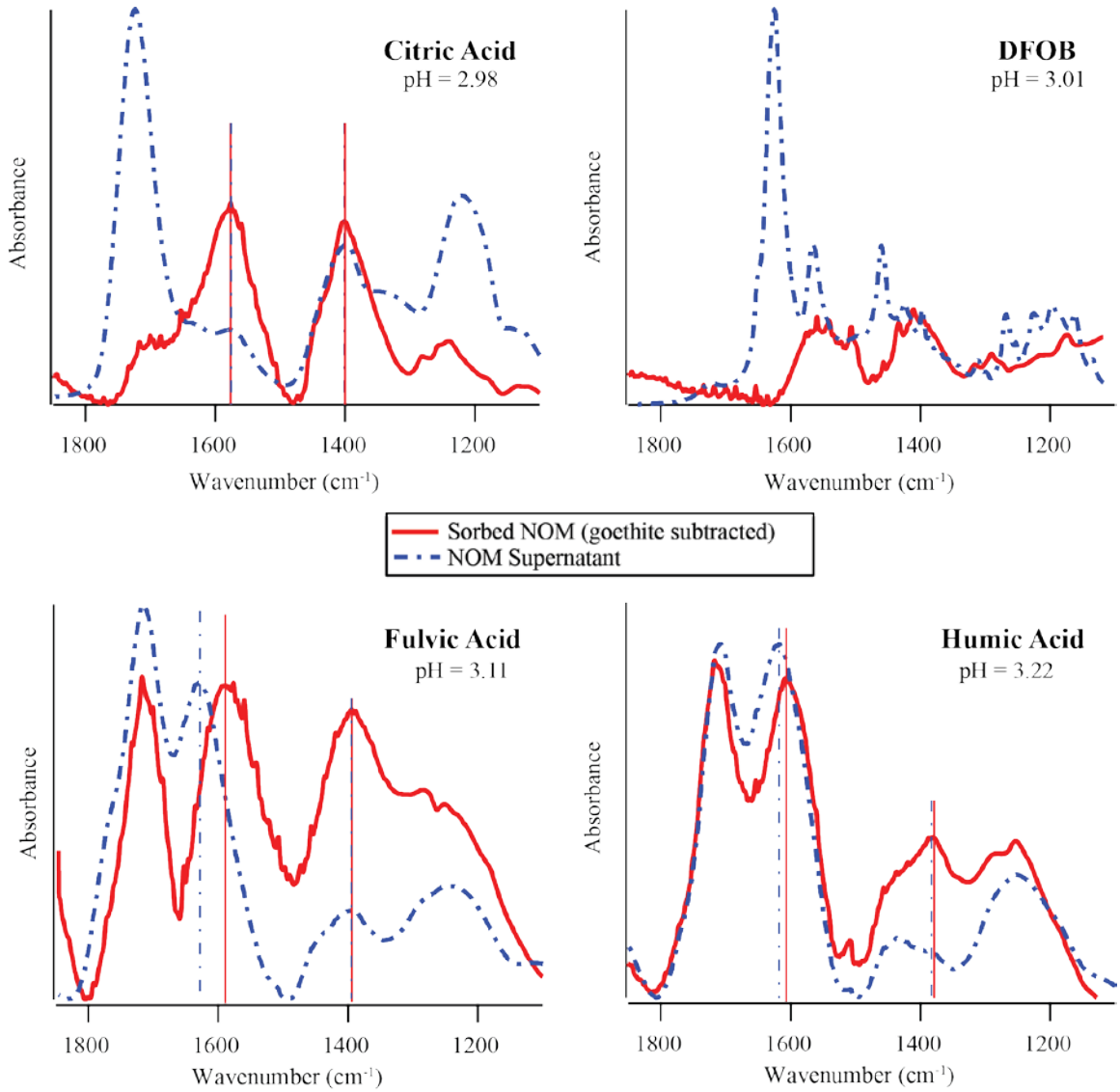

Figure 3.3. ATR-FTIR spectra of NOM sorbed to goethite and supernatant at pH 3.

Effect of NOM on Plutonium Sorption

In order to understand the influence of NOM on Pu sorption, we must first understand Pu sorption to goethite in the absence of NOM. This study found that >95% of Pu(IV) was sorbed to goethite above pH 5.1 (Figure 3.4.; green circles). This agrees well with Sanchez et al.[10], where >95% of Pu(IV) was sorbed to goethite above pH 4.8 in the

absence of a ligand. Pu concentrations were well below the estimated concentration of available reactive sites (~7.9×10^{-6} M, assuming 2.31 sites·nm^{-2}), therefore, site saturation was not a concern. Considering the starting oxidation state of Pu in this work (91% ±0.15% Pu(IV); 3.4% ±0.02% Pu(V); 5.4% ±0.04% Pu(VI)) determined by solvent extraction[32], and previous observations that Pu(IV) is the dominant Pu oxidation state in the presence of humic substances [27,33–37], little to no Pu(V) or Pu(VI) is expected in these experiments. Also under oxic conditions, no Pu(III) is expected at circumneutral pH.

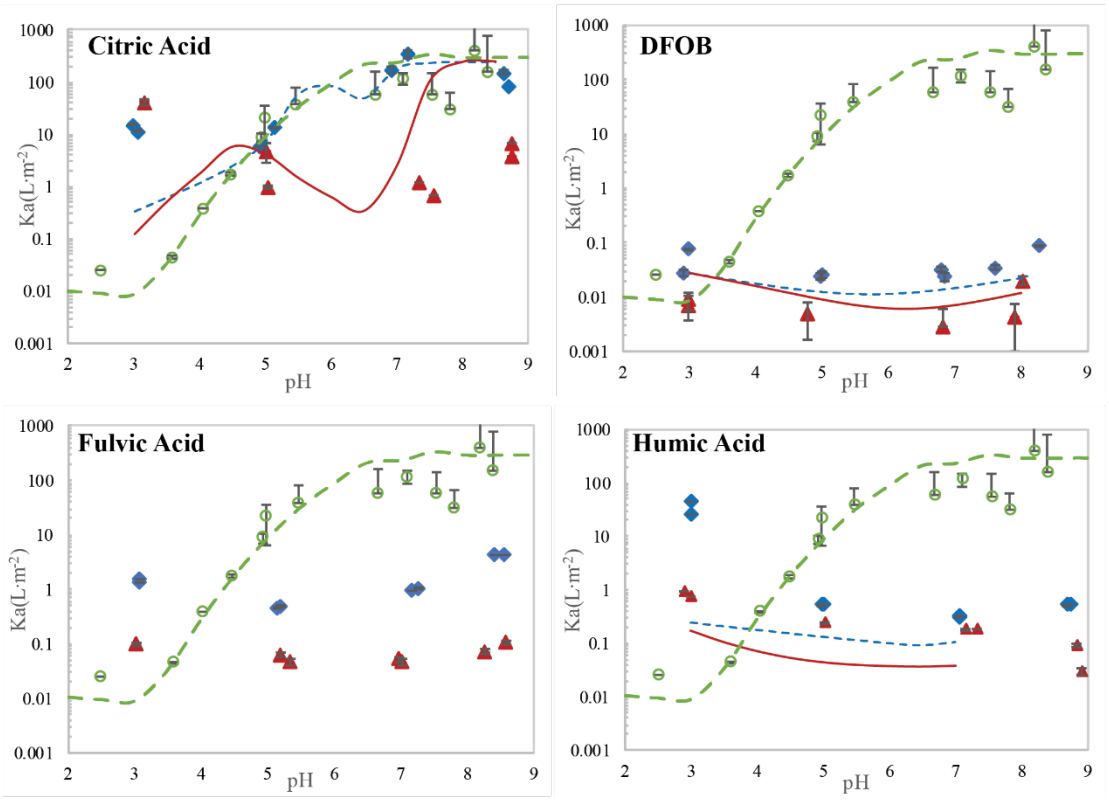

Figure 3.4. Pu sorption to goethite (0.1 $g \cdot L^{-1}$) in the presence of NOM at 5 $mg_C \cdot L^{-1}$ (blue diamonds) & 50 $mg_C \cdot L^{-1}$ (red triangles) in 0.01 M NaCl after 30 days (CA after 45 days); NOM free system in green circles. Thermodynamic models shown with green dashed line (NOM free), dashed blue line (5 $mg_C \cdot L^{-1}$), and solid red line (50 $mg_C \cdot L^{-1}$). Error bars calculated from counting statistics.

CA enhanced Pu sorption at low pH. At pH 3, CA sorption reached 4.60×10^{-4} and 3.39×10^{-3} mol $CA \cdot g_{goethite}^{-1}$ in the 5 and 50 $mg_C \cdot L^{-1}$ experiments, respectively (Figure 3.2). Pu concentrations on goethite reached 5.78×10^{-9} and 6.99×10^{-9} mol $Pu \cdot g_{goethite}^{-1}$, respectively, at the same pH. The molar ratios of Pu:CA on the goethite surface were

therefore 1.26×10^{-5} and 2.06×10^{-6}, indicating a drastic excess of CA on the surface for Pu binding. We propose that the enhanced Pu sorption at low pH was due to formation of ternary complexes, where CA formed a surface coating on goethite and binds Pu through moieties, that are either directly or indirectly bound to the surface themselves. The Pu:CA molar ratios in solution were 4.26×10^{-7} and 1.71×10^{-8} in the 5 and 50 $mg_C \cdot L^{-1}$ experiments, respectively. Greater Pu:CA ratios on the goethite surface over the aqueous solution is an indication of the favorability of a ternary, goethite-CA-Pu, surface complex.

From pH 5 to 7, CA sorption decreased substantially whilst Pu sorption in the 5 $mg_C \cdot L^{-1}$ system increased and in the 50 $mg_C \cdot L^{-1}$ system decreased with respect to the ligand-free system. This suggested a transition from ternary complexes at low pH to binary sorption similar to the ligand-free system at high pH. The higher concentration of CA outcompetes Pu-hydrolysis and subsequent binary sorption to a higher pH than the lower concentration; hence the observed decrease in Pu sorption compared to the ligand-free system at both pH 7 and 9, but also an increase in Pu sorption from pH 7 to 9 due to increasing Pu-hydrolysis and subsequent sorption. Modeling binary Pu-CA and $Pu(OH)_x$ species in the presence of goethite using constants available in the literature[44,50] indicated a change from CA complexation to hydrolysis and binary Pu-goethite sorption near pH 7 (Figure A9). At pH 7, Pu sorption in the presence of $5 mg_C \cdot L^{-1}$ CA is slightly enhanced relative to the ligand-free system. This likely reflects the stabilization of Pu in the Pu(IV) oxidation state in the presence of organic matter, as trace amounts of oxidation to Pu(V)

in the absence of a complexing ligand would result in decreased Pu sorption (Figure 3.4, green dots).

Compared to the CA-Pu-goethite system, the behavior of Pu in the presence of DFOB is relatively straightforward. DFOB significantly reduced Pu sorption to goethite across the entire pH range studied. Strong DFOB-Pu(IV) complexation and marginal DFOB sorption kept Pu(IV) bound to DFOB without the prospect of ternary complex formation involving the goethite surface. It must be noted that in the DFOB systems, mesylate is present in equimolar quantities due to the DFOB mesylate salt reagent. While three-coordinate chelation effects, demonstrated by reported[43,51] log K values > 10^{30}, make Pu(IV)-DFOB complexes the most probable aqueous Pu species, stabilization of aqueous Pu could be promoted by Pu-mesylate complexes as well.

Fulvic acid decreased Pu sorption at pH 5, 7, and 9 due to strong Pu complexation. Nevertheless, slight increases in sorption at pH 9, relative to pH 5 or 7, may reflect Pu hydrolysis products and the subsequent binary $Pu(OH)_x$-goethite sorption. At pH 3, Pu sorption in the presence of FA was enhanced (Figure 3.4), but to a lesser extent than with CA, indicating either higher stability of Pu-FA aqueous complexes relative to Pu-CA and/or weaker sorption of FA to goethite leading to less favorable conditions for ternary complex formation; less FA was sorbed at pH 3 than CA (Figure 3.2).

HA also decreased Pu sorption at pH 5, 7, and 9. At pH 3 however, HA led to greater Pu sorption than FA did. Assuming Pu removal was entirely due to goethite sorption, the sorbed Pu concentrations were 1.86×10^{-4} and 1.56×10^{-3} $mol\cdot g^{-1}$ for the 5 and 50 $mg_C\cdot L^{-1}$

experiments, respectively at pH 3. However, sorption may be “apparent” due to the tendency of HA to aggregate, particularly at low pH.

To study the effect of HA aggregation on Pu removal from solution, a similar batch sorption study was performed with 6 $mg_C \cdot L^{-1}$ and 64 $mg_C \cdot L^{-1}$ HA and in the absence of goethite (Figure 3.5).

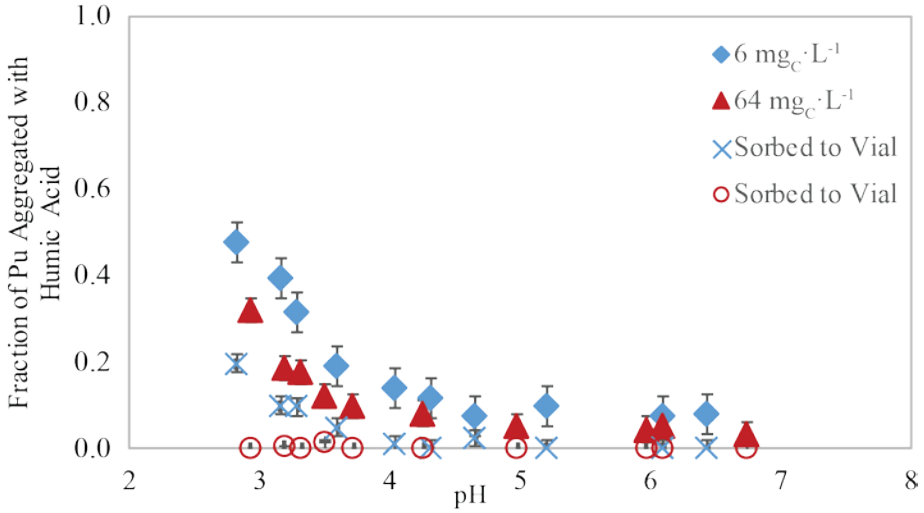

Figure 3.5. Pu (10^{-10} M) removal by HA aggregation in the presence of 6 $mg_C \cdot L^{-1}$ (blue diamonds) and 64 $mg_C \cdot L^{-1}$ (red triangles) HA in 0.01 M NaCl; fraction of Pu sorbed to vial wall indicated by “×” and “○” symbols, respectively. Error bars calculated from counting statistics.

At low pH values, Pu was removed from solution by both 6 mgC·L-1 and 64 mgC·L-1 HA (in the absence of goethite). Pu removal at low pH was likely due to HA aggregation and Pu sorption to the aggregate or sequestration within the aggregate. Lower concentrations of HA however, also made Pu less resistant to vial sorption at pH < 4. Dynamic light scattering verified a strong correlation between average HA aggregate size

and pH (Figure 3.6, left), demonstrating that the hydrophobic driven precipitation of HA at low pH is a gradual process. Meanwhile zeta potential measurements (Figure 3.6, right) revealed greater instability of the particles present in 6 mgC·L-1 systems than 46 mgC·L-1, which resulted in greater Pu removal at lower HA concentrations. Sorption data in the presence of goethite and HA must therefore be interpreted cautiously, particularly at low pH, as a significant fraction of Pu can be sequestered by intrinsic HA colloids.

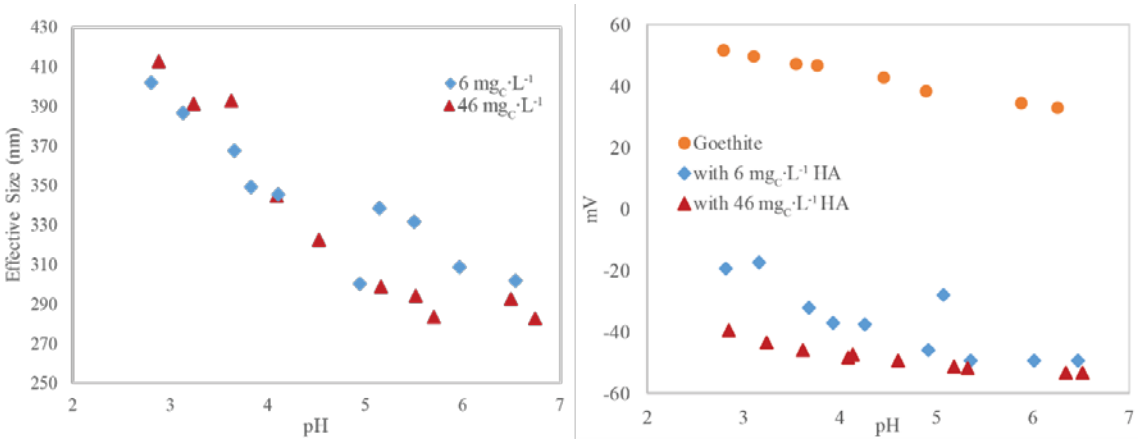

Figure 3.6. HA particle effective diameter with respect to pH (left); zeta potential in goethite suspensions (0.1g·L^{-1}) in the absence and presence of 6 mg_C·L^{-1} and 46 mg_C·L^{-1} HA.

Thermodynamic Modeling

Modeling of the binary Pu-goethite system followed that of Wang *et al.*[52], in which a Diffuse Layer Model (DLM) was used to simulate adsorption behavior. The same goethite surface charge reactions from Wang *et al.*[52] were used to account for the surface charge dependence on pH (Table S1), which agree with the goethite pzc measurements from this study (pzc = 8.3; Figure A14). The same surface site density (2.31 × 10^{18}

sites·m^{-2}) was also used. The binary Pu-goethite system was modeled using two surface species: $FeOPu^{3+}$ (logβ = 17.05) and $FeOPu(OH)_3$ (logβ = -0.54). Traditional surface complexation modeling (SCM) was problematic for modeling the ternary systems presented here. The resolution of the dataset, particularly at low pH where ternary complexes were expected, did not warrant detailed SCM. Therefore, to evaluate the effect of NOM on Pu(IV) sorption to goethite, total Pu(IV) interactions with each NOM were modeled by aqueous speciation calculations while the formation of ternary complexes or aggregates was determined empirically. This hybrid approach allowed interrogation of the data, without the false impression of true SCM. To model the ternary systems, the speciation of Pu in solution was calculated using complexation constants from literature for the CA[44], DFOB[43], and HA[28], experiments (Pu(IV)-FA complexation constants are not readily available). Pu binary goethite sorption constants for the NOM-free case from this study were used. NOM sorption was approximated empirically by fitting NOM sorption data to a line, and therefore, was only valid within the bounds of the empirical data. Ternary Pu-NOM sorption was then estimated by assuming that the sorption of free NOM and complexed Pu-NOM was equivalent (Equation 2).

$$\frac{[PuNOM]_{SORBED}}{[PuNOM]_{TOTAL}} \approx \frac{[NOM]_{SORBED}}{[NOM]_{TOTAL}} \quad \text{Equation 2.}$$

From this assumption, we can estimate the partitioning of Pu between the aqueous and solid phases by Equation 3. It should be noted that this model does not account for the preferential formation of ternary complexes. As a result, model underestimates of Pu sorption in the ternary sorption data are indicative of preferential formation of ternary complexes, as described below.

$$K_a(L \cdot m^{-2}) = \frac{[Pu]_{SORBED(Binary)} + \frac{[NOM]_{SORBED}}{[NOM]_{TOTAL}}[PuNOM]_{TOTAL}}{[Pufree]_{aq} + \frac{[NOM]_{aq}}{[NOM]_{TOTAL}}[PuNOM]_{TOTAL}} \times \frac{1}{[SS]} \times \frac{1}{SA}$$

Equation 3.

Modeled Pu K_a in the presence of 5 $mg_C \cdot L^{-1}$ and 50 $mg_C \cdot L^{-1}$ CA, DFOB, and HA are given in Figure 3.4. The CA ternary model agreed well with the observed data at pH 5 and 7 and it successfully captured the transition from ternary sorption species to aqueous complex to sorbed hydrolyzed species; as well as the dependence on CA concentration. At pH 3 modeling predicted less Pu sorption than was observed and the Pu:CA ratio on the surface exceeded the Pu:CA ratio in solution, by more than could be accounted for by binary Pu sorption. This corroborates the favorability of a ternary complex at pH 3. Less Pu sorption was observed than was predicted at high pH in the presence of 50 $mg_C \cdot L^{-1}$ CA, which suggests Pu-CA complexes persist to higher pH than the literature values would suggest. It is worth noting that there are no Pu(IV)-citrate values currently endorsed by the Nuclear Energy Agency (NEA), and that uncertainty in Pu hydrolysis constants makes speciation models at pH 7 and 9 particularly speculative. Model predictions in the presence of DFOB agreed well with observed data. Both the model and data indicated little or no ternary complex formation. In fact, the Pu:DFOB ratio on the surface was less than the Pu:DFOB ratio in solution, suggesting that sorbed DFOB is less able to complex Pu than free DFOB. The HA ternary model is truncated at pH 7 due to the arbitrary pKa = 7 complexation site used to fit the $Pu(OH)_2(HA)^+$ species.[28] The model consistently under predicted Pu removal by sorption or aggregation, signifying that HA sorption and aggregation are biased towards Pu inclusion (the removed Pu:HA ratio

exceeded that of free Pu:HA). Pu(IV)-FA aqueous complexation constants are not readily available. When HA complexation constants were used to predict FA behavior however, model predictions were within an order of magnitude of measured data between pH 3-7. This is consistent with previous studies,[53,54] suggesting that HA and FA metal complexation constants do not differ substantially.

Comparing the four different NOM species used in this work provides insight into how NOM influences Pu migration in the environment. CA and FA increased Pu sorption to goethite at pH 3, likely through ternary complex formation, while HA also does so through aggregation which incorporates Pu. At more environmentally relevant pH (5-9), all ligands decreased Pu sorption to goethite relative to a ligand free system, likely by forming soluble complexes. The observed decrease in Pu sorption in this pH range with respect to NOM type (50 $mg_C \cdot L^{-1}$) was CA < HA < FA < DFOB. NOM sorption and its influence on Pu sorption appears to be primarily controlled by 1) the strength of the Pu-NOM complex and 2) the affinity of NOM for goethite. These two factors influence formation of aqueous Pu-NOM and ternary goethite-NOM-Pu complexes, respectively. Pu sorption tends to increase from pH 7 to 9. This is likely due to the greater stability of Pu(IV) hydrolysis species over Pu-NOM complexes at high pH and the formation of hydrolyzed binary Pu-goethite surface complexes. NOM–goethite surface interactions were characterized by ATR-FTIR, and provide clear evidence of CA and FA binding to goethite at low pH. This provides a strong indication of ternary surface complex formation. Spectroscopic and batch sorption studies suggest that HA behaves more like

an aggregated particle at pH 3. ATR-FTIR experiments saw no indication of DFOB sorption to goethite, which was corroborated by bulk sorption experiments.

The presence of NOM in hydrogeological systems can have a profound effect on Pu speciation, solubility, and transport. This study demonstrates that NOM can influence Pu sorption through complexation with dissolved NOM, NOM aggregation that sequesters Pu, and through ternary complex formation on mineral surfaces. At environmentally relevant pH values, formation of Pu-NOM aqueous complexes tends to enhance the mobility of Pu. These results are consistent with field observations at the NNSS and RFETS, which suggest enhancement of Pu mobility as a result of Pu interaction with mobile NOM components in groundwater and surface waters.

References

(1) Kersting. Plutonium Transport in the Environment. *Inorg. Chem.* **2013**, *52* (7), 3533–3546.

(2) Cantrell, K. J. Transuranic Contamination in Sediment and Groundwater at the US DOE Hanford Site. *Pac. Nortwet Natl. Lab.* **2009**.

(3) Carlton, W.; Evans, A.; Murphy, C. J.; Pinder, J.; Strom, R. Assessment of Plutonium in the Savannah River Site Environment (U). *WSRC-92-879 Rev 1* **1992**.

(4) Ackland, L. *Making a real killing: Rocky Flats and the nuclear West*, 1st ed.; University of New Mexico Press: Albuquerque, 1999.

(5) Santschi, P. H.; Roberts, K. A.; Guo, L. Organic nature of colloidal actinides transported in surface water environments. *Environ. Sci. Technol.* **2002**, *36* (17), 3711–3719.

(6) UNSCEAR. *Sources and Effects of Ionizing Radiation*; 2000.

(7) Kersting, A. B.; Efurd, D. W.; Finnegan, D..; Rokop, D. J.; Smith, D. K.; Thompson, J. L. Migration of plutonium in ground water at the Nevada Test Site. *Nature* **1999**, *397*, 56–59.

(8) Kersting, A. B.; Zavarin, M. Colloid-Facilitated Transport of Plutonium at the Nevada Test Site, NV, USA. In *Actinide Nanoparticle Research*; Springer: Berlin; London, 2010; pp 399–412.

(9) *Actinide nanoparticle research*; Kalmykov, S. N., Denecke, M. A., Eds.; Springer: Berlin; London, 2010.

(10) Sanchez, A. L.; Murray, J. W.; Sibley, T. H. The adsorption of plutonium IV and V on goethite. *Geochim. Cosmochim. Acta* **1985**, *49*, 2297–2307.

(11) Simpkins, L. Influence of Natural Organic Matter on Plutonium Sorption to Gibbsite, Clemson University, 2011.

(12) Romanchuk, A. Y.; Kalmykov, S. N.; Aliev, R. A. Plutonium sorption onto hematite colloids at femto- and nanomolar concentrations. *Radiochim. Acta* **2011**, *99* (3), 137–144.

(13) Powell, B. A.; Kersting, A. B.; Zavarin, M.; Zhao, P. Development of a Composite Non-Electrostatic Surface Complexation Model Describing Plutonium Sorption to Aluminosilicates. *Lawrence Livermore Natl. Lab. LLNL-TR-408276* **2008**.

(14) Keeney-Kennicutt, W. L.; Morse, J. W. The redox chemistry of $Pu(V)O_2^+$ interaction with common mineral surfaces in dilute solutions and seawater. *Geochim. Cosmochim. Acta* **1985**, *49*, 2577–2588.

(15) Powell, B. A.; Fjeld, R. A.; Kaplan, D. I.; Coates, J. T.; Serkiz, S. M. Pu $(V)O_2^+$ adsorption and reduction by synthetic magnetite (Fe3O4). *Environ. Sci. Technol.* **2004**, *38* (22), 6016–6024.

(16) Kirsch, R.; Fellhauer, D.; Altmaier, M.; Neck, V.; Rossberg, A.; Fanghänel, T.; Charlet, L.; Scheinost, A. C. Oxidation State and Local Structure of Plutonium Reacted with Magnetite, Mackinawite, and Chukanovite. *Environ. Sci. Technol.* **2011**, *45* (17), 7267–7274.

(17) Novikov, A. P.; Kalmykov, S. N.; Utsunomiya, S.; Ewing, R. C.; Horreard, F.; Merkulov, A.; Clark, S. B.; Tkachev, V. V.; Myasoedov, B. F. Colloid transport of plutonium in the far-field of the Mayak Production Association, Russia. *Science* **2006**, *314* (5799), 638–641.

(18) Zhao, P.; Zavarin, M.; Leif, R. N.; Powell, B. A.; Singleton, M. J.; Lindvall, R. E.; Kersting, A. B. Mobilization of actinides by dissolved organic compounds at the Nevada Test Site. *Appl. Geochem.* **2011**, *26* (3), 308–318.

(19) Bryan, N. D.; Abrahamsen, L.; Evans, N.; Warwick, P.; Buckau, G.; Weng, L.; Van Riemsdijk, W. H. The effects of humic substances on the transport of radionuclides: Recent improvements in the prediction of behaviour and the understanding of mechanisms. *Appl. Geochem.* **2012**, *27* (2), 378–389.

(20) Gu, B.; Schmitt, J.; Chen, Z.; Liang, L.; McCarthy, J. F. Adsorption and desorption of natural organic matter on iron oxide: mechanisms and models. *Environ. Sci. Technol.* **1994**, *28* (1), 38–46.

(21) Weng; Van Riemsdijk, W. H.; Koopal, L. K.; Hiemstra, T. Adsorption of Humic Substances on Goethite: Comparison between Humic Acids and Fulvic Acids †. *Environ. Sci. Technol.* **2006**, *40* (24), 7494–7500.

(22) Ghosh, S.; Wang, Z.-Y.; Kang, S.; Bhowmik, P. C.; Xing, B. S. Sorption and fractionation of a peat derived humic acid by kaolinite, montmorillonite, and goethite. *Pedosphere* **2009**, *19* (1), 21–30.

(23) Kang, S.; Xing, B. Humic Acid Fractionation upon Sequential Adsorption onto Goethite. *Langmuir* **2008**, *24* (6), 2525–2531.

(24) Wang, L.; Chin, Y.-P.; Traina, S. J. Adsorption of (poly) maleic acid and an aquatic fulvic acid by geothite. *Geochim. Cosmochim. Acta* **1997**, *61* (24), 5313–5324.

(25) Weng, L.; Van Riemsdijk, W. H.; Hiemstra, T. Adsorption of humic acids onto goethite: Effects of molar mass, pH and ionic strength. *J. Colloid Interface Sci.* **2007**, *314* (1), 107–118.

(26) Tinnacher, R. M.; Begg, J. D.; Mason, H.; Ranville, J.; Powell, B. A.; Wong, J. C.; Kersting, A. B.; Zavarin, M. Effect of Fulvic Acid Surface Coatings on Plutonium Sorption and Desorption Kinetics on Goethite. *Environ. Sci. Technol.* **2015**, *49* (5), 2776–2785.

(27) Buda, R.; Banik, N. L.; Kratz, J. V.; Trautmann, N. Studies of the ternary systems humic substances – kaolinite – Pu(III) and Pu(IV). *Radiochim. Acta* **2008**, *96* (9-11).

(28) Zimmerman, T.; Zavarin, M.; Powell, B. A. Influence of humic acid on plutonium sorption to gibbsite: Determination of Pu-humic acid complexation constants and ternary sorption studies. *Radiochim. Acta* **2014**, *102* (7).

(29) Stockdale, A.; Bryan, N. D. The influence of natural organic matter on radionuclide mobility under conditions relevant to cementitious disposal of radioactive wastes: A review of direct evidence. *Earth-Sci. Rev.* **2013**, *121*, 1–17.

(30) Tinnacher, R. M.; Honeyman, B. D. A New Method to Radiolabel Natural Organic Matter by Chemical Reduction with Tritiated Sodium Borohydride. *Environ. Sci. Technol.* **2007**, *41* (19), 6776–6782.

(31) Powell, B. A.; Duff, M. C.; Kaplan, D. I.; Fjeld, R. A.; Newville, M.; Hunter, D. B.; Bertsch, P. M.; Coates, J. T.; Eng, P.; Rivers, M. L. Plutonium oxidation and subsequent reduction by Mn (IV) minerals in Yucca Mountain tuff. *Environ. Sci. Technol.* **2006**, *40* (11), 3508–3514.

(32) Conroy, N. A.; Wylie, E. M.; Powell, B. A. A Novel Method for Tracer Concentration Plutonium(V) Solution Preparation. *Anal. Chem.* **2016**, *88* (8), 4196–4199.

(33) Dardenne, K.; Seibert, A.; Denecke, M. A.; Marquardt, C. M. Plutonium(III, IV, VI) speciation in Gorleben groundwater using XAFS. *Radiochim. Acta* **2009**, *97*, 91-97.

(34) Choppin, G. R. Actinide speciation in the environment. *Radiochim. Acta* **2003**, *91*, 645–649.

(35) Andre, C.; Choppin, G.. Reduction of Pu(V) by humic acid. *Radiochim. Acta* **2000**, *88*, 613–616.

(36) Marquardt, C. M.; Seibert, A.; Artinger, R.; Denecke, M. A.; Kuczewski, B.; Schild, D.; Fanghanel, T. The redox behaviour of plutonium in humic rich groundwater. *Radiochim. Acta* **2004**, *92*, 617–623.

(37) Kaplan, D. I.; Powell, B. A.; Demirkanli, D. I.; Fjeld, R. A.; Molz, F. J.; Serkiz, S. M.; Coates, J. T. Influence of oxidation states on plutonium mobility during long-term transport through an unsaturated subsurface environment. *Environ. Sci. Technol.* **2004**, *38* (19), 5053–5058.

(38) Currie, L. A. Limits for qualitative detection and quantitative determination. Application to radiochemistry. *Anal. Chem.* **1968**, *40* (3), 586–593.

(39) Tunesi, S.; Anderson, M. A. Surface effects in photochemistry: an in situ cylindrical internal reflection-Fourier transform infrared investigation of the effect of ring substituents on chemisorption onto titania ceramic membranes. *Langmuir* **1992**, *8* (2), 487–495.

(40) Tejedor-Tejedor, M. I.; Yost, E. C.; Anderson, M. A. Characterization of benzoic and phenolic complexes at the goethite/aqueous solution interface using cylindrical internal reflection Fourier transform infrared spectroscopy. Part 1. Methodology. *Langmuir* **1990**, *6* (5), 979–987.

(41) Yost, E. C.; Tejedor-Tejedor, M. I.; Anderson, M. A. In situ CIR-FTIR characterization of salicylate complexes at the goethite/aqueous solution interface. *Environ. Sci. Technol.* **1990**, *24* (6), 822–828.

(42) Nakamoto, K. *Infrared and Raman spectra of inorganic and coordination compounds*, 6th ed.; Wiley: Hoboken, N.J, 2009.

(43) Boukhalfa, H.; Reilly, S. D.; Neu, M. P. Complexation of Pu(IV) with the Natural Siderophore Desferrioxamine B and the Redox Properties of Pu(IV)(siderophore) Complexes. *Inorg. Chem.* **2007**, *46* (3), 1018–1026.

(44) Chemical thermodynamics of compounds and complexes of U, Np, Pu, Am, Tc, Se, Ni, and Zr with selected organic ligands; Hummel, W., Mompean, F. J., Eds.; Chemical thermodynamics; Elsevier: Amsterdam, **2005**.

(45) Givan, A.; Loewenschuss, A.; Nielsen, C. J. Infrared spectrum and ab initio calculations of matrix isolated methanesulfonic acid species and its 1:1 water complex. *J. Mol. Struct.* **2005**, *748* (1-3), 77–90.

(46) Guo, Z.; Li, Y.; Wu, W. Sorption of U(VI) on goethite: Effects of pH, ionic strength, phosphate, carbonate and fulvic acid. *Appl. Radiat. Isot.* **2009**, *67* (6), 996–1000.

(47) Fu, H.; Quan, X. Complexes of fulvic acid on the surface of hematite, goethite, and akaganeite: FTIR observation. *Chemosphere* **2006**, *63* (3), 403–410.

(48) Lefevre, G.; Precanin, T.; Lutzenkirchen, J. Attenuated Total Reflection - Infrared Spectroscopy Applied to the Study of Mineral - Aqueous Electrolyte Solution Interfaces: A General Overview and a Case Study. In *Infrared spectroscopy - materials science, engineering and technology*; Theophanides, T. M., Ed.; InTech: Rijeka, **2012**.

(49) Petteys, M. P.; Schimpf, M. E. Characterization of hematite and its interaction with humic material using flow field-flow fractionation. *J. Chromatogr. A* **1998**, *816* (2), 145–158.

(50) Delany, J.; Lundeen, S. R. The LLNL Thermochemical Database; UCRL-21658. Lawrence Livermore National Laboratory **1990**.

(51) Chemical thermodynamics of compounds and complexes of U, Np, Pu, Am, Tc, Se, Ni, and Zr with selected organic ligands; Hummel, W., Mompean, F. J., Eds.; Chemical thermodynamics; Elsevier: Amsterdam, **2005**.

(52) Wang, P.; Anderko, A.; Turner, D. R. Thermodynamic Modeling of the Adsorption of Radionuclides on Selected Minerals. I: Cations. *Ind. Eng. Chem. Res.* **2001**, *40* (20), 4428–4443.

(53) Reiller, P.; Moulin, V.; Casanova, F.; Dautel, C. Retention behaviour of humic substances onto mineral surfaces and consequences upon thorium (IV) mobility: case of iron oxides. Appl. Geochem. 2002, 17 (12), 1551–1562.

(54) Nash, K.; Choppin, G. Interaction of Humic and Fulvic Acids with Th(IV). J. Inorg. Nucl. Chem. 1980, 42, 1045–1050.

Acknowledgement

This work was supported by the Subsurface Biogeochemical Research Program of the U.S. Department of Energy's Office of Biological and Environmental Research.

CHAPTER FOUR

TERNARY MINERAL-CITRATE-PLUTONIUM(IV) SPECIES ON GOETHITE AND GIBBSITE

Nathan A. Conroy[1], Mavrik Zavarin[2], Annie B. Kersting[2], Brian A. Powell[1]

[1]Department of Environmental Engineering & Earth Sciences,

Clemson University, Clemson, South Carolina, 29634

[2]Glenn T. Seaborg Institute, Physical and Life Scie nces Directorate, Lawrence

Livermore National Laboratory

7000 East Avenue, Livermore, California, 94550

Abstract

Plutonium sorption to gibbsite and goethite was studied in the presence of 10^{-6} – 10^{-4} M citric acid and diffuse-layer surface complexation models were used to describe plutonium sorption to both minerals. Ternary mineral-citrate-Pu(IV) surface complexes were necessary to describe plutonium sorption to both minerals from pH 2 – 4. The ternary species $\equiv AlCitPu^{2+}$ (log K = 31.0) was fit to the gibbsite data and the ternary species $\equiv FeOPu(OH)_2Cit^{2-}$ was fit to the goethite system. The stoichiometries of the ternary species suggested type A and type B sorption for the gibbsite and goethite surfaces, respectively. Development of the ternary models also required modeling citrate sorption to both minerals, which was accomplished using a ligand exchange species, $\equiv Fe(OOC)\text{-}C_3H_5O(COOH)_2^0$, below pH 4 and a 3:1 surface site:citrate species, $(\equiv FeOH\cdots OOC)_3^{-}$

$C_3H_5O^{3-}$, at intermediate pH. Under surface-site saturated conditions (10^{-4} M citrate), citrate sorption could be fit below pH 4 using the same ligand exchange reaction, but model fits were inadequate above pH 4. In addition to surface species, aqueous Pu-citrate binding constants at alkaline pH are proposed. Experimental conditions were maintained such that the 4+ oxidation state of plutonium would dominate under all experimental conditions, and lanthanum fluoride co-precipitation based oxidation state analysis was preformed to confirm the oxidation state wherever possible. The results demonstrate that ternary surface complexes are necessary to model Pu sorption to both goethite and gibbsite below pH 4.

Introduction

Plutonium (Pu) has been introduced into the environment from multiple sources including nuclear weapons production and testing, nuclear power plant accidents, reprocessing plant discharges, and accidents resulting in unexpected satellite reentry. Trace Pu poses minimal risk to human or environmental health, and the widely distributed Pu fallout from weapons testing or satellite accidents is not generally considered to be a major health concern. Contrarily, the substantially higher Pu concentrations found at non-public sites, where Pu weapons were either tested or their materials produced, could pose risks if their propensity for transport are not adequately understood and mitigated.

The mobility of Pu in a subsurface depends on the chemical composition of its source-term and the biogeochemical conditions it encounters that may impact its chemical speciation. Due to low solubility and strong sorption of Pu(IV) at environmentally relevant pH, Pu is not expected to be highly-mobile under field conditions. Further, reduction of the more mobile forms of Pu, Pu(V) and Pu(VI), has been observed on numerous mineral surfaces, including those considered oxidizing.[1–6] Despite the anticipated lack of mobility,

long-range transport of Pu has been observed at both the Nevada National Security Site (NNSS), in the United States, and the Mayak Production Association (MPA), in Russia. At the NNSS, Kersting *et al.*[7] measured Pu 1.3 km from its source, and determined that > 99 % of that mobile Pu was associated with inorganic colloids, primarily clays and zeolites. At the MPA, Novikov *et al.*[8] measured consistent Pu_{aq}:$Pu_{colloid}$ ratios within 2.15 km of the source, but a greater $Pu_{colloid}$ fraction as distance exceeded 2.5 km. This suggests that colloid-bound Pu was the more mobile form. At the MPA, Pu was measured up to 4 km from the source, Lake Karachai.[8]

The effect of natural organic matter (NOM) on Pu speciation has been well recognized by previous studies, and has been shown to be both direct and indirect. Dissolved NOM can form soluble complexes with Pu,[9–13] and intrinsic NOM aggregates have been shown to incorporate Pu,[14,15] either by adsorption or by absorption. Additionally, NOM coatings can increase Pu affinity for mineral surfaces, such as inorganic colloids or the host rock.[14,16] Indirectly, NOM may control Pu redox chemistry, which has profound effects on Pu hydrolysis, speciation, and sorption properties. Also indirectly, NOM coatings can affect the fate of inorganic colloids that may have associated Pu. Coatings that increase the absolute surface potential can stabilize colloids, while surface-charge neutralization can promote aggregation and destabilize colloids.

Citric acid is a tricarboxylic prevalent NOM known to form relatively strong complexes with Pu(IV).[17] The known chemical structure, solubility, and acid-base chemistry of citrate make it an appealing proxy for more complex NOMs and their effect on radionuclide complexation and migration. In addition to its use as a NOM analog, citrate itself is a

common organic ligand introduced to groundwater by microorganisms and by root exudation, as well as from the decomposition of organisms and soil organic matter. Furthermore, citrate has been introduced into radioactive wastes from ammonium citrate containing decontaminating agents, although the longevity of anthropogenic citrate is unclear.[18,19] Despite the multifaceted need to understand Pu-citrate complexation behavior at environmentally relevant conditions, relatively little research has been done. Pu(IV)-citrate complexation values vary widely in the literature and the Nuclear Energy Administration (NEA) does not endorse any values.[17]

In addition to being an aqueous Pu complexant, NOMs have been shown to promote Pu sorption through ternary surface complexes. Ternary Pu-NOM-mineral surface complexes have been studied with pure mineral phases such as kaolinite[20], gibbsite[21], silica[22], and goethite[14,16]. Conroy *et al.*[14] produced a hybrid model to predict Pu sorption to goethite in the presence of citrate, desferoxamine B, and Leonardite humic acid. The hybrid model fit NOM sorption empirically and input the results into a diffuse-layer surface complexation model (DLM), which included reactions from the literature describing Pu complexation with the ligands present in each system and binary sorption with the mineral. The hybrid approach inherently made the assumption that Pu:ligand ratios would be the same in the bulk solution as they would be on the surface. However, Pu sorption was underestimated at low pH, the region of greatest NOM sorption, and suggested that ternary complexes were thermodynamically preferential. Unfortunately, the data from the previous study lacked the necessary resolution to develop a true ternary DLM. Hence, this study seeks to produce that model. In addition, it is apparent that Pu(IV)-citrate complexation in aqueous solutions

and at alkaline pH is lacking in the literature. In order to propose Pu-citrate binding constants at alkaline pH, competitive Pu(IV) binding experiments between citrate and a commercially available solid resin surface were conducted from pH 4 – 10.

Materials and Methods

Citrate Stock Preparations

All experiments were performed in background 0.01 M NaCl (BDH Lot # 0094C504) prepared in H_2O (18.2 MΩ). Citric acid monohydrate (BDH Lot # 95097) solutions were prepared in 0.01 M NaCl at citrate concentrations of 10^{-6} and 10^{-4} M. For the resin sorption experiments, the citrate solutions were prepared in 0.01 M NaCl previously degassed in a vacuum chamber and transferred to a 100 % nitrogen atmosphere glovebox. These solutions were then spiked with 52 µL of a 1.4×10^5 Bq·mL^{-1} ^{14}C-citrate solution in water (reconstituted from 50 – 60 mCi·mmol^{-1} ^{14}C-citrate solution from American Radiolabeled Chemicals Inc.). For mineral batch sorption experiments, the citrate solutions were spiked with 310 µL of the 1.4×10^5 Bq·mL^{-1} ^{14}C-citrate solution. It should be noted that the ^{14}C spike consisted of only 2.2×10^{-8} - 1.3×10^{-7} moles of citrate, and therefore, did not significantly alter the total citrate concentration.

Plutonium Stock Preparations

Pu(IV) solutions were prepared by pipetting a small volume of 2.75×10^6 Bq·L^{-1} ^{238}Pu, in 0.1 M HCl, into a Teflon® vial and evaporating the liquid off over low heat. The Pu was then reconstituted in a volume of the 10^{-6} or 10^{-4} M citrate solutions described previously. This evaporative step has been shown to produce high purity Pu(IV) solutions at low Pu concentrations.[6] Final Pu concentrations ranged from 1.1×10^{-10} M - 1.2×10^{-10} M in citrate-containing experiments and 5.7×10^{-11} M - 6.3×10^{-11} M in citrate-free experiments.

Plutonium solutions for the resin sorption experiments were reconstituted in a 100 % N_2 atmosphere glovebox. Oxidation state analysis (OSA) was performed on the citrate-free Pu solution 10 minutes after the solution was prepared to confirm that Pu was in the 4+ oxidation state. Oxidation state analysis was preformed using a lanthanum fluoride (LaF_3) coprecipitation following the procedure described by Conroy *et al.*[23]. While the oxidation state of the Pu in the 10^{-4} M citrate experiments could not be determined by this method, previous studies indicate Pu(IV) will be the dominate oxidation state under the conditions of the experiments containing citrate.[24]

Mineral Suspensions

Gibbsite was purchased from Ward's Natural Science Establishment Inc. The average surface area was 1.9 $m^2 \cdot g^{-1}$ measured by N_2(g) adsorption (Quadrasorb SI surface area analyzer with QuadraWin™ v.5.02 software, Quantachrome Instruments). Goethite was synthesized using the procedure described by Schwertmann *et al.*[25] and confirmed by power X-ray diffraction (Bruker D8 X-ray diffractometer). The average surface area was 38.8 $m^2 \cdot g^{-1}$ measured by N_2(g) adsorption (Quadrasorb); and the point of zero charge (pzc) was 8.3, measured by mass titration (Figure C.1). Prior to use, both minerals were washed three-times in low carbon (< 2ppb) H_2O (18.2 MΩ) adjusted to pH 10; followed by H_2O adjusted to pH 3; followed by H_2O at pH 7. After washing, minerals were lyophilized and stored dry. Mineral suspensions were prepared by suspending 0.037 g of goethite and 1.83 g of gibbsite, each into 330 mL of the 10^{-6} or 10^{-4} M citrate solutions described previously. This resulted in stock mineral suspensions of 0.11 $g \cdot L^{-1}$ and 5.5 $g \cdot L^{-1}$ for goethite and gibbsite, respectively.

Mineral Batch Sorption Experiments

Samples were prepared by mixing 9 mL of citrate-mineral suspensions with 1 mL of citrate-plutonium solutions. Samples were promptly pH-adjusted to closely spaced pH values from 2 – 10 using small additions of 0.01 – 1 M HCl or 0.01 – 0.1 M NaOH. The pH of each sample was measured periodically and adjusted as necessary. Sampling occurred 4 weeks (28 days) and 6 weeks (52 days) after Pu and mineral suspensions were initially mixed. During each sampling event a 1.3 mL aliquot of each Pu-citrate-mineral suspension was removed and centrifuged (Beckman Coulter Allegra X22R) for 40 minutes at 8000 RPM (6596 RCF) using a Beckman 2402 rotor; this is calculated by Stokes' Law to remove particles greater than 70 nm. A 1 g sample of the supernatant was then mixed with 4.5 mL of Hi Safe 3 (Perkin Elmer) scintillation cocktail and counted 120 minutes for α and β activity using a Tri-Carb liquid scintillation analyzer. Surface area normalized solid-water distribution ratios (K_a) were determined using Equation 8.

Equation 8

$$K_a(L \cdot m^{-2}) = \frac{[C]_{total} - [C]_{aq}}{[C]_{aq}} \times \frac{1}{[SS]} \times \frac{1}{SA}$$

Where $[C]_{total}$ and $[C]_{aq}$ are the total and aqueous molar concentrations, respectively, of either Pu or citrate, [SS] is the concentration of mineral ($kg \cdot L^{-1}$), and SA is the average surface area of the mineral ($m^2 \cdot kg^{-1}$). Mineral sorption data are presented as surface area normalized distribution ratios to facilitate comparison with other studies and other minerals. Uncertainty, given in figures as error bars, was calculated by counting statistics.

Resin Sorption versus Citrate Complexation Experiments

Inside of a 100% N_2 atmosphere glovebox, 0.01 g of Analig-Pu02 (IBC) resin was suspended into 80 mL of degassed 10^{-4} M citrate solutions or 0.01 M NaCl. Four mL aliquots of these suspensions were transferred into 15 mL centrifuge tubes (polypropylene, VWR) and the pH was adjusted prior to adding a 1 mL spike from a Pu(IV) solution, either with 10^{-4} M citrate (with ^{14}C citrate tracer) or citrate-free. Samples were pH adjusted again and mixed end-over-end overnight in a 100 % N_2 atmosphere. During a sampling event, the resin was allowed to settle by gravity before a 1 g sample of the supernatant was mixed with 4 mL of Hi Safe 3 (Perkin Elmer) scintillation cocktail and counted 20 minutes for α and β activity using a Tri-Carb liquid scintillation analyzer. The pH of each supernatant was measured. In the 10^{-4} M citrate experiments a ^{14}C citrate tracer was used to confirm citrate did not sorb to the resin. Additionally, 0.5 g of supernatant was removed from each cirate-free suspension for LaF_3 OSA.

Thermodynamic Modeling

Thermodynamic models were generated using FIT4FD, a modified version of FITEQL, which allows for speciation database integration with surface complexation model fitting. Pu(IV) hydrolysis constants and citrate protonation constants from the NEA database were used.[17,26] Gibbsite and goethite surface acid-base chemistry values were taken from Karamalidis and Dzombak[27] and Dzombak and Morel,[28] respectively. All complexation constants from previous studies are reported in Table 4.2. Activity corrections were performed using the Davies equation. Surface complexation modeling approaches assume that complexation with the surface occurs at discrete binding sites analogous to

complexation in solution. Surface reactions include acid-base proton exchange, cation binding, and ligand exchange with surface hydroxyl groups. Analogous to reactions in solution, surface complexation equilibrium reactions abide by a mass conservation law, and therefore, the activities of aqueous reactants and of surface sites must be considered. In the diffuse-layer model, the surface/water interface is considered to consist of two layers of charge, a fixed surface layer (σ-plane) and a diffuse-layer (d-plane). Because there is no empirical difference between chemically sorbed and electrostatically sorbed species, sorption reaction constants will inherently incorporate a chemical term and a coulombic term, corresponding to the free energy of surface binding chemically or through electrostatic interactions.

Results and Discussion

Selection of Appropriate Pu(IV)-Citrate Binding Constants

Two previous studies that had modeled Pu(IV)-citrate thermodynamic behavior were identified, along with one additional study that modeled Th(IV)-citrate thermodynamic behavior, which served as a surrogate for Pu(IV). The experimental conditions and approaches of those studies varied considerably in pH, background electrolyte, and method. Those differences are summarized in Table 4.1 and the reactions and associated constants from those studies are reported in Table 4.2.

Table 4.1. Experimental Conditions of Previous Pu(IV)-Citrate Studies

Reference	[Pu]/[Th]	[Cit^{3-}]	Ionic Medium	pH	Method
Metivier & Guillaumont[29]	10^{-7} – 10^{-8}	10^{-1}	1 M $LiClO_4$	0 -7	solvent extraction
Nebel[17,30]	10^{-3}	10^{-1}	0.5 M $NaClO_4$	0.8 – 4	redoxpotential
Raymond *et al.*[31]	10^{-3}	10^{-3}-10^{-4}	0.1 M NaCl	1 - 6	titration

Selection of the most appropriate Pu(IV)-citrate binding constants under the experimental conditions of the current study was non-trivial. The values presented by Nebel were not chosen because those experiments were conducted under highly acidic conditions and subsequent modeling attempts demonstrated that Pu-citrate complexation at environmentally relevant pH was likely significantly over-predicted by those values (reported in SI). The pH range studied in the works by Metivier and Guillaumont and by Raymond *et al.* both overlap with the lower half of the pH range encompassed by this study. The ionic medium of the current study is most closely matched by that of Raymond *et al.*, however their reported values were based on Th(IV) complexation. Therefore, Pu speciation under the solution conditions of our experiments (no solids) was predicted from the Pu/Th-citrate binding constants of both Metivier and Guillaumont and Raymond *et al.* and compared. Those speciation models are shown in Figure 4.1. Although Raymond *et al.* studied Th(IV) complexation with citrate, Pu(IV) hydrolysis constants were used in these predictive models to better represent the experimental conditions of the current study.

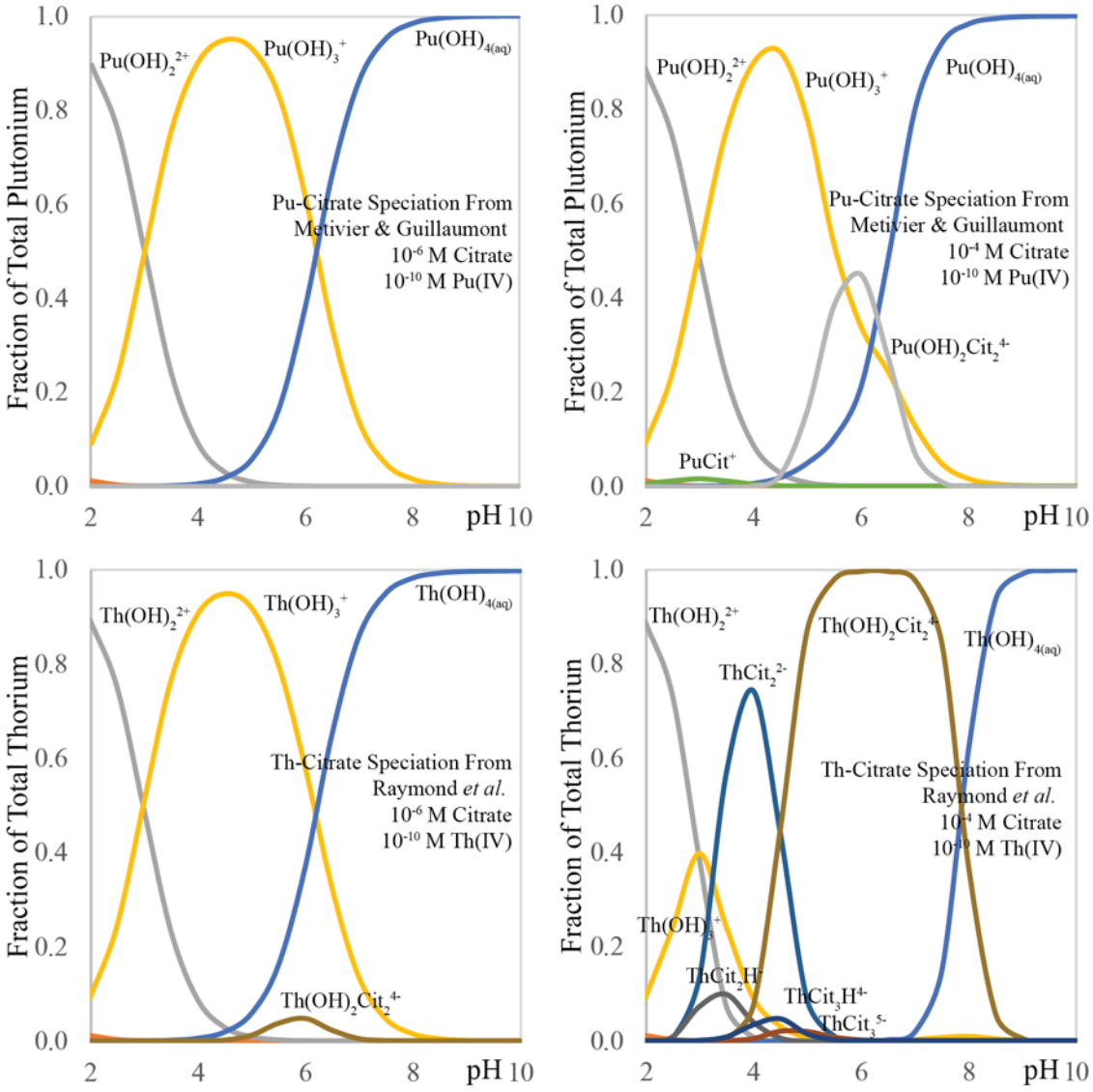

Figure 4.1. Pu/Th (10^{-10} M) speciation predicted by the Pu-citrate binding constants from Metivier and Guillaumont[29] (top) and Raymond *et al.*[31] (bottom) under the solution conditions of the current study; 0.01 M NaCl, 10^{-6} M citrate (left), and 10^{-4} M citrate (right).

Table 4.2. Thermodynamic Literature Values Used in Diffuse-Layer Modeling

Reaction	Log K	Ref.
$H_2O \leftrightarrow OH^- + H^+$	-13.997	
$Pu^{4+} + H_2O \leftrightarrow Pu(OH)^{3+}$	0.6 ± 0.2	NEA Database[26]
$Pu^{4+} + 2H_2O \leftrightarrow Pu(OH)_2^{2+}$	0.6 ± 0.3	
$Pu^{4+} + 3H_2O \leftrightarrow Pu(OH)_3^{+}$	-2.3 ± 0.4	
$Pu^{4+} + 4H_2O \leftrightarrow Pu(OH)_4^{0}$	-8.5 ± 0.5	
$Cit^{3-} + H^+ \leftrightarrow HCit^{2-}$	6.36	NEA Database[17]
$Cit^{3-} + 2H^+ \leftrightarrow H_2Cit^-$	11.14	
$Cit^{3-} + 3H^+ \leftrightarrow H_3Cit^0$	14.27	
$\equiv FeOH \leftrightarrow \equiv FeO + H$	8.93 ± 0.07	Dzombak & Morel[28]
$\equiv FeOH + H \leftrightarrow \equiv FeOH_2$	-7.29 ± 0.10	
$\equiv AlOH \leftrightarrow \equiv AlO + H$	11.18 ± 0.22	Karamalidis & Dzombak[27]
$\equiv AlOH + H \leftrightarrow \equiv AlOH_2$	-7.17 ± 0.19	
$Pu^{4+} + 2H^+ + Cit^{3-} \leftrightarrow PuH_2Cit^{3+}$	17.12	Metivier & Guillaumont[29]
$Pu^{4+} + H^+ + Cit^{3-} \leftrightarrow PuHCit^{2+}$	16.12	
$Pu^{4+} + Cit^{3-} \leftrightarrow PuCit^{+}$	14.37	
$Pu^{4+} + H_2O + Cit^{3-} \leftrightarrow Pu(OH)Cit^0 + H^+$	8.64	
$Pu^{4+} + 2H_2O + Cit^{3-} \leftrightarrow Pu(OH)_2Cit^{1-} + 2H^+$	4.42	
$Pu^{4+} + 5H^+ + 2Cit^{3-} \leftrightarrow Pu(H_3Cit)(H_2Cit)^{3+}$	32.54	
$Pu^{4+} + 4H^+ + 2Cit^{3-} \leftrightarrow Pu(H_2Cit)_2^{2+}$	32.04	
$Pu^{4+} + 2H^+ + 2Cit^{3-} \leftrightarrow Pu(HCit)_2^0$	27.01	
$Pu^{4+} + 2H_2O + 2Cit^{3-} \leftrightarrow Pu(OH)_2Cit_2^{4-} + 2H^+$	11.94	
$Pu^{4+} + 2Cit^{3-} \leftrightarrow Pu(Cit)_2^{2-}$	21.04	
$Pu^{4+} + Cit^{3-} \leftrightarrow PuCit^{+}$	15.5	Nebel[17,30]
$Pu^{4+} + 2Cit^{3-} \leftrightarrow Pu(Cit)_2^{2-}$	30.0	
$Th^{4+} + Cit^{3-} \leftrightarrow ThCit^{3+}$	14.13	Raymond *et al.*[31]
$Th^{4+} + 2Cit^{3-} \leftrightarrow Th(Cit)_2^{2-}$	24.29	
$Th^{4+} + H^+ + 2Cit^{3-} \leftrightarrow Th(HCit)(Cit)^{1-}$	27.21	
$Th^{4+} + 2H_2O + 2Cit^{3-} \leftrightarrow Th(OH)_2Cit_2^{4-} + 2H^+$	14.67	
$Th^{4+} + 3Cit^{3-} \leftrightarrow Th(Cit)_3^{5-}$	28.00	
$Th^{4+} + H^+ + 3Cit^{3-} \leftrightarrow Th(HCit)(Cit)_2^{4-}$	33.31	

The Metivier and Guillaumont reactions predicted 45 % of Pu at pH 6 would be associated with citrate in the 10^{-4} M experiments, and a very small amount (< 1 %) of Pu at pH 3 would be associated with citrate. Negligible Pu-citrate complexation was predicted by the Metivier and Guillaumont values in our 10^{-6} M citrate experiments. The Raymond *et al.* reactions predicted nearly all Pu would be associated with citrate from pH 4 – 7 in the 10^{-4} M experiments and a small, but not insignificant (~ 5 %), fraction of Pu would be associated with citrate at pH 6 in the 10^{-6} M experiments. Meanwhile, the data from the 10^{-4} M citrate experiments of this study indicated that Pu(IV)-citrate complexation must outcompete Pu hydrolysis at pH 6. Additionally, a significant decrease in Pu sorption to gibbsite and goethite was observed in the 10^{-4} M citrate experiments, when compared to the citrate-free or the 10^{-6} M citrate experiments (Figures 3.4 and 3.5). Only if the Pu(IV)-citrate complexes were considerably more thermodynamically favorable than Pu hydrolysis would we observe such a decrease in Pu sorption. For that reason, the Raymond *et al.* Pu-citrate binding constants were selected for use in the diffuse-layer models presented here. While this is the best means of modeling Pu-citrate complexation for the current study, there are fundamental limitations associated with assuming that Th-citrate binding will behave identically to Pu-citrate binding. The results of the same modeling exercises using the Metivier and Guillaumont constants are available in the supporting materials.

Determination of Pu(IV)-Mineral Binding Constants

Binary Pu(IV)-mineral surface complexation was re-modeled using data from previous studies that had utilized different mineral acid-base chemistry constants. The average surface areas of gibbsite and goethite were 1.9 $m^2 \cdot g^{-1}$ and 38.8 $m^2 \cdot g^{-1}$, respectively.

Available site densities for both minerals were estimated by assuming complete saturation of available surface sites by citrate in the 10^{-4} M citrate experiments. The lack of pH dependence on citrate sorption in the presence of 10^{-4} M citrate strongly suggests a site-saturation effect. Site densities of 1.2×10^{18} sites·m^{-2} and 2.3×10^{18} sites·m^{-2} were estimated by this method for gibbsite and goethite, respectively. The site density estimation for goethite wholly agree with values seen in the literature.[28,32–34] The site density estimated for gibbsite was low compared with literature recommendations. For example, a site density of 8×10^{18} sites·m^{-2} was recommended in the gibbsite surface complexation model review by Karamalidis and Dzombak.[27] Binary Pu(IV)-mineral sorption data was modeled using two surface species each. Surface reactions and their associated log K values are listed in Table 4.3, and pH dependent models are presented in Figure 4.2 as fraction sorbed (left) and surface area normalized K_a (right). Presenting sorption data as both fraction sorbed and distribution coefficient is crucial as poor model fits at the boundaries are easily concealed by fraction sorbed plots. Conversely, poor model fits are easily suppressed by distribution coefficient plots at moderate sorbed fractions (10 – 90 %).

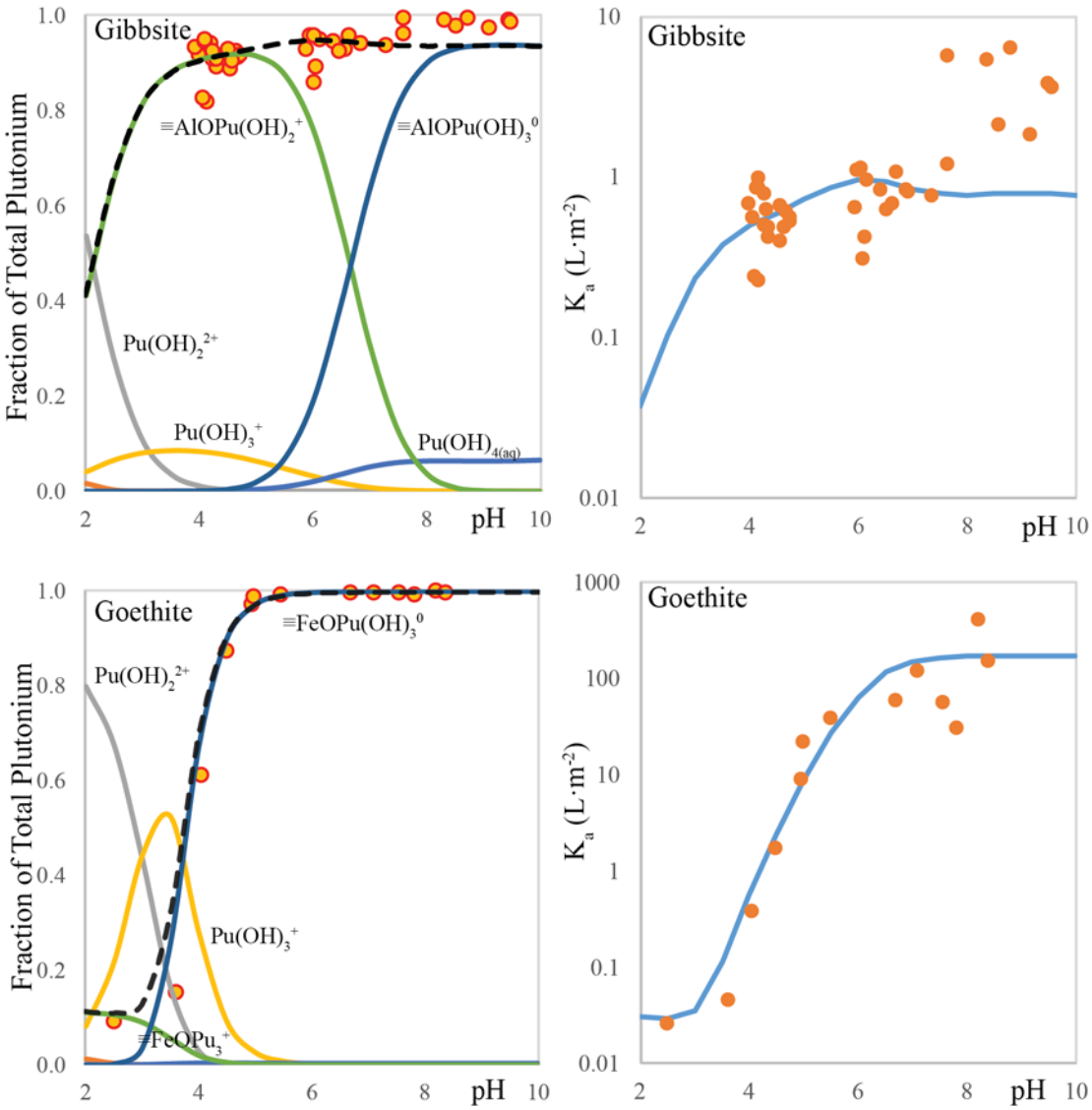

Figure 4.2. Binary Pu (10^{-10} M) sorption models in fraction sorbed (left) and surface area normalized distribution coefficent (right); 5.5 g·L^{-1} gibbsite (top) and 0.11 g·L^{-1} goethite (bottom). The total sorbed fraction is given as a fine-dashed black line.

Table 4.3. Binary Pu(IV) Sorption to Gibbsite & Goethite Species

Reactions	log K
$\equiv AlOH + Pu^{4+} + H_2O \leftrightarrow \equiv AlOPu(OH)^{2+} + 2H^+$	12.45
$\equiv AlOH + Pu^{4+} + 3H_2O \leftrightarrow \equiv AlOPu(OH)_3 + 4H^+$	-2.91
$\equiv FeOH + Pu^{4+} + \equiv FeOPu^{3+} + H^+$	19.19
$\equiv FeOH + Pu^{4+} + 3H_2O \equiv FeOPu(OH)_3 + 4H^+$	-0.73

The observed Pu^{4+} sorption to both solids is typical of cation sorption to metal oxide solids with pH-dependent surface charge.

Determination of Citrate-Mineral Binding Constants

Citrate surface complexation was modeled assuming all citrate sorbed as a binary species (no Pu). Under the conditions of these experiments, where citrate concentrations exceeded Pu concentrations by a factor of more than 10,000 and sorption fractions were relatively high, this was a good assumption. Citrate sorption to gibbsite and goethite was modeled using two citrate-mineral surface species each. Surface reactions, and associated log K values are listed in Table 4.4 and pH dependent models are presented in Figure 4.3.

The observed citrate sorption was typical of anion adsorption to a solid with pH-dependent surface charge, as well as numerous previous studies.[14,35–37] Citrate clearly forms strong complexes with both solids as sorption occurs at alkaline pH, where both the surface and the citrate are negatively charged. Under unsaturated conditions (10^{-6} M citrate), the species used to fit the citrate sorption data consisted of a 1:1 surface:citrate ligand exchange reaction below pH 4 and a 3:1 surface:citrate species, without explicit proton exchange, at intermediate pH. The 1:1 species was analogous to a single carboxylic acid of citrate interacting with a single surface site, and the remaining citrate carboxylic groups being protonated. Meanwhile, the fit of the 3:1 species implies a Van der Waals

interaction at intermediate pH, with each carboxylic acid of citrate weakly interacting with a surface site, the combined strength of the weak interactions resulting in the observed sorption. While some models would designate this as an outer-sphere complex, the two-layer model does not distinguish between inner and outer-sphere complexes. Under unsaturated conditions (10^{-6} M citrate), models of citrate sorption were satisfactory from pH 2 to pH 6 or 8 for the gibbsite and goethite experiments, respectively. Complications associated with modeling citrate sorption at alkaline pH are discussed shortly under saturated conditions. Due to poor fit of 10^{-6} M citrate sorption models above pH 6 and 8, model lines throughout this study are presented as a dashed line above those pH values for gibbsite and goethite, respectively.

Citrate sorption below pH 4 in the 10^{-4} M citrate experiments was fit using the same ligand exchange reaction. The model fit in saturated conditions (10^{-4} M citrate) above pH 4 to both minerals was inadequate. This shortcoming is not unsurprising as it would require saturating a mineral surface above its pzc with a -3 anion. While this condition it certainly possible to fit in isolation, the log K values required to overcome the electrostatic repulsion terms are so large that citrate sorption is vastly over-predicted under the unsaturated surface-site condition. It is also possible to simultaneously fit sorption of both concentrations of citrate if Na^+ is included in the surface species. This strategy effectively neutralizes the repulsive charges and allows the model to place citrate on an uncharged surface. Unfortunately, no literature could be found to suggest that Na-citrate would be a thermodynamically favorable citrate complex under the solution conditions of this study. Additionally, a previous study by Redden *et al.*[35] noted little effect of Na^+ concentration on

citrate sorption to either goethite, gibbsite, or kaolinite. A study by Balistrieri and Murray[38] did propose equilibrium reactions for Na^+ ion adsorption to goethite. The proposed equilibrium constant however, indicated that no appreciable Na^+ sorption would be expected below pH 9 under the conditions of these experiments, and that sorption would remain below 10 % up to pH 10. Without any previous indication that Na-citrate would jointly sorb to a mineral surface, these modeling efforts are presented with the acknowledgement that sorption models of anionic ligands to minerals at alkaline pH need improvement. For that reason, we present 10^{-4} M citrate model lines above pH 4 with a dashed line. The raw data will be made available in the supporting materials, should other researchers seek to improve upon this model.

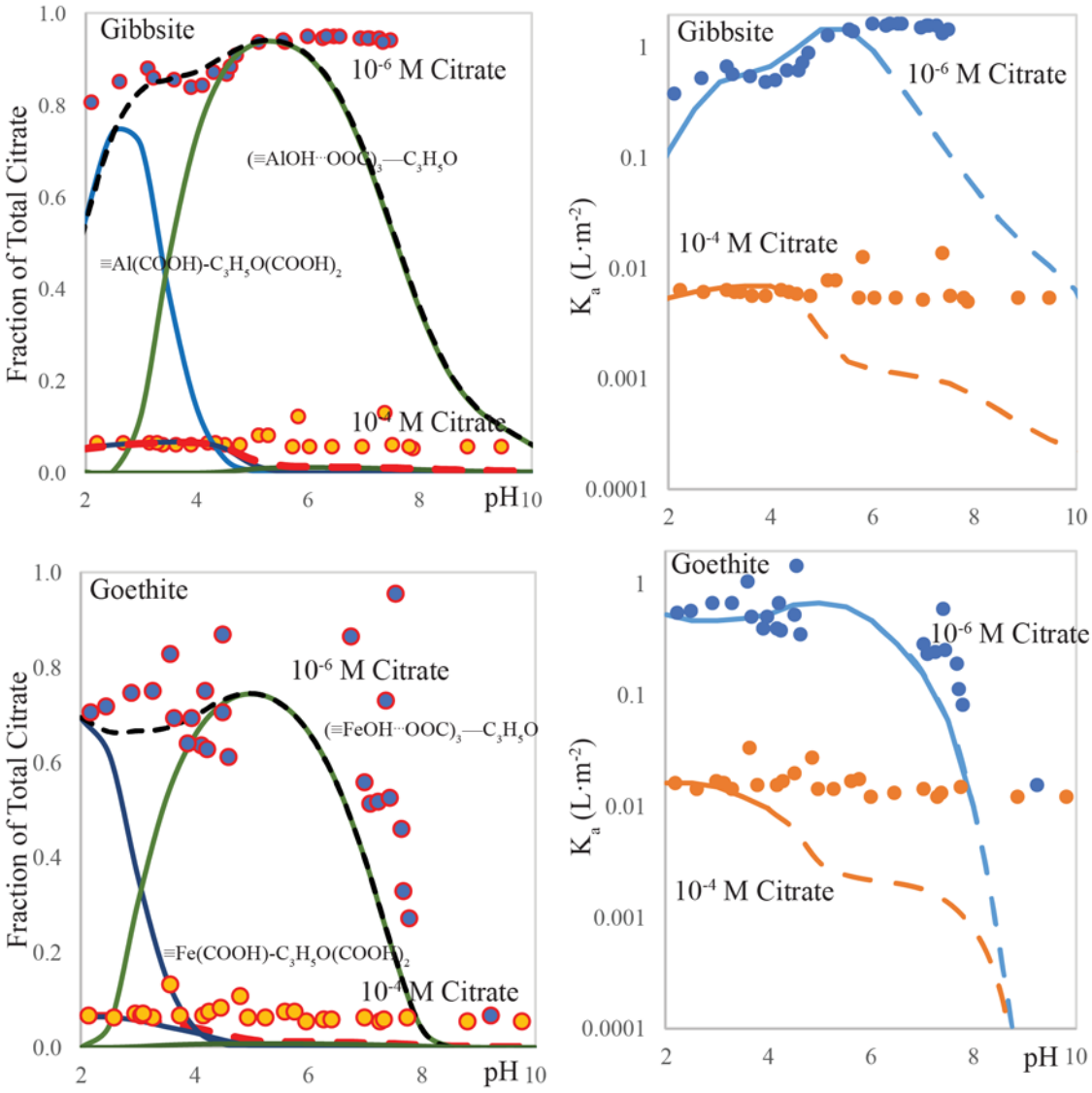

Figure 4.3. Citrate sorption to 5.5 g·L^{-1} gibbsite (left) and 0.11 g·L^{-1} goethite (right) at 10^{-6} M and 10^{-4} M citrate. Data given by circles, model fit by lines. The total sorbed fraction is given as a fine-dashed black line.

Table 4.4. Citrate-Mineral Surface Complexation Constants

Reaction	log K
$\equiv AlOH^0 + 3H^+ + C_6H_5O_7^{3-} \leftrightarrow \equiv Al(COOH)\text{-}C_3H_5O(COOH)_2^0 + H_2O$	21.23
$3(\equiv AlOH) + Cit^{3-} \leftrightarrow (\equiv AlOH\cdots OOC)_3{-}C_3H_5O^{3-}$	14.9
$\equiv FeOH^0 + 3H^+ + C_6H_5O_7^{3-} \leftrightarrow \equiv Fe(COOH)\text{-}C_3H_5O(COOH)_2^0 + H_2O$	26.8
$3(\equiv FeOH) + Cit^{3-} \leftrightarrow (\equiv FeOH\cdots OOC)_3{-}C_3H_5O^{3-}$	13.69

Determination of Ternary Mineral-Pu(IV)-Citrate Binding Constants

The effect of citrate on Pu sorption to both gibbsite and goethite was significant. As previous studies have shown, citrate will increase Pu in solution at circumneutral pH and will increase Pu sorption at acidic pH by means of ternary surface complexes. Ternary Pu sorption data were coupled with the binary Pu-mineral sorption models and the binary citrate sorption models to propose ternary mineral-Pu-citrate reactions and thermodynamic K values. From those ternary sorption experiments, it was immediately apparent that the presence of citrate increased Pu sorption to gibbsite and goethite below pH 4. This was observed in experiments of both 10^{-4} M and 10^{-6} M citrate. Additionally, it was clear that Pu-citrate complexes were able to stabilize Pu in solution from pH 4 – 8, outcompeting both mineral surfaces for Pu. While this decrease in Pu sorption was distinctive in the 10^{-4} M citrate dataset, it was not evident in the 10^{-6} M citrate dataset. The estimated concentration of surface sites in both systems was approximately 10^{-5} M. Therefore, the affinity of citrate and the surfaces for Pu from pH 4 – 8 is likely similar. Plutonium-citrate ternary sorption to gibbsite and goethite was fit using one ternary species for each mineral. Surface reactions and the associated log K values are listed in Table 4.5 and pH dependent

models presented in Figures 4.4 and 4.5 as fraction sorbed (left) and surface area normalized K_a (right).

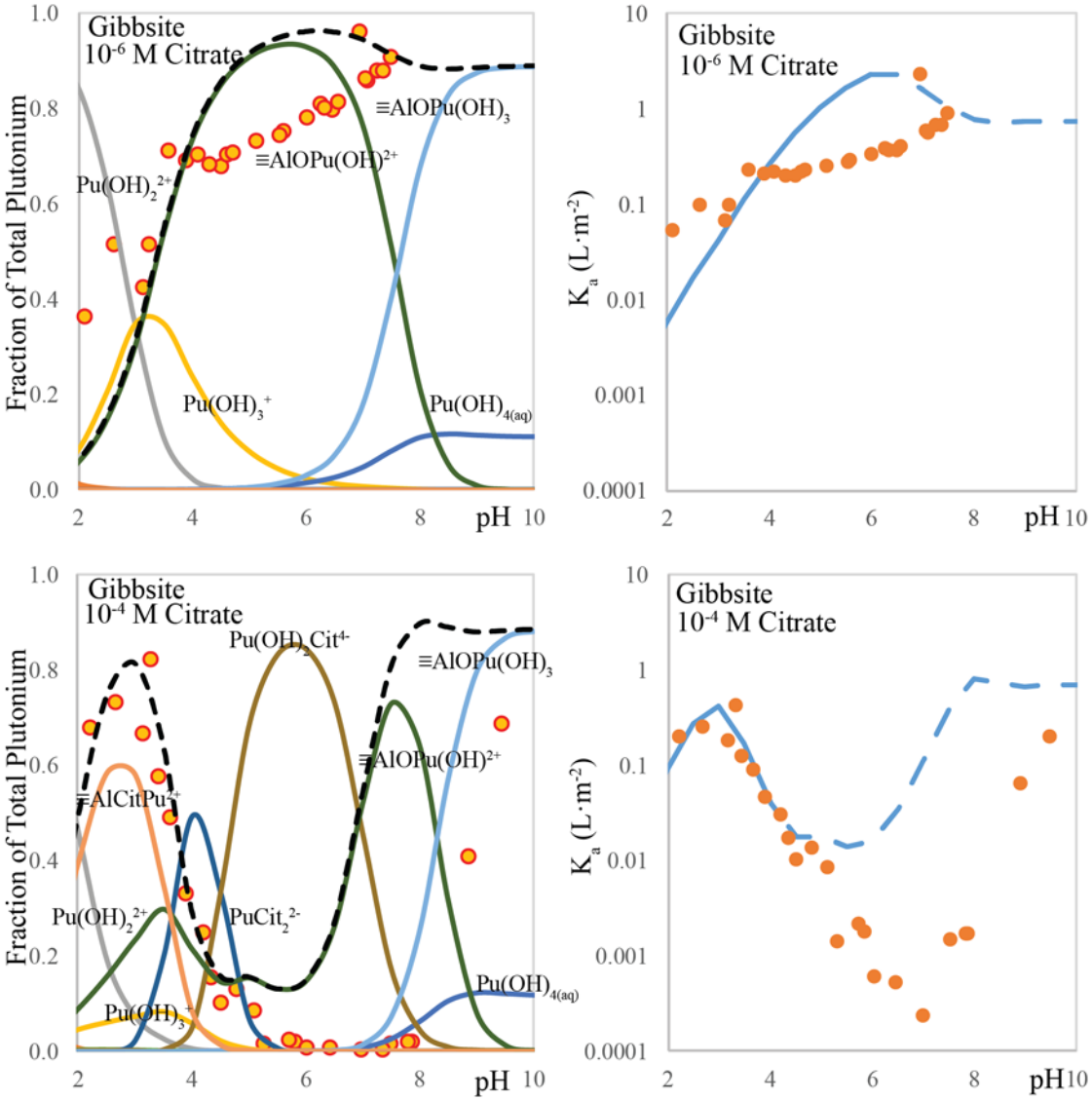

Figure 4.4. Pu (10^{-10} M) sorption to 5.5 g·L^{-1} gibbsite in the presence of 10^{-6} M (top) and 10^{-4} M (bottom) citrate. Fraction sorbed (left) and surface area normalized distribution coefficent (right). Data given by circles, model fit by lines. The total sorbed fraction is given as a fine-dashed black line.

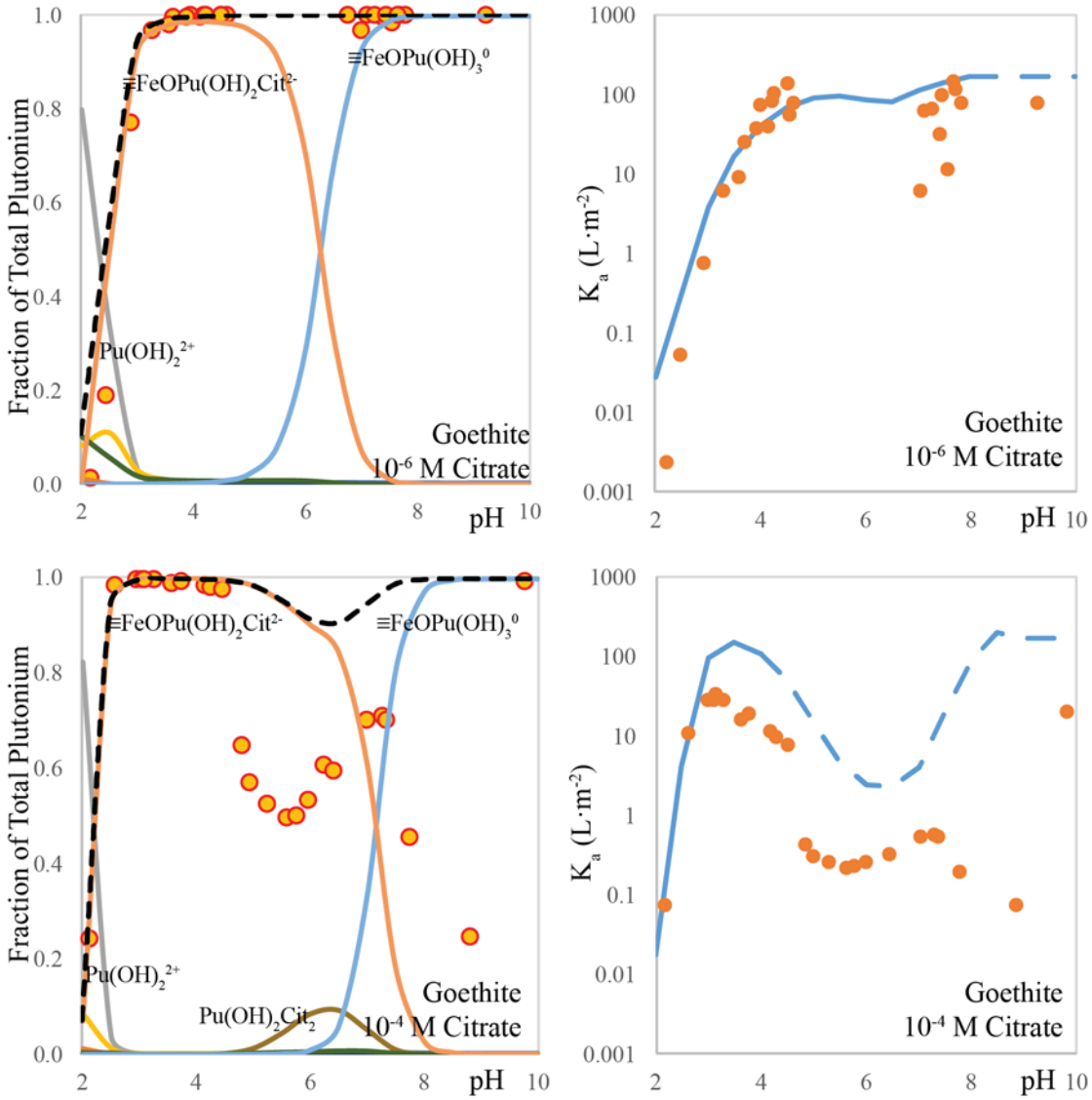

Figure 4.5. Pu (10^{-10} M) sorption to 0.11 g·L^{-1} goethite in the presence of 10^{-6} M (top) and 10^{-4} M (bottom) citrate. Fraction sorbed (left) and surface area noramlized distribubtion coefficent (right). Data given by circles, models by lines. The total sorbed fraction is given as a fine-dashed black line (left).

The ternary species $\equiv AlCitPu^{2+}$ (log K = 31.0) was fit to the gibbsite system. The stoichiometry of this species suggests a type B ternary complex. By contrast, the ternary species $\equiv FeOPu(OH)_2Cit^{2-}$ was fit the goethite system, the stoichiometry of which suggests a type A ternary complex. While the authors will caution readers from conclusively deciding mechanistic information from diffuse-layer modeling, the contrast is readily explained by the differing affinities of both surfaces for Pu and for citrate. Gibbsite has a similar affinity for Pu and citrate at pH 3 as seen in Figures 2 and 3, respectively. Meanwhile, citrate concentration significantly exceeds Pu concentration, and approximately 10 % of surface sites are estimated to be occupied by citrate. These citrate molecules are expected to sorb via a 1:1 surface complex and therefore, have available carboxylic acid moieties to bind Pu. Therefore, there are plentiful citrate complexation sites on the surface that likely have similar favorability as Pu-citrate complexation in solution. Conversely, goethite has a significantly greater affinity for Pu than for citrate and also a greater affinity for Pu than gibbsite. Therefore, it is intuitive that a goethite-Pu-citrate ternary complex would orient with the Pu towards the surface.

Predicting Pu speciation from pH 2 – 4 in the presence of citrate and gibbsite or goethite required inclusion of a ternary surface species. Because speciation controls mobility, understanding the thermodynamic behavior of ternary surface complexes will be necessary in assessing the transport of Pu in groundwater. Even though pH 2 – 4 is acidic for groundwater, acidic waste may have been co-disposed of with Pu, and that possibility warrants a more detailed understand of ternary complexes their long-term stability. Accurate transport risk assessment will also require improved organic ligand to mineral

sorption models, particularly in groundwater with high organic carbon and at moderately to more alkaline pH. With an improved representation of citrate sorption, our ability to predict Pu speciation will certainly improve. Speciation of both Pu and organic ligands, particularly at alkaline pH, deserves more detailed study. The extremely high pH of many tanks wastes, as well as the inadequacies in our understand of Pu-ligand behavior at alkaline pH ought to provide sufficient motivation to study these systems in greater detail.

Table 4.5. Ternary Citrate-Pu-Mineral Surface Complexation Constants

Reaction	log K
$\equiv FeOH^0 + Pu^{4+} + Cit^{3-} + 2H_2O \leftrightarrow \equiv FeOPu(OH)_2Cit^{2-} + 3H^+$	10.28
$\equiv AlOH^0 + Pu^{4+} + Cit^{3-} + H^+ \leftrightarrow \equiv AlCitPu^{2+} + H_2O$	31.0

Improvements in Pu-Citrate Binding Modeling at Alkaline pH

While the Pu-citrate constants produced by Raymond *et al.* permitted modeling of ternary Pu-citrate-goethite/gibbsite sorption at acidic pH, it was very apparent that understating of Pu-citrate complexation at alkaline pH is insufficient. In order to propose Pu-citrate binding constants at alkaline pH, competitive Pu(IV) binding experiments between citrate and a solid resin surface were conducted from pH 4 – 10. A commercially available resin, Analig-Pu02, was used for these experiments. While there have been numerous studies of distribution coefficients and kinetics of Pu(IV) sorption to Analig-Pu02,[39–41] no studies were found that included a pH dependence. Therefore, pH adjusted Pu(IV) solutions were contacted with the resin in the absence of citrate to first estimate binary Pu(IV)-Analig-Pu02 adsorption. Following the binary Pu-resin sorption experiment, an oxidation state analysis was performed on the Pu remaining in each supernatant. Well within the assumed 5 % margin of error for lanthanum fluoride co-precipitation OSA, all

of the Pu that remained un-sorbed was in the 4+ oxidation state (Figure 4.6, left). An identical experiment was then conducted with 10^{-4} M citrate in solution. A ^{14}C citrate tracer was used to confirm citrate did not sorb to the resin (see SI). The decrease in Pu sorption to the resin from pH 4 – 10 was best fit using two 1:1 Pu:citrate species with different degrees of Pu hydrolysis. Plutonium-citrate complexation reactions and their associated log K values are listed in Table 4.6 and pH dependent models presented in Figure 4.6.

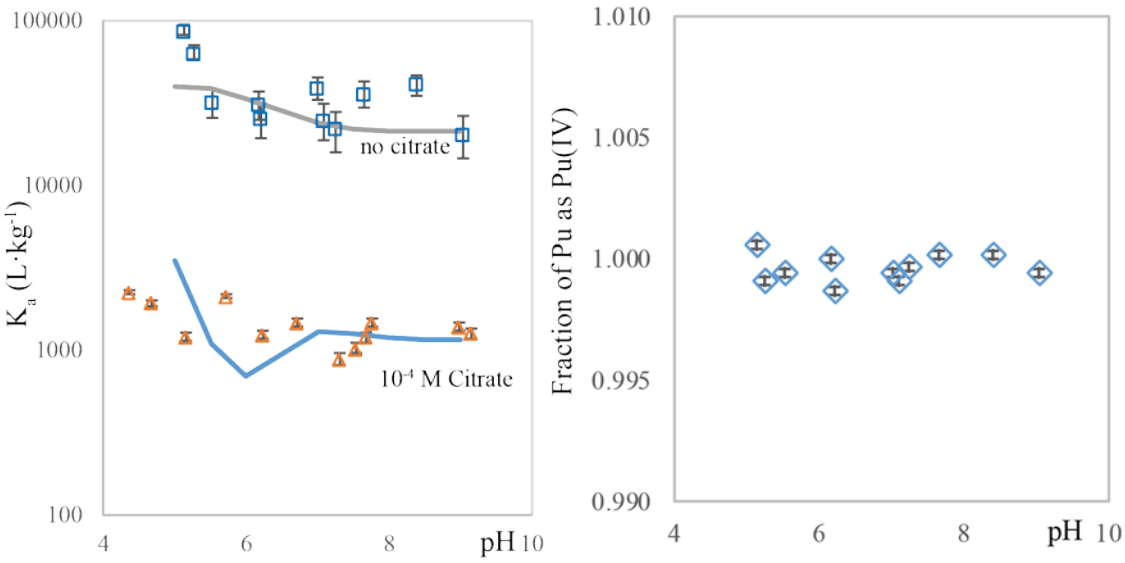

Figure 4.6. Pu (10^{-9} M) sorption to Analig-Pu02 resin in the absence (open squares) and presence (open triangles) of 10^{-4} M citrate (left) and fraction of aqueous Pu as Pu(IV) in citrate free experiments (right). Data given by circles, model fit by solid lines. Error bars calculated from counting statistics.

Table 4.6. Pu-Citrate Binding Constants at Alkaline pH

Reaction	log K
$Pu^{4+} + 2Cit^{3-} + 2H_2O \leftrightarrow Pu(OH)_2Cit^{2-} + 2H^+$	13.4
$Pu^{4+} + Cit^{3-} + 4H_2O \leftrightarrow Pu(OH)_4Cit^{3-} + 4H^+$	-4.1

Of the two species used to fit the competitive complexation data, $Pu(OH)_4Cit^{3-}$ is new and $Pu(OH)_2Cit^{2-}$ was used in previous studies by Raymond *et al.* and by Metivier and Guillimont. Raymond *et al.* proposed a log K value of 14.67 for $Th(OH)_2Cit^{2-}$ as an analog for $Pu(OH)_2Cit^{2-}$ and that value agrees reasonably closely to that of the competitive complexation experiment. Metivier and Guillimont proposed a value of 11.94, but also included a similar $Pu(OH)_2Cit^{+}$ species in their work, preventing a direct quantitative comparison. The Pu-citrate complexation reactions and constants proposed here will likely require refinement and certainly need to be validated by other methods. The results however, demonstrate that Pu-citrate complexation persists to higher pH than previously recognized and provides an estimated strength of Pu-citrate complexation at alkaline pH.

Citrate has been shown to have a profound effect on Pu aqueous speciation and sorption to gibbsite and goethite. While an increase in aqueous Pu at neutral pH was only observed in the presence of 10^{-4} M citrate, and not 10^{-6} M citrate, both concentrations of citrate had a clear influence below pH 4, increasing Pu sorption through ternary surface complexes. It was also demonstrated that binary citrate sorption strongly influenced Pu sorption through surface-site competition, and by controlling the concentrations of citrate available in solution to complex Pu. It seems likely that further improvement of binary citrate sorption models, will likewise improve Pu sorption models in the same pH range. These results indicate that accurately predicting natural organic matter sorption, complexation with Pu, and formation of ternary complexes will be essential in accurately assessing the risks associated with the fate and transport of Pu in the environment.

References

(1) Sanchez, A. L.; Murray, J. W.; Sibley, T. H. The adsorption of plutonium IV and V on goethite. *Geochim. Cosmochim. Acta* **1985**, *49*, 2297–2307.

(2) Keeney-Kennicutt, W.; Morse, J. The redox chemistry of $Pu(V)O^{2+}$ interaction with common mineral surfaces in dilute solutions and seawater. *Geochim. Cosmochim. Acta* **1985**, *49*, 2577–2588.

(3) Romanchuk, A. Y.; Kalmykov, S. N.; Aliev, R. A. Plutonium sorption onto hematite colloids at femto- and nanomolar concentrations. *Radiochim. Acta* **2011**, *99* (3), 137–144.

(4) Powell, B. A.; Fjeld, R. A.; Kaplan, D. I.; Coates, J. T.; Serkiz, S. M. $Pu(V)O^{2+}$ adsorption and reduction by synthetic magnetite (Fe3O4). *Environ. Sci. Technol.* **2004**, *38* (22), 6016–6024.

(5) Kirsch, R.; Fellhauer, D.; Altmaier, M.; Neck, V.; Rossberg, A.; Fanghänel, T.; Charlet, L.; Scheinost, A. C. Oxidation State and Local Structure of Plutonium Reacted with Magnetite, Mackinawite, and Chukanovite. *Environ. Sci. Technol.* **2011**, *45* (17), 7267–7274.

(6) Powell, B. A.; Duff, M. C.; Kaplan, D. I.; Fjeld, R. A.; Newville, M.; Hunter, D. B.; Bertsch, P. M.; Coates, J. T.; Eng, P.; Rivers, M. L.; et al. Plutonium oxidation and subsequent reduction by Mn (IV) minerals in Yucca Mountain tuff. *Environ. Sci. Technol.* **2006**, *40* (11), 3508–3514.

(7) Kersting, A. B.; Efurd, D. W.; Finnegan, D.; Rokop, D. J.; Smith, D.; Thompson, J. L. Migration of Plutonium in ground water at the Nevada Test Site. *Nature* **1999**, *397* (6714), 53–56.

(8) Novikov, A. P.; Kalmykov, S. N.; Utsunomiya, S.; Ewing, R. C.; Horreard, F.; Merkulov, A.; Clark, S. B.; Tkachev, V. V.; Myasoedov, B. F. Colloid Transport of Plutonium in the Far-Field of the Mayak Production Association, Russia. *Science* **2006**, *314*, 638–641.

(9) Banik, N. L.; Buda, R. A.; Bürger, S.; Kratz, J. V.; Trautmann, N. Speciation and interactions of plutonium with humic substances and kaolinite in aquifer systems. *J. Alloys Compd.* **2007**, *444–445*, 522–525.

(10) Boukhalfa, H.; Reilly, S. D.; Neu, M. P. Complexation of Pu(IV) with the Natural Siderophore Desferrioxamine B and the Redox Properties of Pu(IV)(siderophore) Complexes. *Inorg. Chem.* **2007**, *46* (3), 1018–1026.

(11) Kantar, C.; Honeyman, B. D. Plutonium (IV) complexation with citric and alginic acids at low PuT concentrations. *Radiochim. Acta* **2005**, *93* (12/2005), 757–766.

(12) *Effects of humic substances on the migration of radionuclides: complexation of actinides with humic substances ; final report*; Czerwinski, K. R., Europäische Kommission, Eds.; EUR; Office for Official Publ. of the European Communities: Luxembourg, 1996.

(13) Xu, C.; Zhang, S.; Kaplan, D. I.; Ho, Y.-F.; Schwehr, K. A.; Roberts, K. A.; Chen, H.; DiDonato, N.; Athon, M.; Hatcher, P. G.; et al. Evidence for Hydroxamate Siderophores and Other N-Containing Organic Compounds Controlling ^{239,240} Pu Immobilization and Remobilization in a Wetland Sediment. *Environ. Sci. Technol.* **2015**, *49* (19), 11458–11467.

(14) Conroy, N. A.; Zavarin, M.; Kersting, A. B.; Powell, B. A. Effect of Natural Organic Matter on Plutonium Sorption to Goethite. *Environ. Sci. Technol.* **2017**.

(15) Santschi, P. H.; Roberts, K. A.; Guo, L. Organic nature of colloidal actinides transported in surface water environments. *Environ. Sci. Technol.* **2002**, *36* (17), 3711–3719.

(16) Tinnacher, R. M.; Begg, J. D.; Mason, H.; Ranville, J.; Powell, B. A.; Wong, J. C.; Kersting, A. B.; Zavarin, M. Effect of Fulvic Acid Surface Coatings on Plutonium Sorption and Desorption Kinetics on Goethite. *Environ. Sci. Technol.* **2015**, *49* (5), 2776–2785.

(17) *Chemical thermodynamics of compounds and complexes of U, Np, Pu, Am, Tc, Se, Ni, and Zr with selected organic ligands*; Hummel, W., Mompean, F. J., Eds.; Chemical thermodynamics; Elsevier: Amsterdam, 2005.

(18) Riley, R. G.; Zachara, J. M. *Chemical Contaminants on DOE Lands and Selection of Contaminant Mixtures for Subsurface Science Research*; DOE/ER--0547T; US Department of Energy, 1992.

(19) Zachara, J. M.; Serne, J.; Freshley, M.; Mann, F.; Anderson, F.; Wood, M.; Jones, T.; Myers, D. Geochemical Processes Controlling Migration of Tank Wastes in Hanford's Vadose Zone. *Vadose Zone J.* **2007**, *6* (4), 985.

(20) Banik, N. L.; Buda, R. A.; Bürger, S.; Kratz, J. V.; Trautmann, N. Sorption of tetravalent plutonium and humic substances onto kaolinite. *Radiochim. Acta* **2007**, *95* (10).

(21) Zimmerman, T.; Zavarin, M.; Powell, B. A. Influence of humic acid on plutonium sorption to gibbsite: Determination of Pu-humic acid complexation constants and ternary sorption studies. *Radiochim. Acta* **2014**, *102* (7).

(22) Roberts, K. A.; Santschi, P. H.; Honeyman, B. D. Pu(V) reduction and enhancement of particle-water partitioning by exopolymeric substances. *Radiochim. Acta* **2008**, *96* (9–11).

(23) Conroy, N. A.; Wylie, E. M.; Powell, B. A. A Novel Method for Tracer Concentration Plutonium(V) Solution Preparation. *Anal. Chem.* **2016**, *88* (8), 4196–4199.

(24) *The chemistry of the actinide and transactinide elements*; Morss, L. R., Ed.; Springer: Dordrecht, 2010.

(25) Schwertmann, U.; Cornell, R. M. *Iron oxides in the laboratory: Preparation and characterization*; VCH: Weinheim, 1991.

(26) *Update on the chemical thermodynamics of uranium, neptunium, plutonium, americium and technetium*; Guillaumont, R., Mompean, F. J., OECD Nuclear Energy Agency, Eds.; Chemical thermodynamics; Elsevier ; Nuclear Energy Agency, Organisation for Economic Co-Operation and Development: Amsterdam ; Boston : Paris, 2003.

(27) Karamalidis, A. K.; Dzombak, D. A. *Surface complexation modeling: gibbsite*; Wiley: Hoboken, N.J, 2010.

(28) Dzombak, D. A.; Morel, F. M. M. *Surface complexation modeling: hydrous ferric oxide*; Wiley: New York, 1990.

(29) Metivier, H.; Guillaumont, R. Complexes Citriques Du Plutonium Tetravalent. *Radiochem Radional Lett.* **1972**, *10* (4), 239–250.

(30) Nebel, D. Potentiometrische Untersuchungen des Gleichgewichtes Pu(IV)-Citrat in wäβriger Lösung. *Z Phys Chem* **1966**, *232*, 368–376.

(31) Raymond, D. P.; Duffield, J. R.; Williams, D. R. Complexation of Plutonium and Thorium in Aqueous Environments. *Inorganica Chim. Acta* **1987**, *140*, 309–313.

(32) Wang, P.; Anderko, A.; Turner, D. R. Thermodynamic Modeling of the Adsorption of Radionuclides on Selected Minerals. I: Cations. *Ind. Eng. Chem. Res.* **2001**, *40* (20), 4428–4443.

(33) Goldberg, S. Inconsistency in the triple layer model description of ionic strength dependent boron adsorption. *J. Colloid Interface Sci.* **2005**, *285* (2), 509–517.

(34) Davis, J. A.; Kent, D. B. Surface Complexation Modeling in Aqueous Geochemistry. *Rev. Mineral. Geochem.* **1990**, *23* (1), 177–260.

(35) Redden, G.; Li, J.; Leckie, J. O. Adsorption of U(VI) and Citric Acid on Goethite, Gibbsite, and Kaolinite. In *Adsorption of Metals by Geomedia*; Academic Press, 1998; pp 291–315.

(36) Filius, J.; Hiemstra, T.; Van Riemsdijk, W. H. Adsorption of Small Weak Organic Acids on Goethite: Modeling of Mechanism. *J. Colloid Interface Sci.* **1997**, *195*, 368–380.

(37) Noerpel, M. R.; Lenhart, J. J. The impact of particle size on the adsorption of citrate to hematite. *J. Colloid Interface Sci.* **2015**, *460*, 36–46.

(38) Balistrieri, L. S.; Murray, J. W. The Surface Chemistry of Goethite (αFeOOH) in Major Ion Seawater. *Am. J. Sci.* **1981**, *281*, 788–806.

(39) Gardoňová, V.; Labaška, M.; Antalík, I.; Kuruc, J. Statistical suitability testing of the Aliquat-336, AnaLig® Pu-02 and TRU® Resin use for the 239,240Pu, 238Pu determination. *J. Radioanal. Nucl. Chem.* **2013**, *295* (2), 1353–1360.

(40) Pathak, S. K.; Tripathi, S. C.; Singh, K. K.; Mahtele, A. K.; Kumar, M.; Gandhi, P. M. Simultaneous separation and purification of plutonium and americium from aqueous nitrate solutions using extractant impregnated macroporous polymeric beads. *J. Radioanal. Nucl. Chem.* **2016**, *308* (1), 47–57.

(41) Dulanská, S.; Remenec, B.; Mátel, Ľ.; Galanda, D. The selective separation of Pu isotopes using molecular recognition technology product AnaLig® Pu02 gel and extraction chromatography TRU® resin. *J. Radioanal. Nucl. Chem.* **2011**, *287* (3), 841–845.

Acknowledgement

This work was supported by the Subsurface Biogeochemical Research Program of the U.S. Department of Energy's Office of Biological and Environmental Research.

CHAPTER FIVE

A NOVEL METHOD FOR TRACER CONCENTRATION PLUTONIUM(V) SOLUTION PREPARATION

Nathan A. Conroy**,** *E. Miller Wylie, Brian A. Powell

Accepted March 15, 2016 to Analytical Chemistry:

Conroy, N. A.; Wylie, E. M.; Powell, B. A. A Novel Method for Tracer Concentration Plutonium(V) Solution Preparation. *Anal. Chem.* **2016**, *88* (8), 4196–4199.

DOI: 10.1021/acs.analchem.6b00229

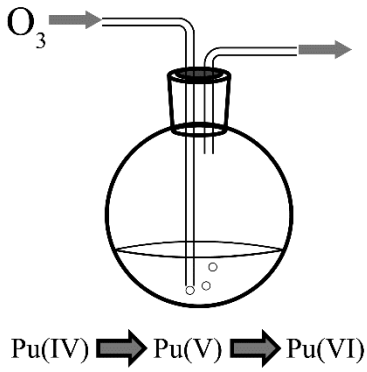

Figure 5.1. Schematic of ozonation apparatus (abstract art).

Abstract

Preparation of relatively pure low concentration Pu(V) solutions for environmental studies is non-trivial due to the complex redox chemistry of Pu. Ozone gas generated by an inexpensive unit designed for household-use was used to oxidize a 2×10^{-8} M Pu(IV) solution to predominantly Pu(VI) with some Pu(V) present. Over several days, the Pu(VI) in the solution reduced to Pu(V) without further reducing to Pu(IV). The reduction from Pu(VI) to Pu(V) could be accelerated by raising the pH of the solution, which led to an immediate conversion without substantial conversion to Pu(IV). The aqueous Pu was found to be stable as predominately Pu(V) for greater than one month from pH 3 – 7, however at circumneutral pH a sizeable fraction of Pu was lost from solution either by precipitation or by sorption to the vial walls. This method provides a fast means of preparing Pu(V) solutions for tracer concentration studies without numerous extractions or cleanup steps.

Introduction

Pentavalent plutonium (Pu) is the dominant aqueous oxidation state of Pu in ocean waters and many surface waters.[1-3] Therefore, understanding environmental transport of Pu requires laboratory studies of Pu(V) behavior. However, the mobility of Pu(V) in the environment is hindered by reduction to immobile and insoluble Pu(IV) on mineral surfaces.[2, 4-7] The thermochemical prevalence of Pu(V) in the aqueous phase and Pu(IV) on mineral surfaces under oxic conditions has been recently demonstrated by Marsac et al.,[8] in an examination of Pu sorption to kaolinite clay. The Pu(IV) surface complexes have an extended stability field with respect to the pH and E_H due to the strength of the Pu(IV) surface complexes while Pu(V) maintains as a stable aqueous actinyl cation.[8] Oxidation of

sorbed Pu(IV) to mobile Pu(V) was also found to be responsible for a stepwise mobilization of Pu in the vadose zone of the Department of Energy, Savannah River Site.[9] While Pu(V) and Pu(IV) are generally expected to persist in most environments, plutonium can simultaneously exist in four oxidation states in a single solution and the redox potentials of the Pu(III)-Pu(VI) couples are sufficiently close together to make them very sensitive to redox transformations.[10, 11] Thus, Pu(III) and Pu(VI) are also expected to be present in some environments. While many environmental systems are fairly well understood, unexpected migration of Pu has been observed at several legacy nuclear weapons production sites. While these studies have primarily identified colloidal transport of Pu as the underlying mechanism for enhanced transport, a significant amount of aqueous Pu remains in these samples. To perform laboratory studies examining this observed migration of Pu, pure oxidation state solutions are required. Preparation of such solutions, particularly Pu(V), is difficult due to the profoundly complicated redox chemistry of Pu.

Preparation of relatively pure oxidation state Pu(V) solutions is non-trivial. Previously reported methods have used electrochemical methods or chemical extractions to separate mixed oxidation states of Pu.[2, 4, 12-15] Generally, a mixed oxidation state solution is forcibly oxidized to Pu(VI) prior to inducing reduction to Pu(V). Following this approach, Saito et al.[16] called for oxidation of a Pu solution using $KMnO_4$ followed by extraction of the Pu(VI) into thenoyltrifluoroacetone (TTA) in the absence of light. The Pu(VI) was then partially reduced photochemically using fluorescent light and the Pu(V) backextracted into an aqueous phase. While there was no evidence of other oxidation states present, yields were only 60 % of the original activity and preparation leaves some residual organic

solvent within the aqueous stock solution. Furthermore, the TTA is light sensitive and must be purified by vacuum sublimation prior to each use.

In this technical note, we report a method which consists of an oxidation step using ozone gas, followed by autoreduction of Pu(VI) to Pu(V). Using ozone as the oxidant eliminates the need to perform extractions to remove oxidizing chemicals. This procedure calls for minimal chemical intervention, as all that is necessary after the initial ozone treatment is adjustment of pH. This simple and effective procedure yields 10^{-8} M Pu solutions which are > 80 % Pu(V), and can generally be completed over the course of 24 – 72 hours.

Experimental Section

Pu(V) stock preparation

A 2.8 µCi (0.28 g of a 10 µCi/g) aliquot of a NIST traceable ^{238}Pu solution (Eckert & Ziegler Source # 1556-59) in 4 M HNO_3 was pipetted into a flat-bottomed round flask; this solution is initially Pu(IV)(NO3)4. Millipore (>18 MΩ) H_2O was added to this flask to a final mass of 30 g, resulting in a calculated activity of 0.092 µCi·mL^{-1} (3410 Bq·mL^{-1}; 2.26 × 10^{-8} M). An initial pH of 1.5 was measured. The pH was adjusted to 3.5 – 4.0 using drop wise additions of 0.1 M NaOH. The diluted solution was treated with O_3 gas (Aqua-6 ozone generator; A_2Z Inc) for 20 minutes every hour for a total of 72 hours and aliquots were removed periodically for oxidation state analysis. After complete conversion to Pu(V) and Pu(VI), the ozonation was terminated and aliquots removed periodically to determine the stability of the final oxidation states for several days.

Influence of pH on oxidation state stability

Following a similar ozonation to the one described above, 10 mL aliquots of the prepared stock were removed and separately pH adjusted to pH 2.9, 5.2, and 7.2 using dropwise

additions of 0.1 M NaOH and 0.01 M NaOH and vigorous stirring to reduce very high pH localities surrounding the added drops. The oxidation state distribution and pH were monitored in these samples for several days using solvent extraction and lanthanum fluoride coprecipitation, as described below.

Oxidation state analysis

The Pu oxidation state was determined using solvent extraction methods. Lanthanum fluoride coprecipitations were also performed to corroborate the solvent extraction results. These methods distinguish Pu(IV), Pu(V), and Pu(VI). Pu(III) is not considered as it will be unstable under the conditions of these experiments.[11] Solvent extraction methods were performed using 0.025 M 4-benzoyl-3-methyl-1-phenyl-2-pyrazolin-5-one (PMBP) in cyclohexane and 0.5 M bis-(2-ethylhexyl)-phosphoric acid (HDEHP) in cyclohexane.[12, 14, 17] A 0.1 mL aliquot of the Pu solution was diluted to 2.5 mL for analysis. An aliquot of this diluted solution was acidified to pH 0 using 5 M HCl then vigorously mixed with the PMBP or HDEHP extractants for 3 minutes. The vial was centrifuged for 1 minute to aid in phase separation before aliquots of both the organic and aqueous phases were removed for counting by liquid scintillation counting (LSC, Hidex 300 SL). The 0.025 M PMBP solution selectively extracts Pu(IV) into the organic phase, leaving Pu(V) and Pu(VI) in the aqueous phase, whereas the 0.5 M HDEHP solution selectively extracts Pu(IV) and Pu(VI) into the organic phase (Figure 5.2). The oxidation state distribution is determined by the Pu distribution across the phases of these two extractions (Equations 1 -3). These results were corroborated by results from lanthanum fluoride coprecipitations: briefly, 1 mL of 0.8 M HNO_3, 0.25 M H_2SO_4, 0.01 M $La(NO_3)_3$ and 0.005 M $KMnO_4$ was added to

0.5 mL of the diluted plutonium solution.[18] Then 10 µL of concentrated HF was added to the solution before it was mixed for 3 minutes and centrifuged at 8000 RPM for 1 minute. Pu(III) and Pu(IV) will be coprecipitated, therefore, Pu(V) and Pu(VI) remain in the aqueous solution which was counted by LSC (Figure 5.2; Equation 4). These results were compared to the solvent extraction techniques to substantiate those results.

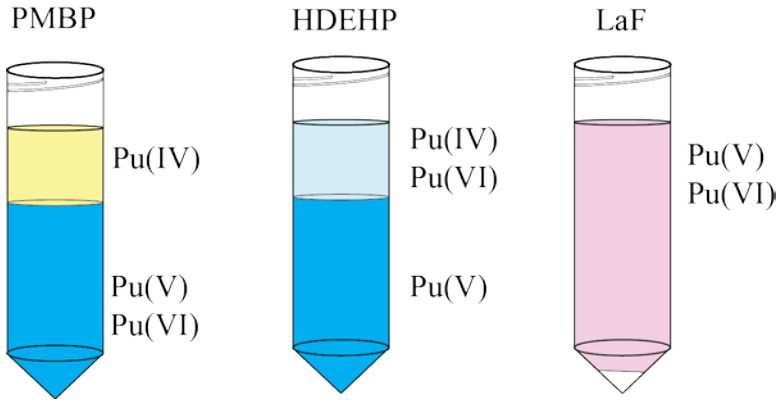

Figure 5.2. Solvent extraction and coprecipitation methods for oxidation state analysis.

$$\frac{\text{PMBP}_{\text{organic}}}{\text{Total Pu}} = \%\ \text{Pu(IV)}$$

Equation 1

$$\frac{\text{HDEHP}_{\text{aqueous}}}{\text{Total Pu}} = \%\ \text{Pu(V)}$$

Equation 2

$$\frac{\text{PMBP}_{\text{aqueous}} - \text{HDEHP}_{\text{aqueous}}}{\text{Total Pu}} = \%\ \text{Pu(VI)}$$

Equation 3.

$$1 - \frac{\text{LaF}_{\text{aqueous}}}{\text{Pu Total}} = \%\ \text{Pu(VI)}$$

Equation 4.

Given the indirect nature of these methods for oxidation state analysis, it must be noted that changes in oxidation state due to the measurement method are possible. A conservative uncertainty of 5 % is assumed for these indirect methods of monitoring Pu oxidation state analysis. This is significantly higher than the uncertainties based on nuclear counting statistics which are generally < 1 %.

Results and Discussion

Pu(V) stock preparation

Significant conversion of Pu(IV) to Pu(V) and Pu(VI) occurs after a single 20 minute bubbling of ozone (Figure 5.2). The Pu(IV) fraction is reduced to less than 1 % of the total plutonium concentration after 23 cycles (1 cycle = 20 minutes bubbling; 40 minutes off) of ozone bubbling. Pu(V) and Pu(VI) fractions are 23 % and 72 %, respectively, after 23 cycles and change marginally up to 70 cycles where they were found to be 26 % and 74 %, respectively. The reduction in pH is hypothesized to be a consequence of nitrogen oxide generation by the ozone generator, which will react with water to form nitrous acid and nitric acid; this is discussed in detail in the supporting information. Error bars are expressed based on nuclear counting statistics, however due to pipetting volume uncertainties as well as the solubility of cyclohexane in water, the authors recommend that a conservative error of 5 % be assumed.

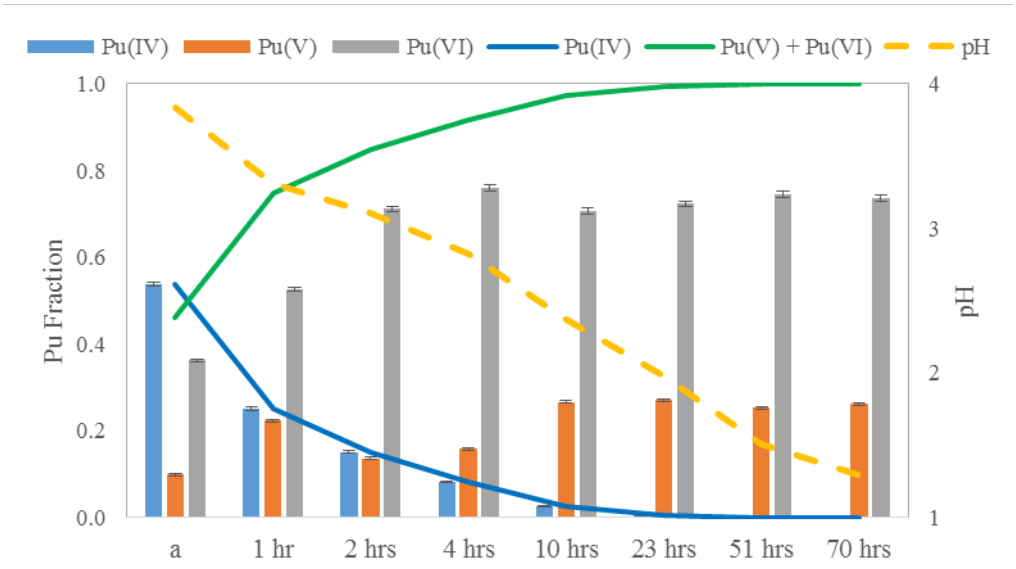

Figure 5.3. Oxidation state of plutonium (2.26×10^{-8} M) with exposure to ozone bubbling.

After ozone treatment and without further intervention, Pu(VI) converted slowly to Pu(V) without significant ingrowth of Pu(IV). A small conversion of Pu(V) to Pu(VI) within the first hour after treatment was attributed to residual ozone in the solution, however this small increase of Pu(VI) and decrease of Pu(V) is within the 5 % error the authors have prescribed. After five days, the Pu(IV) fraction remained below 1 % and the pH of the solution was stable near 1.3 (Figure 5.5). Meanwhile, increasing the pH resulted in an immediate conversion of Pu(VI) to Pu(V) while the Pu(IV) fraction remained effectively unchanged (Figure 5.5).

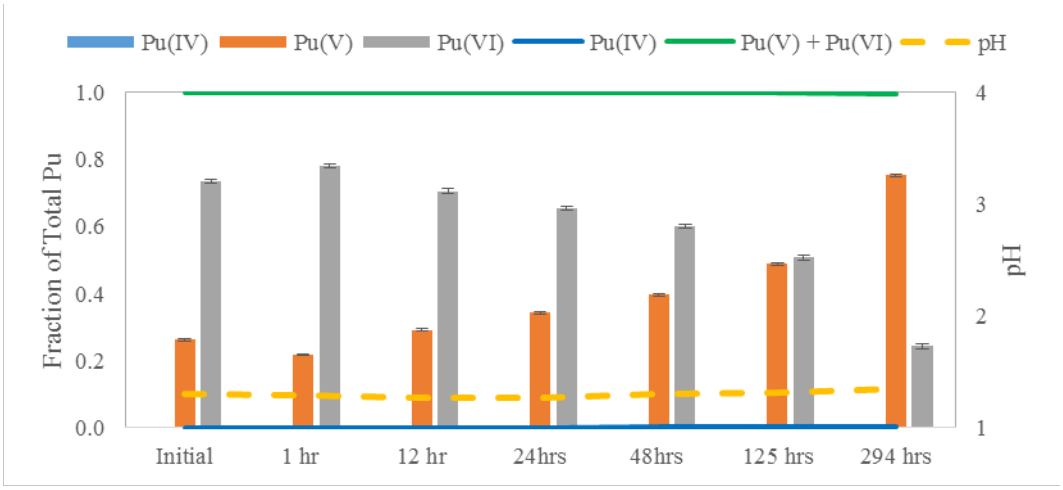

Figure 5.4. Oxidation state of plutonium (2.26×10^{-8} M) with time after ozone bubbling was terminated.

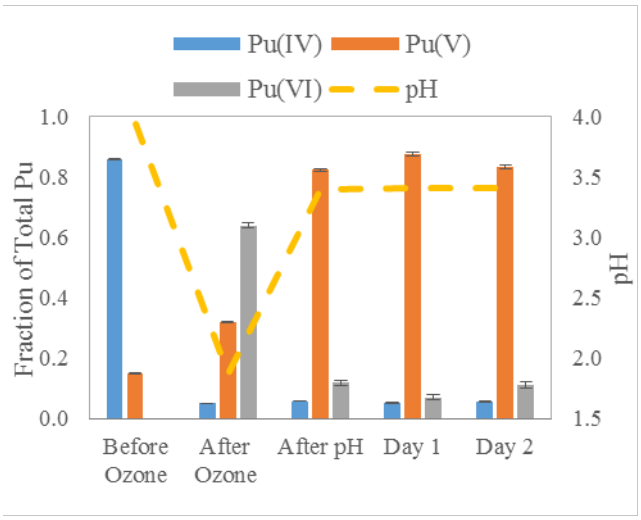

Figure 5.5. Oxidation state changes and stability of plutonium (1.40×10^{-8} M) with ozonation and subsequent pH adjustment.

Pu(V) disproportionation to Pu(IV) and Pu(VI) was avoided by keeping the solution pH > 2[66], and by keeping total Pu concentrations low[67]. At very low concentrations of Pu(III),

as is the case after ozone treatment, disproportionation of Pu(V) is thought to follow the reaction stoichiometry shown in Equation 5[68].

$$2Pu(V)O_2^+ + 4H^+ \rightarrow Pu(VI)O_2^{2+} + Pu(IV) + 2H_2O \qquad \text{Equation 5.}$$

Pu(V) disproportionation will therefore have a fourth-order dependence on H^+ ion concentration and a second-order dependence on $Pu(V)O_2^+$ concentration. Maintaining low total plutonium concentrations (10^{-8} M) and a solution pH from 3 - 6 effectively prevents Pu(V) disproportion for at least 36 days (discussed below) whilst precluding plutonium hydrolysis at high pH. The Pu(V) fraction and pH remained relatively stable over 2 days on monitoring at pH 3.5, therefore, oxidation state stability was studied at additional pH values.

Influence of pH on oxidation state stability

Oxidation state changes were monitored with time at pH 2.9 (Figure 5.6A), pH 5.6 (Figure 5.6B), and pH 7.8 (Figure 5.6C). The pH of the pH 2.9 solution was stable over the 36 day experimental period, whereas the pH 5.6 solution started at pH 5.2 and drifted to 5.8 and the pH 7.8 solution started at 7.2 and drifted to 8.2; average pH values are provided in Figure 5.6. Pu(V) was the predominant oxidation state in the aqueous fraction at all three pH values, however significant Pu was removed from solution at circumneutral pH (Figure 5.6C) either by precipitation or by sorption to vial walls. Particulate and sorbed species are anticipated to be Pu(IV).[19, 20] Pu removal increased with increasing pH, meanwhile the

fraction of Pu(V) present in the aqueous phase was remarkably similar across all pH values studied. Ignoring the fraction of Pu removed, Pu(V) is the dominant aqueous Pu oxidation state after 36 days at any of the pH values studied. The Pu(V) fraction of Pu in the aqueous phase was always > 77 %. The Pu(VI) fraction varied from 8 – 13 %, increasing with increasing pH. The Pu(IV) fraction varied from 4 – 16 %, decreasing with increasing pH.

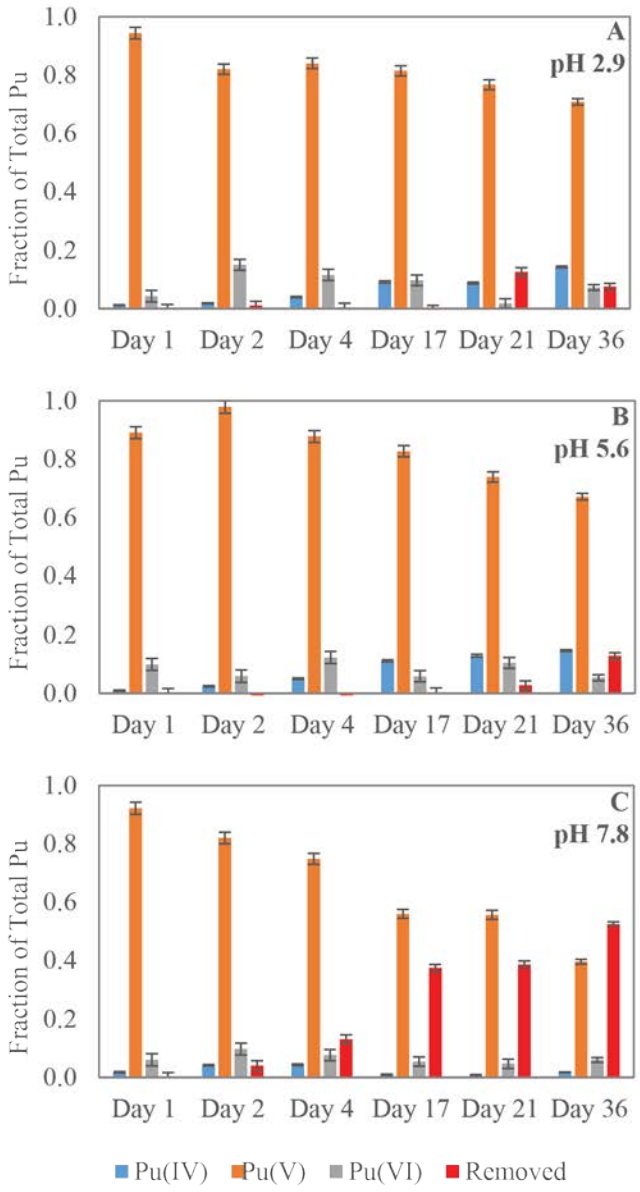

Figure 5.6. Oxidation state of plutonium (5.1×10^{-9} - 9.3×10^{-9} M) with time after pH adjustment to 2.9, 5.6, and 7.8.

Conclusion

Relatively pure Pu(V) solutions were made using a method which is less complex than a previously published method and contains no residual oxidants or organic solvents. Our new method uses fewer reagents and requires less intervention. Even after 36 days, Pu(V) was the predominant aqueous Pu oxidation state at mildly acidic to circumneutral pH. Significant fractions of Pu were removed from solution at pH 7.8 either through precipitation or through sorption to the vial walls. Overall, this is an effective and simple method for preparing Pu(V) stock solutions for low concentration Pu(V) experiments.

References

(1) Orlandini, K. A.; Penrose, W. R.; Nelson, D. M., Pu(V) as the Stable Form of Oxidized Plutonium in Natural-Waters. *Marine Chemistry* **1986,** *18*, (1), 49-57.

(2) Keeney-Kennicutt, W. L.; Morse, J. W., The redox chemistry of Pu(V)O2+ interaction with common mineral surfaces in dilute solutions and seawater. *Geochimica et Cosmochimica Acta* **1985,** *49*, (12), 2577-2588.

(3) Morse, J. W.; Choppin, G. R., The Chemistry of Transuranic Elements in Natural-Waters. *Reviews in Aquatic Sciences* **1991,** *4*, (1), 1-22.

(4) Sanchez, A. L.; Murray, J. W.; Sibley, T. H., The Adsorption of Plutonium-Iv and Plutonium-V on Goethite. *Geochimica Et Cosmochimica Acta* **1985,** *49*, (11), 2297-2307.

(5) Powell, B. A.; Fjeld, R. A.; Kaplan, D. I.; Coates, J. T.; Serkiz, S. M., Pu(V)O-2(+) adsorption and reduction by synthetic magnetite (Fe3O4). *Environ. Sci. Technol.* **2004,** *38*, (22), 6016-6024.

(6) Powell, B. A.; Fjeld, R. A.; Kaplan, D. I.; Coates, J. T.; Serkiz, S. M., Pu(V)O2+ adsorption and reduction by synthetic hematite and goethite. *Environ. Sci. Technol.* **2005,** *39*, (7), 2107-2114.

(7) Romanchuk, A. Y.; Kalmykov, S. N.; Aliev, R. A., Plutonium sorption onto hematite colloids at femto- and nanomolar concentrations. *Radiochim. Acta* **2011,** *99*, (3), 137-144.

(8) Marsac, R.; Banik, N. L.; Lutzenkirchen, J.; Buda, R. A.; Kratz, J. V.; Marquardt, C. M., Modeling plutonium sorption to kaolinite: Accounting for redox equilibria and the stability of surface species. *Chemical Geology* **2015,** *400*, 1-10.

(9) Kaplan, D. I.; Powell, B. A.; Demirkanli, D.; Fjeld, R. A.; Moltz, F.; Serkiz, S. M., Influence of plutonium oxidation-reduction chemistry on transport through Savannah River Site sediments. *Abstracts of Papers of the American Chemical Society* **2004,** *227*, U81-U81.

(10) Clark, D. L.; Hecker, S. S.; Jarvinen, G. D.; Neu, M. P., Plutonium. In *The Chemistry of the Actinides and Transactinide Elements*, Morss, L. R.; Edelstein, N. M.; Fuger, J., Eds. Springer: Dordrecht, 2006; Vol. 2, p 813.

(11) Cleveland, J. M., *The Chemistry of Plutonium*. American Nuclear Society: La Grange Park, IL, 1979.

(12) Neu, M.; Hoffman, D. C.; Roberts, K. E.; Nitsche, H.; Silva, R. J., Comparison of Chemical Extractions and Laser Photoacoustic Spectroscopy for the Determination on Plutonium Species in Near-Neutral Carbonate Solutions. *Radiochim. Acta* **1994,** *66/67*, 251-258.

(13) Nitsche, H., Solubility Studies of Transuranium Elements for Nuclear Waste-Disposal - Principles and Overview. *Radiochim. Acta* **1991,** *52-3*, 3-8.

(14) Nitsche, H.; Lee, S. C.; Gatti, R. C., Determination of Plutonium Oxidation States at Trace Levels Pertinent to Nuclear Waste Disposal. *J. Nucl. Radioanal. Chem.* **1988,** *124*, (1), 171-185.

(15) Silva, R. J.; Nitsche, H., Actinide environmental chemistry. *Radiochim. Acta* **1995,** *70-1*, 377-396.

(16) Saito, A.; Roberts, R. A.; Choppin, G. R., Preparation of Solutions of Tracer Level Plutonium(V). *Analytical Chemistry* **1985,** *57*, (1), 390-391.

(17) Foti, S. C.; Freiling, E. C., The determination of the oxidation states of tracer uranium, neptunium and plutonium in aqueous media. *Talanta* **1964,** *11*, (3), 385-392.

(18) Kobashi, A.; Choppin, G. R.; Morse, J. W., A Study of Techniques for Separating Plutonium in Different Oxidation-States. *Radiochim. Acta* **1988,** *43*, (4), 211-215.

(19) Caceci, M. S.; Choppin, G. R., An Improved Technique to Minimize Cation Adsorption in Neutral Solutions. *Radiochim. Acta* **1983,** *33*, (2-3), 113-114.

(20) Powell, B. A.; Kaplan, D. I.; Serkiz, S. M.; Coates, J. T.; Fjeld, R. A., Pu(V) transport through Savannah River Site soils - an evaluation of a conceptual model of surface- mediated reduction to Pu (IV). *Journal of Environmental Radioactivity* **2014,** *131*, 47-56.

Acknowledgements

This research is funded by the Office of Basic Energy Sciences of the U.S. Department of Energy as part of the Heavy Element Chemistry Program (DE-SC0010355). The authors would like to thank Issac Johnston for thoughtful discussion regarding ozone reaction mechanisms.

CHAPTER SIX

CONCLUSIONS AND FUTURE WORK

General Conclusions

The goal of this research was to improve conceptual models that describe trace plutonium (Pu) geochemical behavior in hydrogeological systems containing natural organic matter (NOM). The preceding chapters demonstrated that the presence of NOM in hydrogeological systems could have a profound influence on Pu mobility by means of influencing Pu speciation and solubility. The magnitude and mechanism of that influence depends on the size and chemical nature of the NOM, which can be highly variable in natural systems. Natural organic matter undergoes sorption, aggregation, and complexation reactions with surfaces, other NOM, and competing ions. All of which impact the fate and transport of the NOM and its ability to sequester Pu. Chapter Three concluded by stating that the influence of NOM of Pu sorption appears to be primarily controlled by 1) the strength of the Pu-NOM complex and 2) the affinity of NOM for the rock material. In the least complex systems, without the influence of colloids or aggregating NOM, those two principles are likely to govern the speciation of Pu; and therefore, its potential for transport. More generally, in order to have an observable impact the NOM must form stronger complexes with Pu than water or the host rock material. This is because water and rock materials will be present at concentrations greatly exceeding NOM, expect under unsaturated conditions or in an organic rich vadose zone, which we would consider unique cases. For the purposes of this discussion, particularly with respect to “Pu transport

potential," fully saturated subsurface conditions are assumed and transport is assumed to occur by prolonged stability in the aqueous phase either as a solute or as a suspended solid. Through this work, natural organic matter was found to influence Pu stability in the aqueous phase either as a solute or as a suspended solid by 1) formation of dissolved Pu-NOM complexes; 2) formation of ternary Pu-NOM-surface complexes; 3) formation of ternary complexes on inorganic colloids; and/or 4) Pu sequestration/sorption to aggregated NOM colloids.

Formation of Dissolved Pu-NOM Complexes

Soluble Pu-NOM complexes will increase the Pu transport potential by means of decreasing the fraction of Pu sorbed to the host rock, relative to an NOM-free system. This was observed in both Chapter Three and Chapter Four at circumneutral pH. Chapter Three noted that the observed decrease in Pu sorption in the presence of $50 mg_C \cdot L^{-1}$ NOM followed the trend DFOB > fulvic acid > humic acid > citric acid. Concluding that the influence of NOM on Pu sorption was primarily controlled by 1) the strength of the Pu-NOM complex and 2) the affinity of NOM for the mineral. Chapter Four found that Pu-citrate species dominated Pu speciation from pH 2 to approximately pH 7 when 10^{-10} M Pu was in the presence of 10^{-4} M citrate, but that 10^{-6} M citrate was unable to out-compete binary Pu sorption to goethite or gibbsite under the same conditions. A typical groundwater might contain $0.7 mg_C \cdot L^{-1}$, which as citrate equals 9.7×10^{-6} M. Therefore, while it is possible that a natural groundwater would contain sufficient DOC to out-compete hydrolysis or sorption, it seems more likely that the DOC of concern from a waste management perspective would be DOC introduced by anthropogenic activity. There are notable exceptions however, such as groundwater associated with gas and oil fields.

Anthropogenic DOC would likely be from co-disposed organic materials or organic debris from repository construction. At higher concentrations of DOC, dissolved Pu-NOM complexes could become a principal transport mechanism so long as the DOC remains mobile. Dominance of Pu-citrate species in the presence of 10^{-4} M citrate (50 $mg_C \cdot L^{-1}$) clearly demonstrates a condition where the affinity of NOM for the mineral will determine the transport potential of the Pu (Chapter Four).

Formation of Ternary Pu-NOM-Surface Complexes

Under some surface/solution conditions, NOM will sorb to minerals. If the NOM maintains its affinity for complexing Pu while sorbed to host rock material, ternary Pu-NOM-surface complexes can form. Chapters Three and Four demonstrate that ternary Pu-NOM-surface complexes are most likely to be present below pH 4. Chapter Four also demonstrates that while citrate will sorb to alkaline pH, it is below pH 4 that citrate is sorbed by a ligand exchange mechanism; and therefore, has free carboxylic groups available to bind Pu. Chapter Three confirms that ligands that exhibit minimal sorption themselves, such as DFOB, do not produce ternary Pu-NOM-surface complexes. In fact, the Pu:DFOB ratio on the surface was less than the Pu:DFOB ratio in solution, suggesting that what little DFOB had sorbed to goethite was less able to simultaneously interact with Pu. An inability to simultaneously interact with Pu and a surface, likely caused by a limited number of reactive functional groups on an NOM molecule, would prevent ternary Pu-NOM-mineral complex formation. This suggests that in some cases, while ternary Pu-NOM-mineral complexes might be thermodynamically favorable, formation could be hindered by steric constraints. In cases where ternary complexes do form, Chapter Three demonstrates that the thermodynamic affinity for ternary complexes increases with the

NOMs thermodynamic affinity for the surface. Ternary Pu-NOM-mineral complexes effectively increase the affinity of Pu for the surface under conditions where binary Pu sorption is out competed by Pu-NOM complexes or surface sites are consumed by NOM coatings. Therefore, so long as ternary Pu-NOM-surface complexes form on an immobile host rock surface, they will reduce the transport potential for Pu.

Formation of Ternary Complexes on Inorganic Colloids

The empirical efforts presented here required complete separation of the soluble and the solid-bound phases in order to measure the extent of sorption to the solid that occurred. Therefore, the preceding chapters do not quantitatively assess the formation of ternary complexes on inorganic colloids. It is important to realize however, that should ternary Pu-NOM-surface complexes form on mobile mineral surfaces, such as mineral colloids, these complexes will increase the transport potential for Pu. This is equally true for binary Pu sorption to mineral colloids. Ternary Pu-NOM-surface complexes are likely to form under similar conditions as NOM coatings on inorganic colloids, which may impact the mobility of those colloids. Natural organic matter coatings have been shown to enhance colloid transport by stabilizing colloids with negatively charged coatings. Unfortunately, the impacts of this effect may be difficult to predict. As in Chapter Three, where zeta potential measurements revealed a stable but positive surface charge on goethite in an NOM-free experiment, a stable but negative surface charge on goethite particles in 46 $mg_C L^{-1}$ humic acid solutions, and an unstable negative surface charge on goethite particles in 6 $mg_C L^{-1}$ humic acid solutions. Intermediate concentrations of NOM may therefore cause inorganic

colloids to aggregate and fall-out, while slightly higher concentrations stabilize the suspended colloid.

Formation of Plutonium-Natural Organic Matter Colloids

Natural organic matter aggregates were shown to have a large impact on Pu speciation under conditions where aggregates will form. In Chapter Three, a significant fraction of Pu was shown to be sequestered by intrinsic humic acid colloids below pH 4. Further, dynamic light scattering measurements demonstrated that the hydrophobically driven precipitation of humic acid with decreasing pH was a gradual process, rather than a discrete process as is often assumed by applying the operational definition of humic acid (soluble at pH > 2). It is ambiguous from this study whether the Pu is co-precipitated with the humic acid or sorbed to the surface of a humic acid particle. This difference, though experimentally difficult to differentiate, could be crucial to assessing Pu transport potential under conditions where such complexes might form. Consider a subsurface region where precipitation of NOM and co-precipitation of Pu is thermodynamically favorable. If transport of the NOM particle occurs, the co-precipitated Pu would be transported with the particle. Should that particle be transported to an environment where co-precipitation of Pu is no longer thermodynamically favorable, but the NOM particle does not disaggregate, the Pu could remain sequestered within the NOM particle despite the lack of thermodynamic favorability. Therefore, hysteretic considerations may be necessary when such aggregates are present in a system. This is an element of this study that warrants future study. Overall, the impact of Pu co-precipitated with NOM on Pu transport potential is dependent on the

mobility of the aggregate; likely governed by several properties including the stability of the aggregate, the size of the aggregate, and the pore size of the subsurface.

Future Work

The research presented here has identified several knowledge gaps key to understanding Pu and NOM speciation in the environment.

Future Research Needs:

1. Models describing NOM sorption to minerals at alkaline pH need improvement. It is evident that NOM will sorb to goethite and gibbsite above the point of zero charge. The diffuse-layer model however, fails to quantitatively describe the observed sorption due to the predicted repulsive electrostatics. In the case of citrate, it is unlikely to be caused by hydrophobicity as could be the case for larger NOM. Therefore, there must be a thermodynamic reason citrate is sorbed at alkaline pH, despite both the citrate and the surface carrying a negative charge. It seems likely that charge neutralization is occurring by some mechanism. If models describing citrate sorption to minerals improve, so will Pu sorption models in the ternary systems.
2. Pu-NOM complexation constants need improvement and trends in NOM character should be correlated to the binding constants. There are infinite molecular structures of organic matter in the world; therefore, it would be valuable to be able to estimate Pu-NOM thermodynamic behavior from the character of the NOM directly (free energy relationships).
3. Understanding the continuum between dissolved organic carbon and particulate organic carbon would facilitate a better understanding of organic carbon

complexation with metals. Previous studies suggest that dissolved organic carbon and particulate organic carbon of the same origin would behave similarly with respect to metal complexes. Experiment evidence of such however, is lacking.

4. Very generally, trace Pu chemistry at alkaline pH warrants further study. Most high-level waste repositories are likely to include concrete in some aspect of waste package or repository construction. The concrete will buffer the interstitial water to alkaline pH. While strong hydrolysis complicates study of Pu interactions with surfaces or organic ligands at alkaline pH, the need to understand trace Pu behavior at alkaline pH should be a sufficient driving force to study those systems.

APPENDICES

Appendix A

The Effect of Natural Organic Matter on Plutonium Sorption to Goethite

Supporting Information

Radiolabeling FA & HA

Radiolabeling of FA and HA was carried out using a procedure adapted from a previous study by Tinnacher and Honeyman[1]. Natural organic matter (10 - 12 mg) in 1 mL water was added to a 50 mL round bottom flask reaction vessel. The weighing vessel was rinsed three times with 0.5 mL of 0.1 M NaOH to ensure complete transfer and solubility of the NOM. A tritiated $NaBH_4$ solution was made from approximately 10 mg tritiated $NaBH_4$ (American Radiolabeled Chemicals, Inc.; S.A. 350 mCi/mmol) and 29.4 mg $NaBH_4$ (≥ 98% Sigma Aldrich) in 2 mL 0.1 M NaOH. This solution was used in all tritium labeling experiments. Through a gas tight addition funnel, 0.5 mL of the tritiated $NaBH_4$ solution was added to the reaction vessel; the funnel was carefully rinsed with DDI after the addition of all reagents to prevent early reduction outside of the reaction vessel. Zero-grade air was continuously bubbled through the reaction solution to remove any evolving hydrogen gas. The air and evolved gas mixture were passed through a column packed with a platinum catalyst (Alfa Aesar, 0.5% Pt on 2.7 – 3.3 mm alumina pellets) bed in order to oxidize any evolved hydrogen gas to water. Gas lines and the column were wrapped with a flexible heating cord and maintained at > 115 °C to prevent condensation of tritiated water in the gas lines. A cold trap was used to capture any water from the system before the remaining gases were vented into a radioisotope fume hood. Vented gases were continuously monitored for hydrogen gas by means of a lower explosive limit gas detector (TIF model:

8800A). The reaction was allowed to proceed at room temperature for 30 minutes, and then warmed in a 60 °C water bath for an additional 4 hours.

Removal of unreacted $NaBH_4$ was accomplished by a series of cleanup steps which differed from the original method of Tinnacher and Honeyman[1]. Cation exchange resin (~1 g, Bio-Rad MP-50) was added to the reaction vessel as a slurry after being preconditioned in columns by 10% HCl and rinsed with DDI. The cation exchange resin absorbs Na^+ ions, transforming $NaBH_4$ to HBH_4, which oxidizes to $B(OH)_3$ in the presence of water; this process can be monitored by measuring the pH as the resin will release significant quantities of H^+ ions during the uptake of Na^+ ions. Zero-grade air was continuously bubbled through the reaction solution while being held at 45 °C to purge tritium gas. In the original procedure, Tinnacher and Honeyman added methanol to react with the byproduct $B(OH)_3$ to form trimethyl borate ($B(OCH_3)_3$), then promptly rotoevaporated the sample to avoid methylation of reactive sites of FA (study was limited to FA) while removing trimethyl borate (b.p. 68 °C). The extent of FA methylation during this step would be difficult to predict and may affect the reactivity of the FA. It was therefore, decided to utilize a boron selective resin that had been used successfully for boron removal from aqueous systems in numerous previous studies[2–4] to prevent methylation of the NOM being labeled.

The solution was taken to dryness by bubbling with zero-grade air. The dried tritium labeled acids were dissolved in 7.5 mL DDI and removed from the reaction vessel. These solutions were treated with Amberlite IRA-743 free base resin (Sigma Aldrich), a boric acid and borate selective resin, after the pH was adjusted to 8; previous studies determined

that maximum boron removal occurred near pH 8.[4] IRA-743 resin has been used successfully for boron removal from aqueous solutions, however data on NOM uptake was unavailable. The procedure used was optimized for boron removal and NOM recovery in a separate experiment. Nine solutions with varying humic acid and boric acid were prepared and 10 mL of each solution was added to a centrifuge tube with 0.4 g of IRA-743 resin. The samples were shaken end-over-end from 1 to 10 minutes. Boron removal was determined by ICP-MS (Thermo Scientific X SERIES 2) and HA recovery was determined by UV-Vis absorption spectroscopy (Spectronic Instruments, SPECTRONIC 20 GENESYS) at 260 nm. The results are shown in Figure A1.

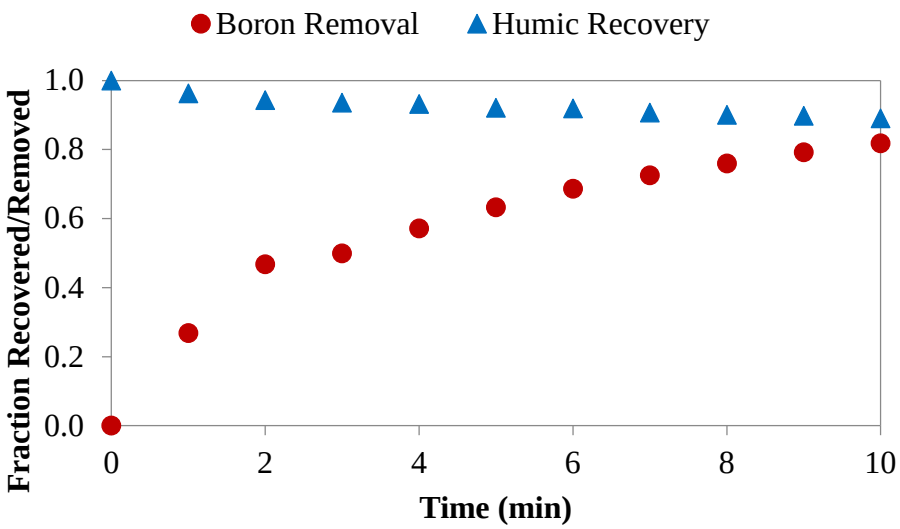

Figure A1. Removal of boric acid and recovery of humic acid using IRA-741 boron selective resin.

For labeling experiments, it was decided to limit resin contact time to 10 minutes to maximize NOM recovery whilst achieving significant boron removal. Although successive

contacts with fresh resin was also studied, a single contact was preferred due to improved HA recovery and reduced loss of solution with each decanting step.

Calculating Minimum Detectable Activity (MDA) & Surface Normalized Kd (Ka):

$$L_D = 4.65\ (\sigma N_B) + 2.71$$

L_D = limit of detection

σN_B = square root of the number of background counts per the count time.

$$MDA_{solution} = \frac{L_D}{(count\ time) \times\ \varepsilon}$$

MDA = minimum detectable activity

ε = counting efficiency

$$MDC_{solution}\ = MDA\ \times \frac{[NOM]}{(Stock\ Count\ Rate)}$$

MDC = minimum detectable concentration

[NOM] = concentration of natural organic matter in solution ($mg_C \cdot L^{-1}$)

"Stock Count Rate" = total activity count rate of Pu or NOM, per an equivalent sampling volume as experimental samplings.

Therefore,

$$K_a = \frac{\left(\frac{mg_C}{L}\right)_{total} - \left(\frac{mg_C}{L}\right)_{solution}}{\left(\frac{mg_C}{L}\right)_{solution}} \times \frac{L}{kg\ goethite} \times \frac{kg\ goethite}{m^2\ surface\ area}$$

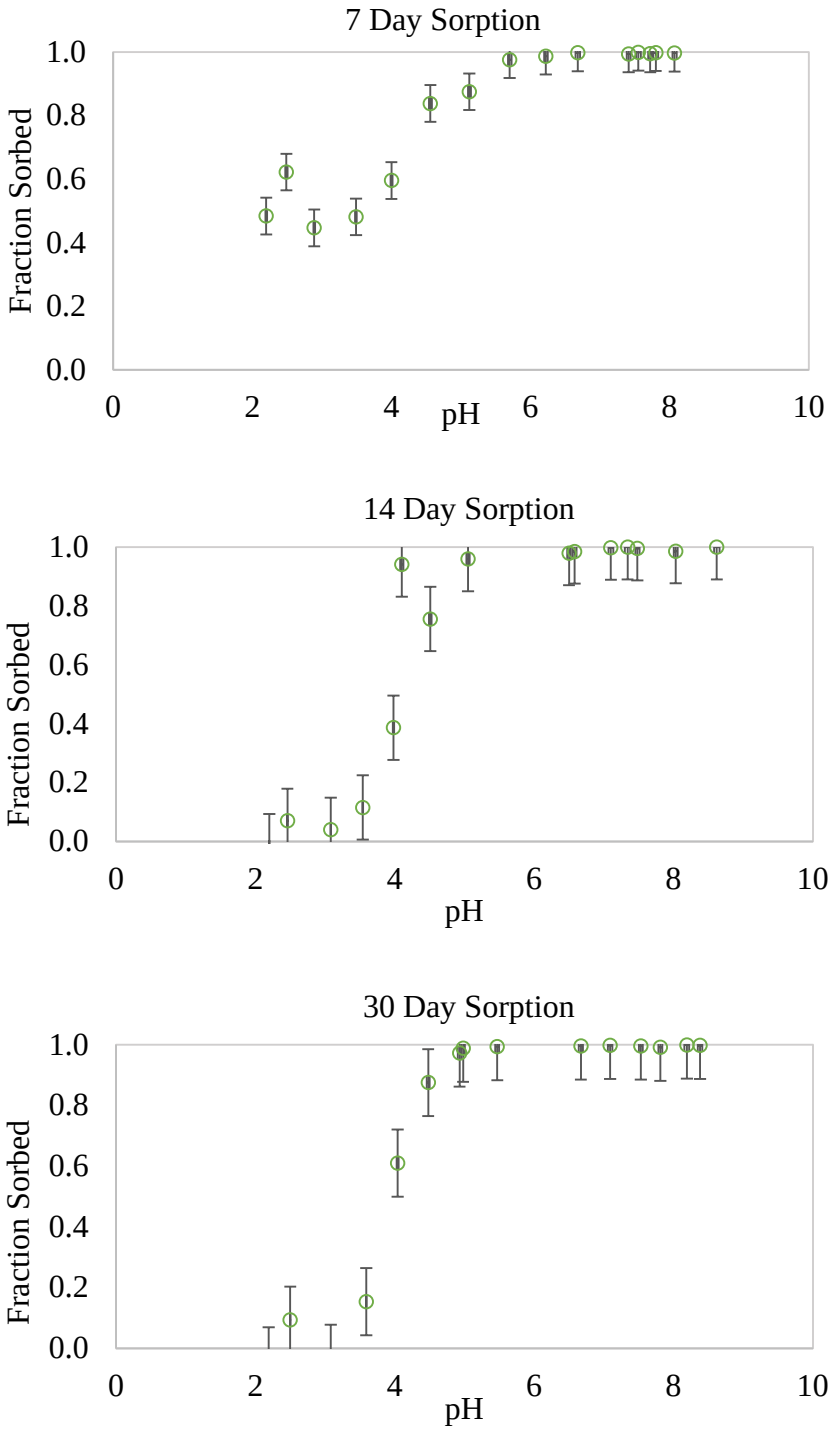

Figure A2. Plutonium (9.4×10^{-5} M) sorption to goethite (no NOM present) at 7, 14, 30 days.

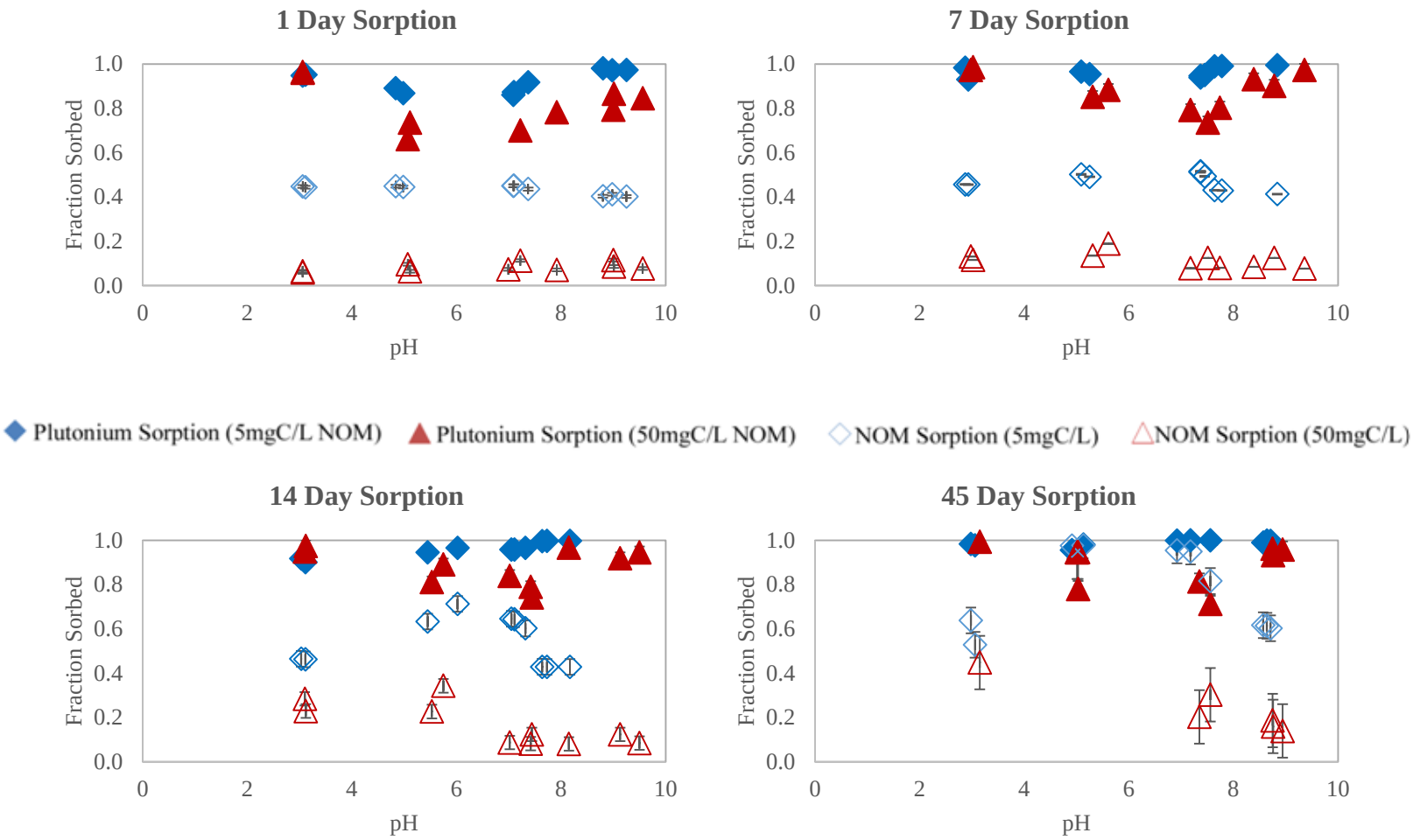

Figure A3. Citric acid and plutonium sorption to goethite at 1, 7, 14, and 45 days.

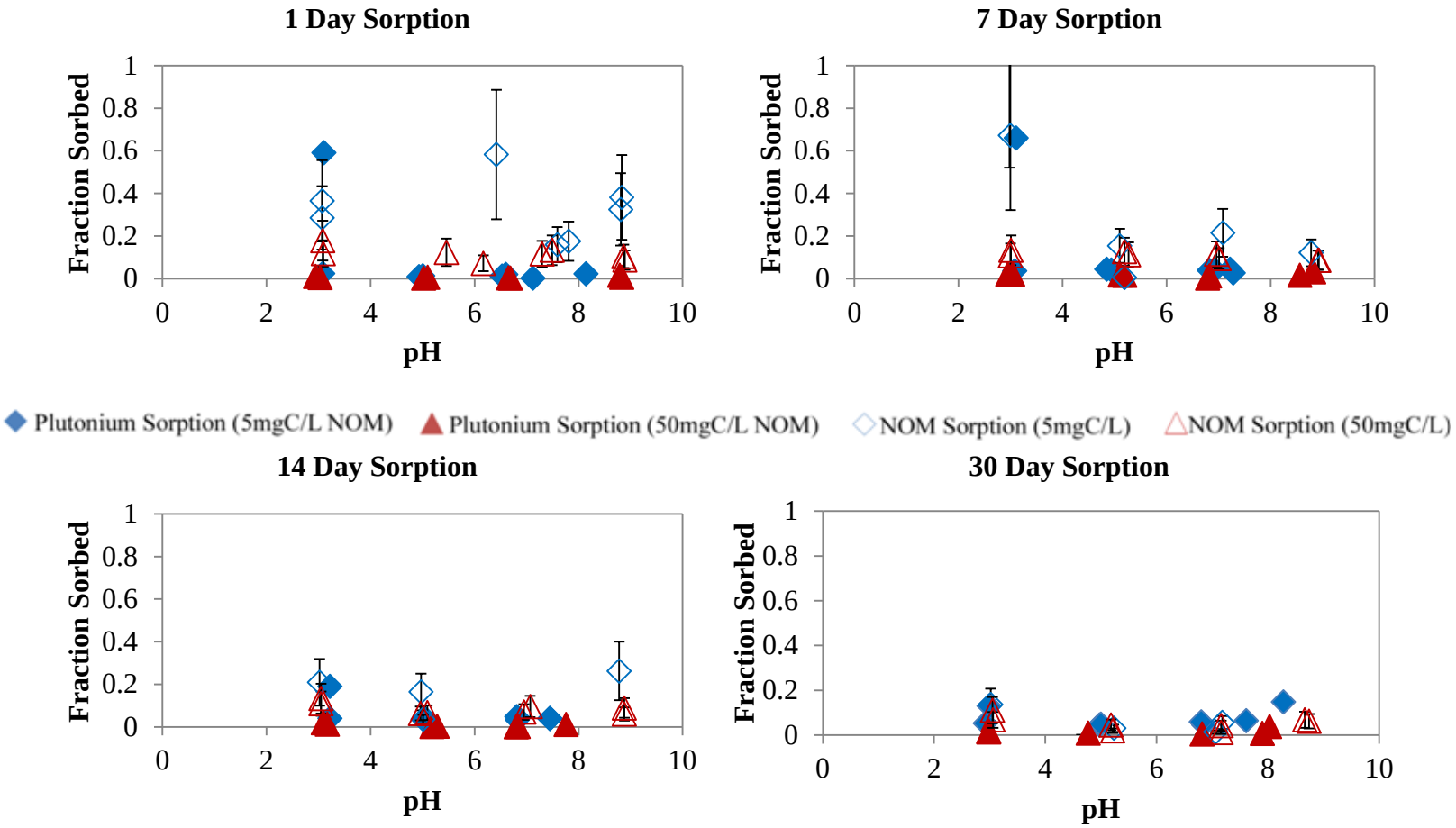

Figure A4. DFOB and plutonium sorption to goethite at 1, 7, 14, and 30 days.

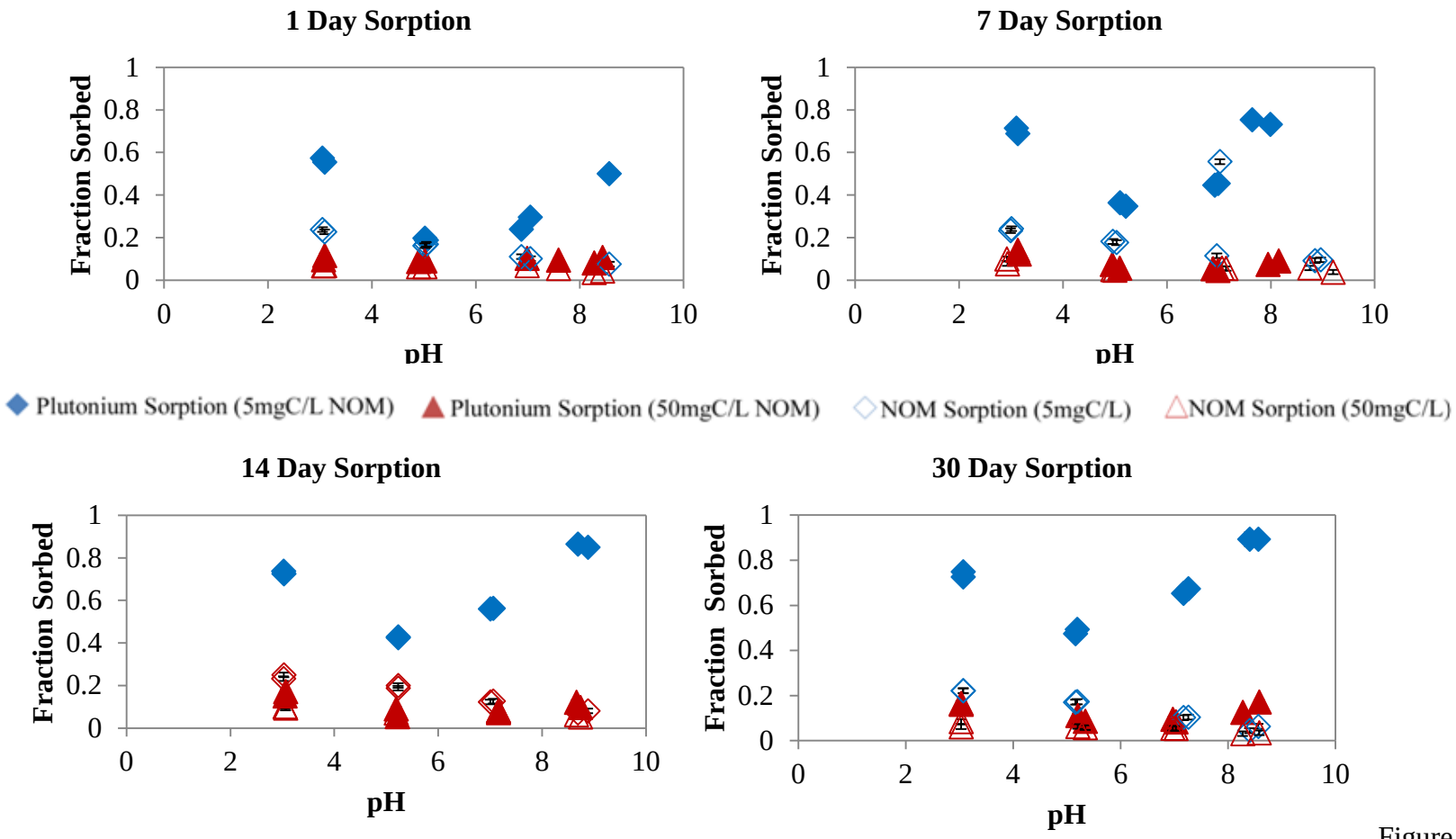

Figure A5. Fulvic acid and plutonium sorption to goethite at 1, 7, 14, and 30 days.

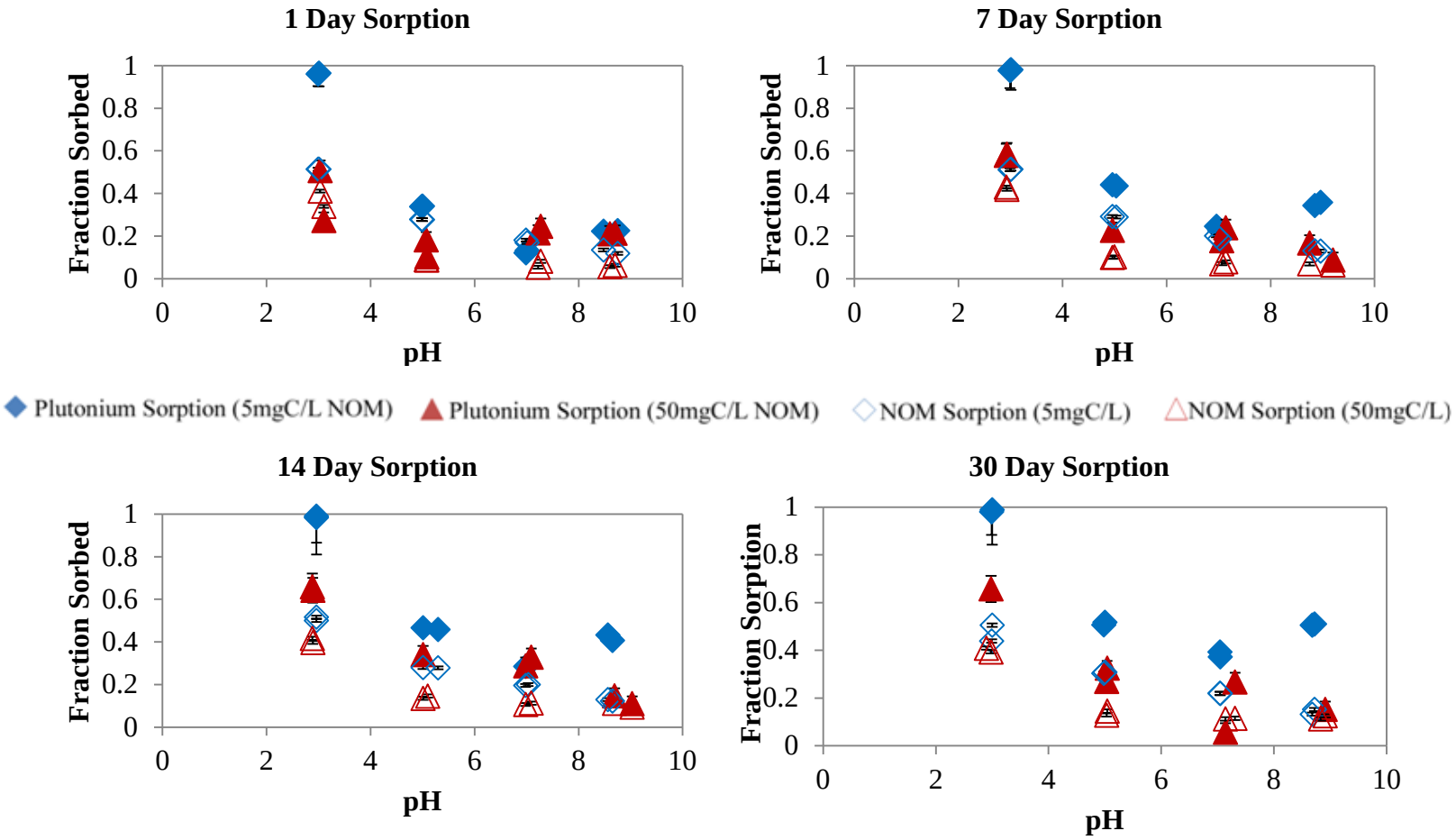

Figure A6. Humic acid and plutonium sorption to goethite at 1, 7, 14, and 30 days.

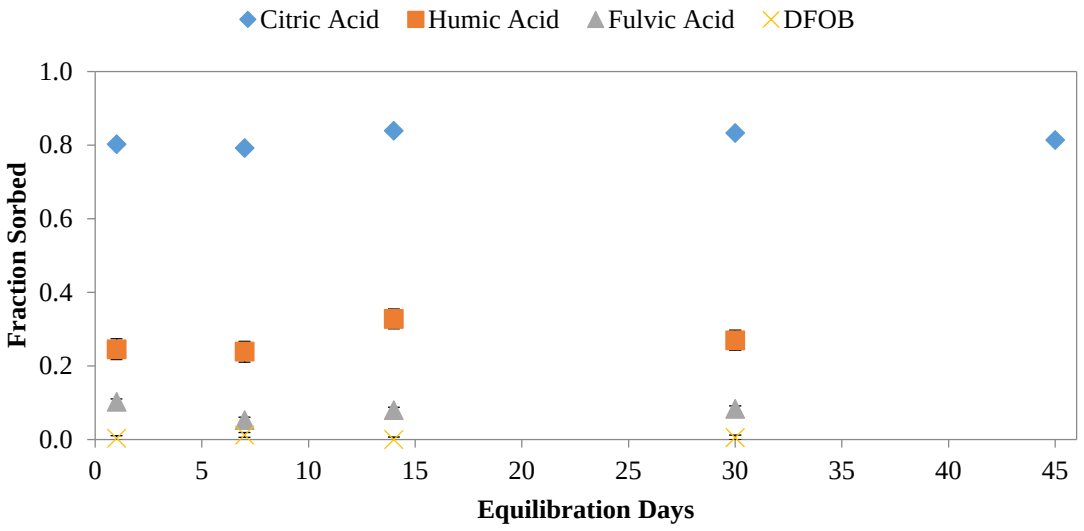

Figure A7. Fraction of ^{238}Pu (10^{-11} M) sorbed to goethite in the presence of the 50 $mg_C \cdot L^{-1}$ citrate, humic acid, fulvic acid, and DFOB, at approximately pH = 7, after 1, 7, 14, and 30 day equilibration periods.

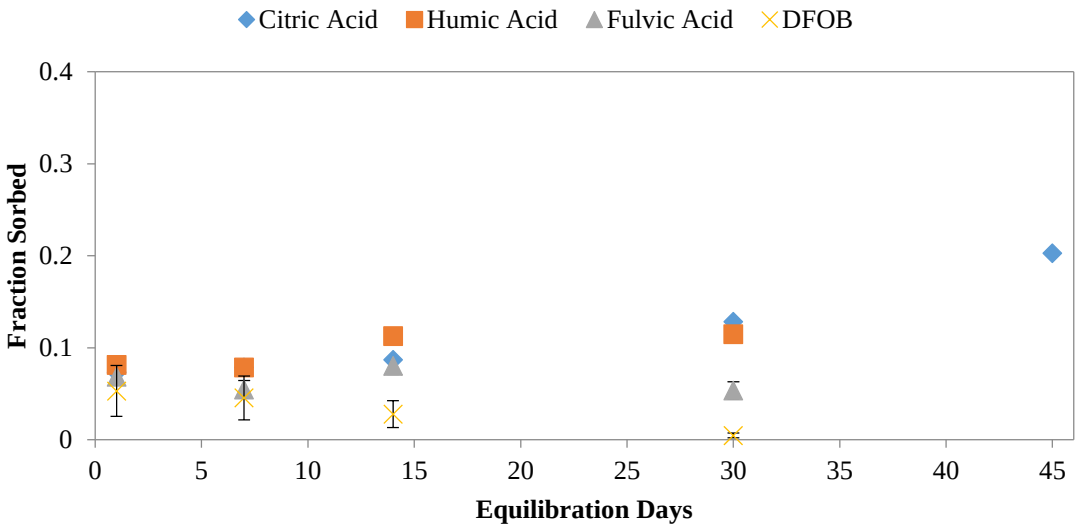

Figure A8. Fraction of NOM (~ 50 $mg_C \cdot L^{-1}$) sorbed to goethite at approximately pH = 7, after 1, 7, 14, and 30 day equilibration periods.

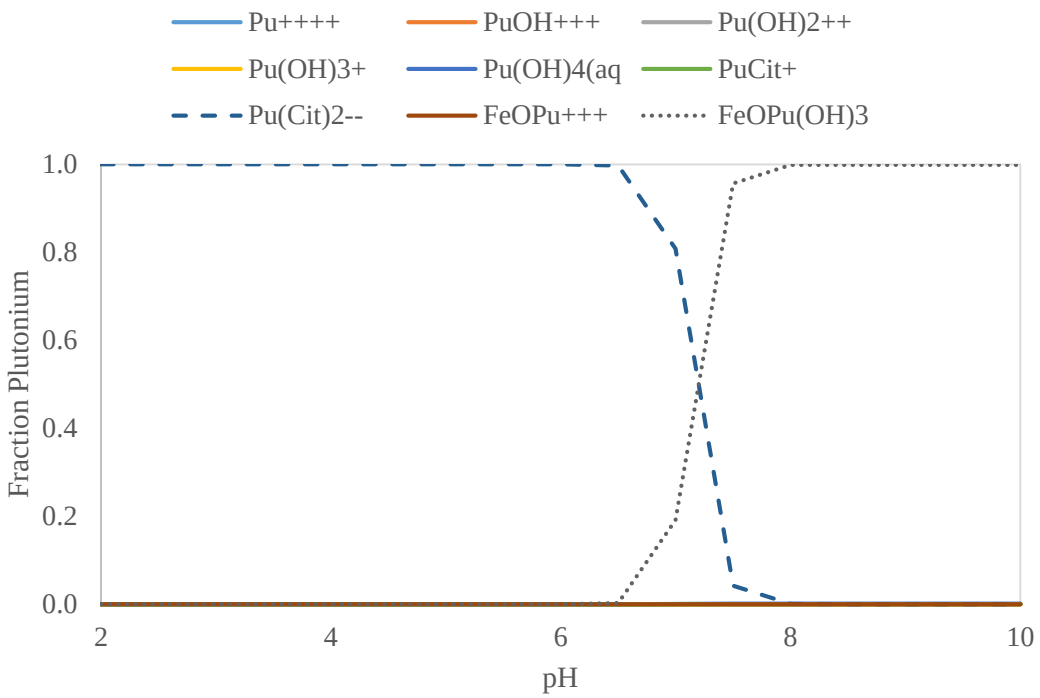

Figure A9. Speciation model of ^{238}Pu (6.5×10^{-10} M) in the presence of citric acid (6.93×10^{-4} M; 50.0 $mg_C \cdot L^{-1}$) and goethite (1.37×10^{-5} M sites; 0.092 $g \cdot L^{-1}$). Only binary Pu-CA, $Pu(OH)_x$, and Pu-goethite species are considered.

Speciation constants used are listed in Table A1. All species included in the model are listed in the legend, however most were not present in significant enough concentrations to be apparent in the figure.

Attenuated Total Reflectance Fourier-Transform Infrared Spectroscopy Experiments

There has been significant previous work identifying the mechanisms of ligand sorption to goethite. For a more detailed discussion of sorption mechanisms with respect to pH, ionic strength, and ligand concentration the authors recommend:

Citric Acid

- Cornell and Schindler, 1980
- Filius, Hiemstra, and Van Riemsdijk, 1997
- Lindegren, Loring, and Persson, 2009

DFOB

- Borer *et al.*, 2009

Fulvic Acid

- Gu *et al.*, 1994
- Fu and Quan, 2006

Humic Acid

- Petteys and Schimpf, 1998

This work sought to validate that the HA and FA used in this study behaved similarly to other NOM used in previous spectroscopic studies. Inferring sorption mechanisms through infrared spectroscopy is normally accomplished by observing differences between spectra of the surface complex and the “free” sorbent in the bulk solution. Here, we qualitatively evaluate those differences as well as apply a spectroscopic mathematical method not

previously used for NOM sorption to goethite. The spectra given here (A10 – A13) include the supernatant (bulk) ligand spectrum, the sorbed ligand spectrum (raw data), as well as a "goethite subtracted" spectrum in which the spectrum of goethite has been subtracted to remove the overtone bands of goethite for clarity (1662 cm^{-1} and 1788 cm^{-1}).

Previous studies of metal carboxylate complexes have found that the change in Δν (where $\Delta\nu = \nu_{as} - \nu_s$ of the carboxylate ion) between the free and sorbed carboxylate species, can be used to infer the sorption mechanism.[5–7] When Δν is significantly smaller for the sorbed carboxylate than the free carboxylate, a bidentate-mononuclear complex is inferred. When Δν increases upon sorption a monodentate-mononuclear complex is inferred. Small decreases in Δν upon sorption is indicative of a bridging-bidentate surface complex, involving both oxygens of the carboxylate and two surface metal atoms.

Citric Acid

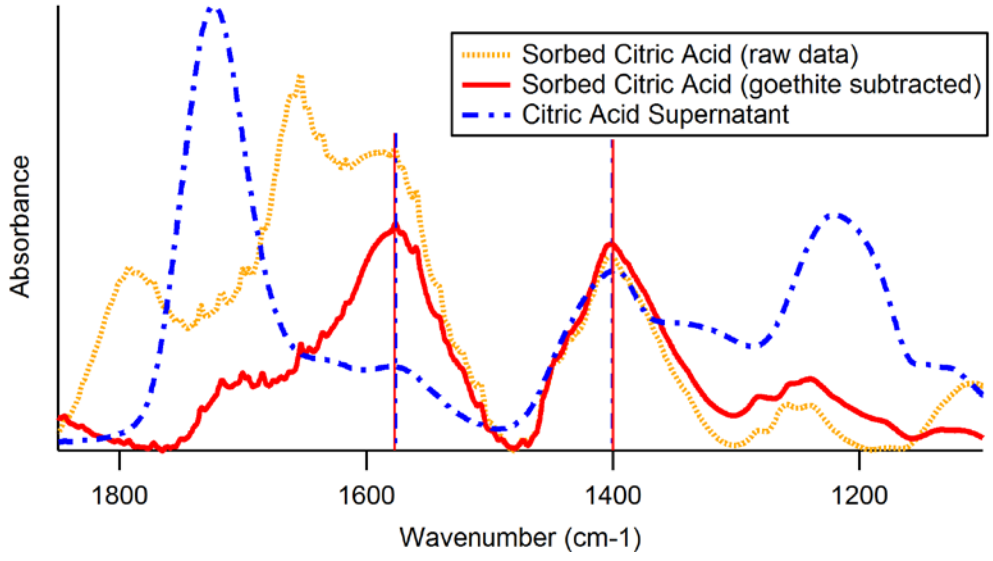

Figure A10. ATR-FTIR spectra of bulk CA and CA sorbed to goethite at pH 2.98.

Spectra from this study suggest bridging bidentate sorption of CA to goethite at both the terminal carboxylic groups. Upon sorption, the C=O peak near 1724 cm^{-1} decreases significantly relative to the $\nu_{as(COO-)}$ and $\nu_{s(COO-)}$ peaks found at 1577 cm^{-1} and 1401 cm^{-1}, respectively. Neither of these peaks was found to shift upon sorption, which together with the disproportionate C=O to COO- peak rations for the given pH strongly suggests a bridging bidentate sorption complex.

DFOB

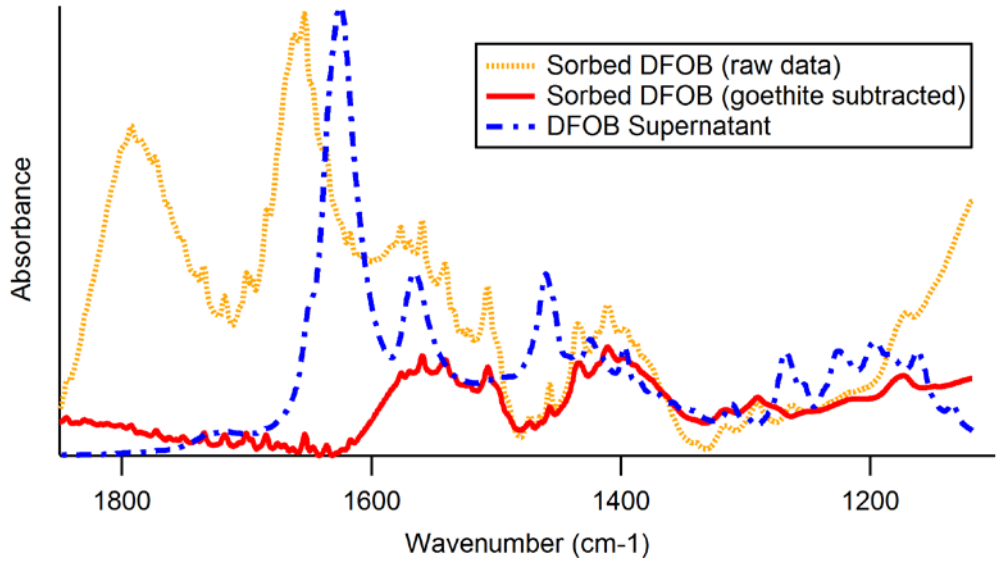

Figure A11. ATR-FTIR spectra of bulk DFOB and DFOB sorbed to goethite at pH 3.01.

There is no spectral evidence of DFOB sorption to goethite. None of the numerous DFOB vibrational bands were observable in the sorbed fraction. The sorbed fraction however, revealed peaks not characteristic of goethite. These peaks were attributed to the mesylate

salt of the DFOB mesylate salt reagent. Methylsulfonic acid has a very low pKa (-1.9) and will exist in solution as a sulfonate. The bands observed in the DFOB – goethite spectrum are consistent with a sorbed mesylate.[8] There is therefore, no spectral evidence of DFOB sorption to goethite, this agrees well with batch sorption data which showed very minimal removal of DFOB from solution by goethite.

Fulvic Acid

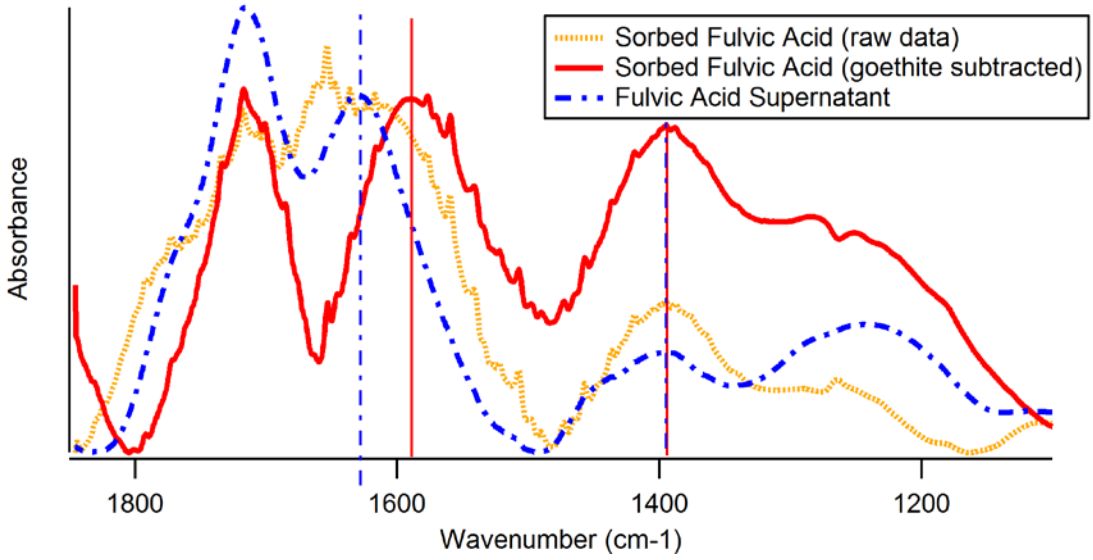

Figure A12. ATR-FTIR spectra of bulk FA and FA sorbed to goethite at pH 3.11.

The ATR-FTIR spectrum of FA after sorption to goethite at pH 3.1 demonstrated significant changes in the carbonyl region that were consistent with observations from previous studies (Gu et al. 1994; Fu and Quan 2006). Briefly, free carbonyl peak assignments were straightforward: $\nu_{(C=O)}$ = 1716 cm^{-1}, $\nu_{as(COO-)}$ = 1628 cm^{-1}, $\nu_{sym(COO-)}$ =

1394 cm^{-1}. Upon sorption, the asymmetric band is shifted 39 cm^{-1} to lower energy at 1589 cm^{-1} and the symmetric band remained centered at 1394 cm^{-1}. These shifts result in an overall decrease in the difference between the asymmetric and symmetric peak locations of 39 cm^{-1}. Such a shift is significant and suggests sorption of FA to goethite is occurring by a bidentate-mononuclear mechanism. It is noteworthy however, that a $\Delta\nu$ shift of 39 cm^{-1} is very near the, albeit arbitrary, cutoff previously cited[9] to delineate a bidentate-mononuclear and a bringing-bidentate complex. This suggests that both surface coordination complexes could be contributors to the overall sorption.

Humic Acid

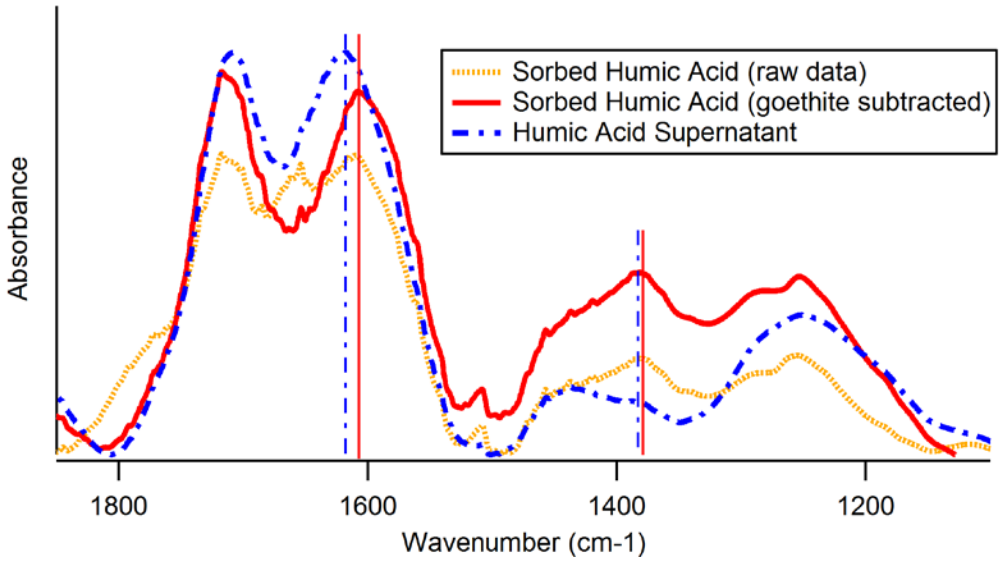

Figure A13. ATR-FTIR spectra of bulk HA and HA sorbed to goethite at pH 3.22.

The ATR-FTIR spectrum of HA sorbed to goethite was marginally different from HA and goethite independently, indicating minimal spectroscopically significant interaction

between HA and the goethite surface. While much of the $\nu_{as(COO-)}$ and $\nu_{a(COO-)}$ intensity appears unchanged, the maximum intensity of the $\nu_{as(COO-)}$ peak is shifted from 1618 cm^{-1} to 1607 cm^{-1} upon sorption and the maximum intensity of the $\nu_{a(COO-)}$ peak is shifted from 1383 cm^{-1} to 1379 cm^{-1} upon sorption. These shifts result in an overall decrease in the difference between the asymmetric and symmetric peak locations of 7 cm^{-1}, which suggests the formation of bridging-bidentate surface complexes. Minimal intensity losses at the free carbonyl peak locations, combined with little observable change in the C=O peak near 1710 cm^{-1} however, suggests minimal spectroscopically significant interaction between HA and the goethite surface. Coagulation of HA to form particle sized intrinsic aggregates could result in significant and sufficiently large HA colloids that the centrifuged retentate contained substantial intrinsic HA. Alternatively, previous studies have shown that HA tends to form multiple adsorption layers on hematite surfaces.[10] Driven by hydrophobicity, the formation of relatively thick layers of HA over a surface could shield the evanescent beam from an ATR-FTIR measurement from interacting with the functional groups at the goethite – HA interface. In the case presented above, since the majority of HA would be aggregated with itself, it would appear spectroscopically similar to aggregated HA. It is worth mentioning that FA tends to form monolayers on the same surfaces.[10] The decrease in intensity of the $\nu_{as(COO-)}$ stretch with respect to the $\nu_{sym(COO-)}$ stretch does not seem to be the result of surface sorption. The same relative decrease in intensity is observed in sample of HA that was hydrated and the freeze dried, which further suggests it is the effect of HA coagulation rather than surface sorption.

Characterization of Synthetic Goethite

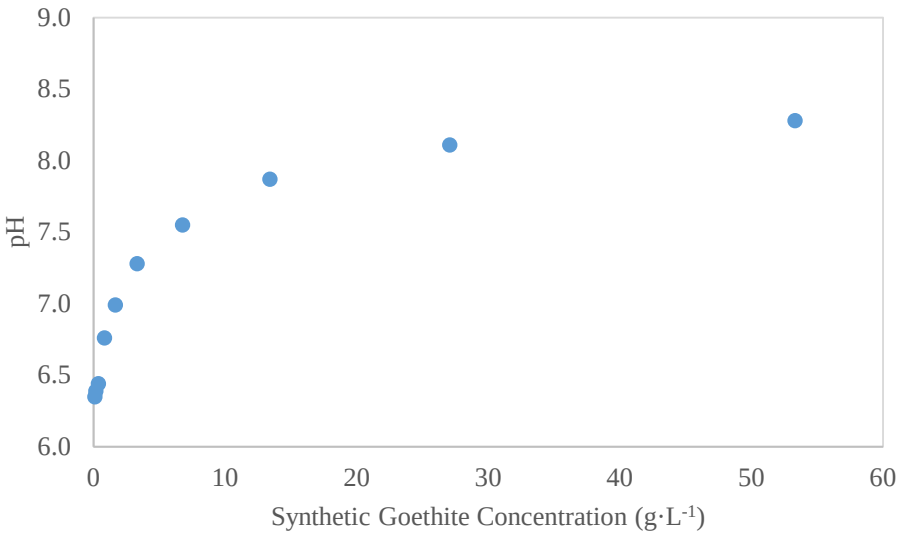

Figure A14. Mass titration of synthetic goethite to determine point of zero charge (pzc). The pzc of the synthetic goethite used in this work was determined to be 8.3 by mass titration in 0.01 M NaCl under anoxic CO_2-free conditions.

Thermodynamic Modeling

The complexation constants used for thermodynamic modeling in this study are listed in Table A1.

Table A1. Equilibrium Constants used in Modeling Approaches

Aqueous Reaction	log K	Reference
$Pu^{4+} + H_2O = Pu(OH)^{3+} + H^+$	0.6	*Neck, 2001*[11]
$Pu^{4+} + 2H_2O = Pu(OH)_2^{2+} + H^+$	0.6	
$Pu^{4+} + 3H_2O = Pu(OH)_3^{+} + H^+$	-2.3	
$Pu^{4+} + 4H_2O = Pu(OH)_4^{0} + H^+$	-8.5	
$Cit^{3-} + H^+ = HCit^{2-}$	6.36 ± 0.02	*Chem. Thermo., 2005*[12]
$Cit^{3-} + 2H^+ = H_2Cit^-$	11.14 ± 0.02	
$Cit^{3-} + 3H^+ = H_3Cit$	14.27 ± 0.02	
$Pu^{4+} + Cit^{3-} = PuCit^+$	15.3 ± 1	
$Pu^{4+} + 2Cit^{3-} = Pu(Cit)^{2-}$	30 ± 1	
$DFOB^{2-} + H^+ = HDFOB^-$	9.71 ± 0.16	*Boukhalfa, 2007*[13]
$DFOB^{2-} + 2H^+ = H_2DFOB$	18.68 ± 0.23	
$DFOB^{2-} + 3H^+ = H_3DFOB^+$	27.03 ± 0.25	
$Pu^{4+} + DFOB^{2-} + 2H^+ = PuH_2DFOB^{4+}$	35.48 ± 0.50	
$Pu^{4+} + DFOB^{2-} + H+ = PuHDFOB^{3+}$	34.87 ± 0.30	
$Pu^{4+} + DFOB^{2-} = PuDFOB^{2+}$	33.98 ± 0.90	
$Pu^{4+} + DFOB^{2-} + H2O = PuDFOB(OH)+$	27.33 ± 0.05	
$Pu^{4+} + 2DFOB^{2-} + 2H^+ = PuH_2DFOB_2^{2+}$	62.30 ± 0.19	
$HA^- + H^+ = H(HA)$	7.00	*Zimmerman, 2014*[14]
$Pu^{4+} + H(HA) + 2H_2O = Pu(OH)_2(HA)^+$	6.76 ± 0.14	
$FeOH = FeO^- + H^+$	-9.17	*Wang, 2001*[15]
$FeOH = FeOH_2^+$	7.35	

A Diffuse Layer Model (DLM) was used to simulate adsorption behavior. Goethite surface charge reactions from Wang *et al.*[15] were used, which agree with the goethite pzc measurements from this study (pzc = 8.3; Figure A14). A surface site density of 2.31 ×

10^{18} sites·m^{-2} was used. The binary Pu-goethite system was modeled using two surface species: $FeOPu^{3+}$ (logβ = 17.05) and $FeOPu(OH)_3$ (logβ = -0.54) (Figure A15).

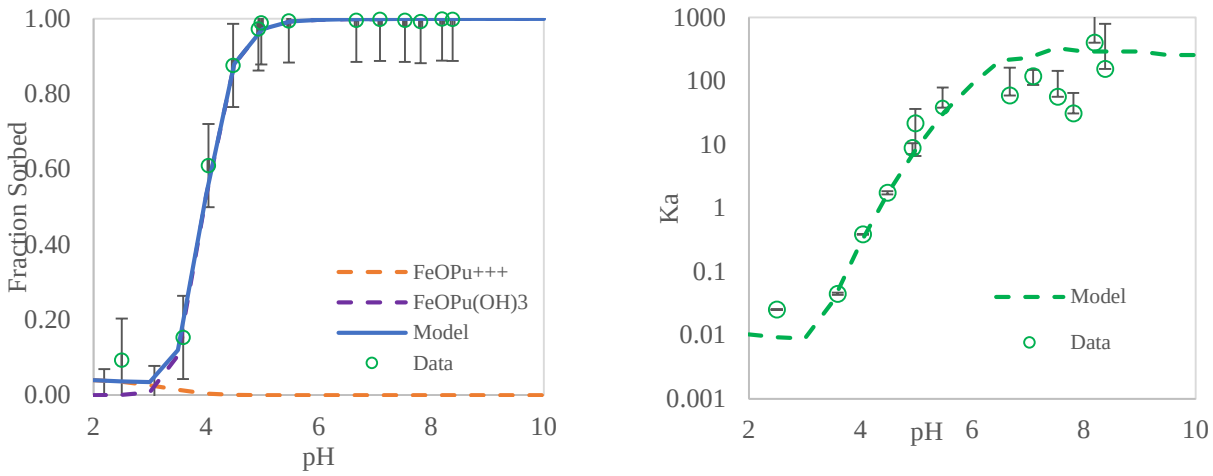

Figure A15. Model Pu sorption to goethite in fraction sorbed (left) and K_a (right).

A comparsion of Pu(IV)-goethite sorption constants with those reported by Wang *et al.* revealed some differences. Wang *et al.*[15] modeled the Sanchez *et al.*[16] dataset using $FeOPu^{3+}$ (logβ = 14.33) and $FeOPu(OH)_3$ (logβ = -3.92), as well as $FeOPu(OH)^{2+}$ (logβ = 8.79) (Figure A16, left). The differences between the work by Wang *et al.*[15] and this study can be partially attributed to the different Pu(IV) hydrolysis constants used. Wang *et al.*[15] used: $Pu(OH)^{3+}$ = -0.5; $Pu(OH)_2^{2+}$ = -2.32; $Pu(OH)_3^{+}$ = -5.38; $Pu(OH)_4^{0}$ = -9.52; while this study used the hydrolysis constants given in Table A2. The best fit to the Sanchez *et al.*[16] dataset using the Pu-hydrolysis constants from this study used the equilibrium constants: $FeOPu^{3+}$ logβ = 16.66; $FeOPu(OH)_3$ logβ = -1.34; and $FeOPu(OH)^{2+}$ logβ = 11.86 (Figure

A16, right); which are inbetween the constants obtained by Wang *et al.* and this study, suggesting a combined effect of different hydrolysis constants, as well as differences in the data.

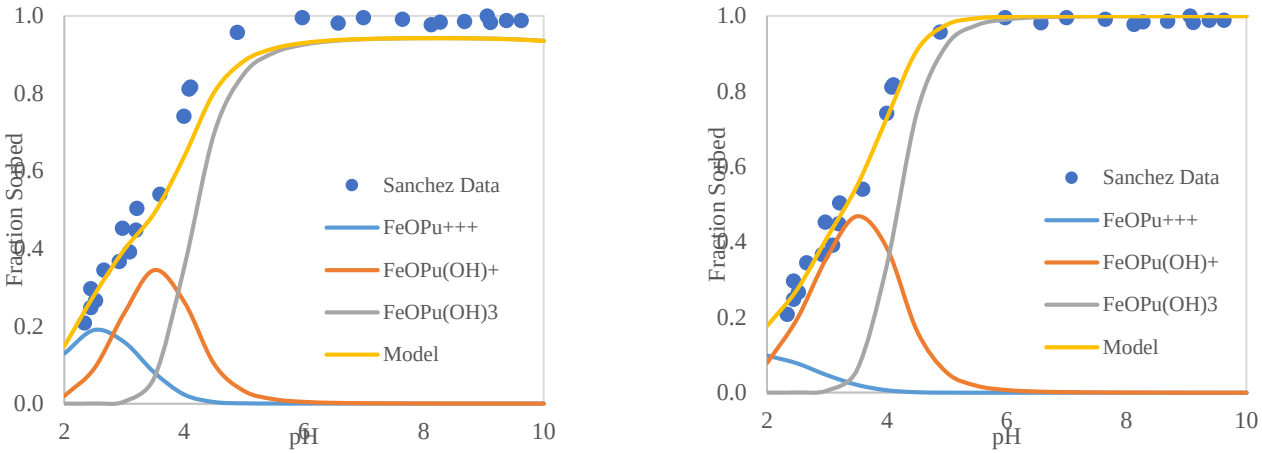

Figure A16. Sanchez *et al.* (1985) 10^{-11}M Pu to goethite soprtion data. Modeled using constants by Wang *et al.* (left), and best fit by this study (right).

Sanchez *et al.*[16] used equilibrium times of 1-24 hours and this study used 30 days, which could account for the differences. When plotted with the surface complexation constants from this study however, and viewed in fraction sorbed rather than Kd, the data match the model quite well. Overall, while there could be small differences in the datasets with regards to sorption time, the differences could just as well be the effect of uncertainties characteristic of the data. .

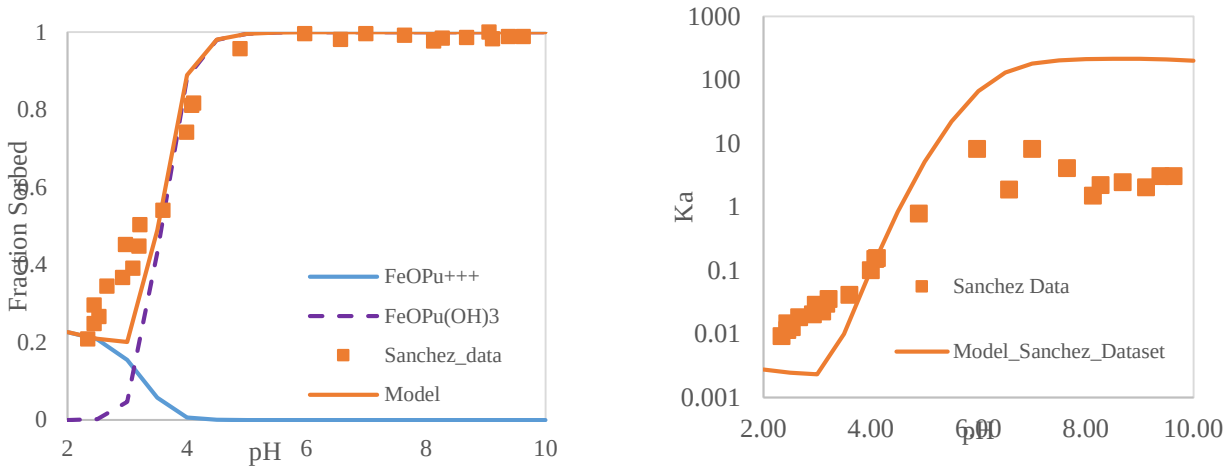

Figure A17. Sanchez *et al.*[16] 10^{-11}M Pu to goethite soprtion data in fraction sorbed (left) and K_a (right). Modeled using constants used in this study.

Only one significant figure was reported of Pu concentration and no counting statistics were reported. Its worth noting that under the conditions reported by Sanchez *et al.* (^{238}Pu; 10^{-11}M) counting times for samples with > 97 % sorption would have needed to exceed 15 hours per sample in order to result in 1 % error. The difference between a reported K_a of 10 and 100 is translated from a fraction sorbed difference of 97.4 % and 99.7%. Therefore, descrepancies in data above pH 4 could be the result of inherant uncertainity in the data reported.

References

(1) Tinnacher, R. M.; Honeyman, B. D. A New Method to Radiolabel Natural Organic Matter by Chemical Reduction with Tritiated Sodium Borohydride. *Environ. Sci. Technol.* **2007**, *41* (19), 6776–6782.

(2) Arias, M. F. C.; Bru, L. V. i; Rico, D. P.; Galvañ, P. V. Comparison of ion exchange resins used in reduction of boron in desalinated water for human consumption. *Desalination* **2011**, *278* (1–3), 244–249.

(3) García-Soto, M. del M. de la F.; Muñoz Camacho, E. Boron Removal by Processes of Chemosorption. *Solvent Extr. Ion Exch.* **2005**, *23* (6), 741–757.

(4) Özdemir, M.; Kıpçak, İ. Boron recovery from borax sludge using solid–liquid extraction followed by sorption with a boron selective resin in column. *Environ. Prog.* **2007**, *26* (4), 375–383.

(5) Tunesi, S.; Anderson, M. A. Surface effects in photochemistry: an in situ cylindrical internal reflection-Fourier transform infrared investigation of the effect of ring substituents on chemisorption onto titania ceramic membranes. *Langmuir* **1992**, *8* (2), 487–495.

(6) Yost, E.; Tejedor-Tejedor, M. I.; Anderson, M. In Situ CIR-FTIR Characterization of Salicylate Complexes at the Goethite/Aqueous Solution Interface. *Environ. Sci. Technol.* **1990**, *24*, 822–828.

(7) Nakamoto, K. *Infrared and Raman Spectra of Inorganic and Coordination Compounds.*, 6th ed.; Wiley: Hoboken, N.J, 2009.

(8) Givan, A.; Loewenschuss, A.; Nielsen, C. J. Infrared spectrum and ab initio calculations of matrix isolated methanesulfonic acid species and its 1:1 water complex. *J. Mol. Struct.* **2005**, *748* (1–3), 77–90.

(9) Lefèvre, G.; Precanin, T.; Lützenkirchen, J. Attenuated Total Reflection - Infrared Spectroscopy Applied to the Study of Mineral - Aqueous Electrolyte Solution Interfaces: A General Overview and a Case Study. In *Infrared Spectroscopy - Materials Science, Engineering and Technology*; 2012.

(10) Petteys, M. P.; Schimpf, M. E. Characterization of hematite and its interaction with humic material using flow field-flow fractionation. *J. Chromatogr. A* **1998**, *816* (2), 145–158.

(11) Neck, V.; Kim, J. Solubility and hydrolysis of tetravalent actinides. *Radiochim. Acta* **2001**, *89*, 1–16.

(12) Martell, A. E.; Smith, R. M. Critical Stability Constants, Standard Reference Database 46, Version 6.0. National Institute of Standards 2001.

(13) Boukhalfa, H.; Reilly, S. D.; Smith, W. H.; Neu, M. P. EDTA and Mixed-Ligand Complexes of Tetravalent and Trivalent Plutonium. *Inorg. Chem.* **2004**, *43* (19), 5816–5823.

(14) Zimmerman, T.; Zavarin, M.; Powell, B. A. Influence of humic acid on plutonium sorption to gibbsite: Determination of Pu-humic acid complexation constants and ternary sorption studies. *Radiochim. Acta* **2014**, *102* (7).

(15) Wang, P.; Anderko, A.; Turner, D. R. Thermodynamic Modeling of the Adsorption of Radionuclides on Selected Minerals. I: Cations. *Ind. Eng. Chem. Res.* **2001**, *40* (20), 4428–4443.

(16) Sanchez, A. L.; Murray, J. W.; Sibley, T. H. The adsorption of plutonium IV and V on goethite. *Geochim. Cosmochim. Acta* **1985**, *49*, 2297–2307.

Appendix B

A Novel Method for Tracer Level Plutonium(V) Solution Preparation

Supporting Information

Reduction in pH with Ozonation

Throughout this work, a significant increase in $\{H^+\}$ activity was measured regardless of the starting conditions. It was deduced nitrogen oxide must be generated within the ozone generator, from the input of room air. Once nitrogen oxide is introduced into an aqueous solution it can react with water to form nitrous acid (pk_a= 3.4) and nitric acid (pk_a= -1.4) by the same mechanism NO_x produces acid rain in the atmosphere:

$$2NO_2 + H_2O \rightarrow HNO_2 + HNO_3$$

Introduction of these acids will reduce the aqueous solution pH regardless of the starting NO_3 or Pu concentrations. Deprotonation of nitric acid in solution will likewise introduce significant concentrations of NO_3. To confirm the introduction of NO_3, ozone was bubbled through distilled deionized water (18 $M\Omega \cdot cm^{-1}$) with an ion-selective electrode sensitive to nitrate (Orion 9300 NO_3 ISE/ Orion 900200 reference electrode) (Figure B1).

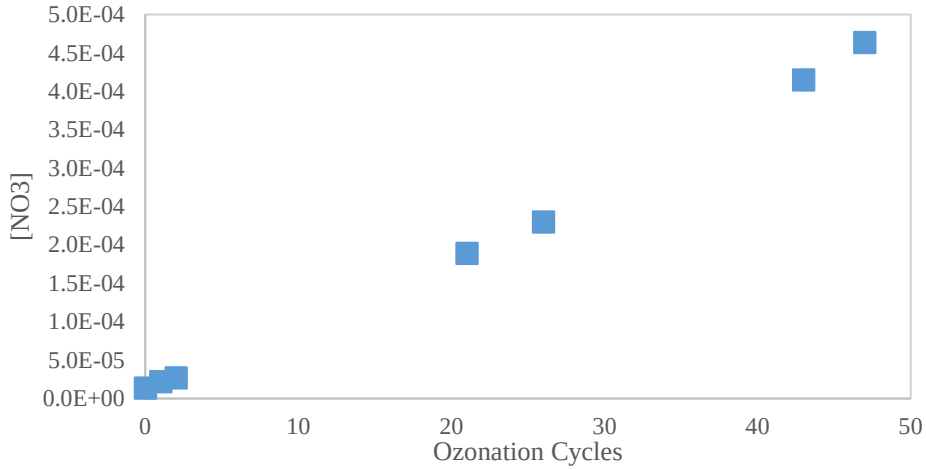

Figure B1. Nitrate concentration in DDI water with ozone generator gases introduced by program 10 (cycle = 20 minutes on / 40 minutes off).

Attempts were made to correlate nitrate concentration to decrease in pH and to confirm that the decrease in pH was similar in the Pu experiment as with only DDI water. We found that the decrease in pH was inconsistent across multiple samples with respect to the number of ozonation cycles (Figure B2); note the differences in pH between two samples of DDI water. The authors attribute this to the rudimentary nature of the ozone generator used as well as inherent inconsistencies in nitrogen oxide and ozone diffusion from a relatively violent bubbling through a small volume.

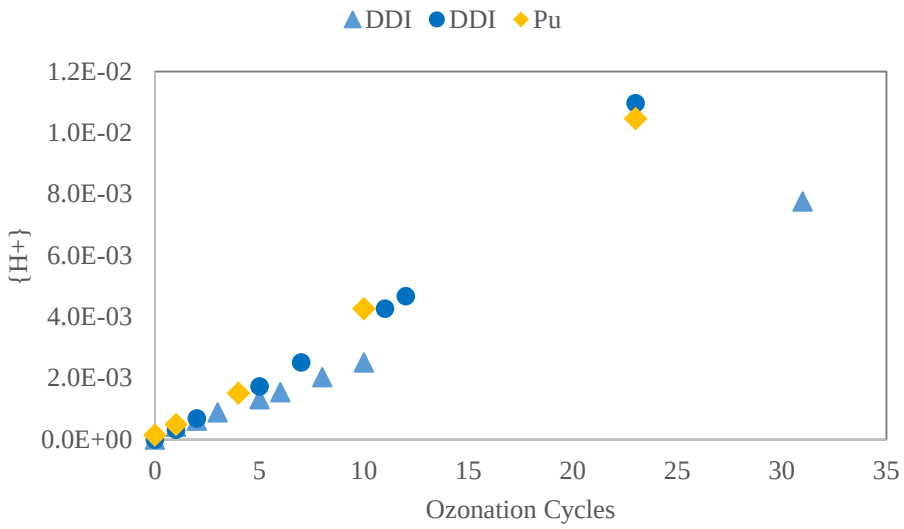

Figure B2. $\{H^+\}$ activity of Pu (2.26×10^{-8} M) solution and DDI H_2O solutions ozone generator gases introduced by program 10 (cycle = 20 minutes on / 40 minutes off).

Nevertheless, despite the crude nature of the ozonation process, stable solutions of Pu(V) were produced in high purity with minimal sample intervention and with few byproducts making this a practical method for trace Pu(V) solution preparation.

Appendix C

Ternary Mineral-Citrate-Plutonium(IV) Speciation on Goethite and Gibbsite

Supporting Information

Mass Titration of Synthetic Goethite

The point of zero charge (pzc) of the synthetic goethite used in this work was determined to be 8.3 by mass titration in 0.01 M NaCl under anoxic CO_2-free conditions.

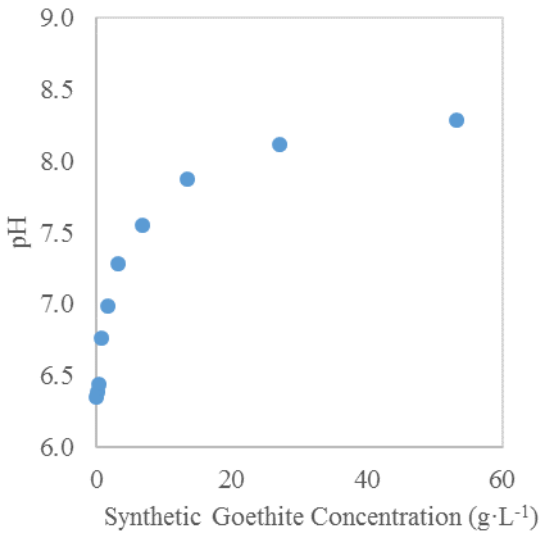

Figure C1. Mass titration of synthetic goethite to determine point of zero charge (pzc).

Speciation of Pu(IV) predicted by Nebel Constants

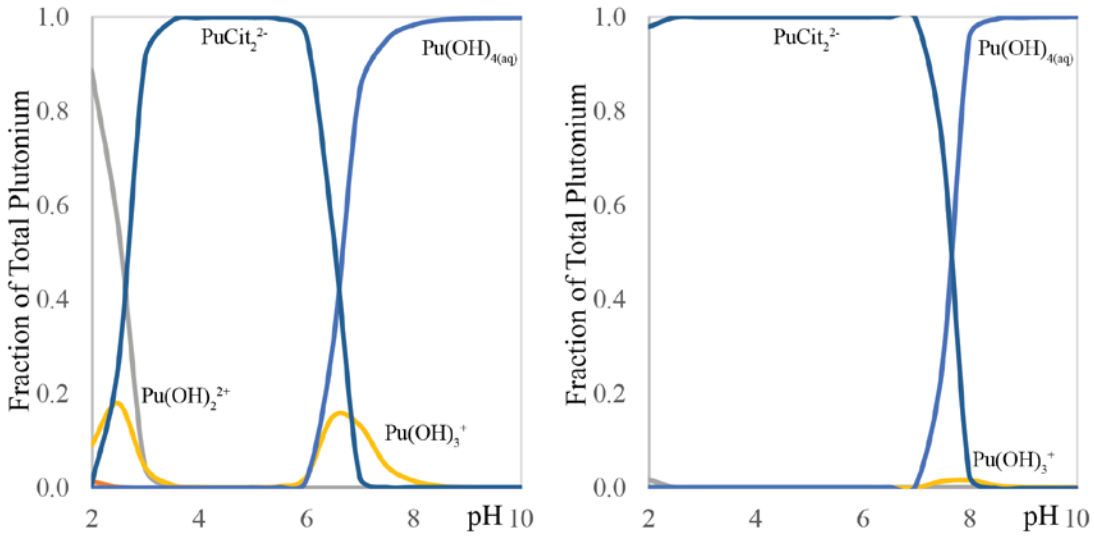

Figure C2. Pu (10^{-10} M) speciation predicted by the Pu-citrate binding constants Nebel[69] under the solution conditions of the current study: 0.01 M NaCl, 10^{-6} M citrate (left), and 10^{-4} M citrate (right).

Modeling Exercises with Metivier & Guillaumont

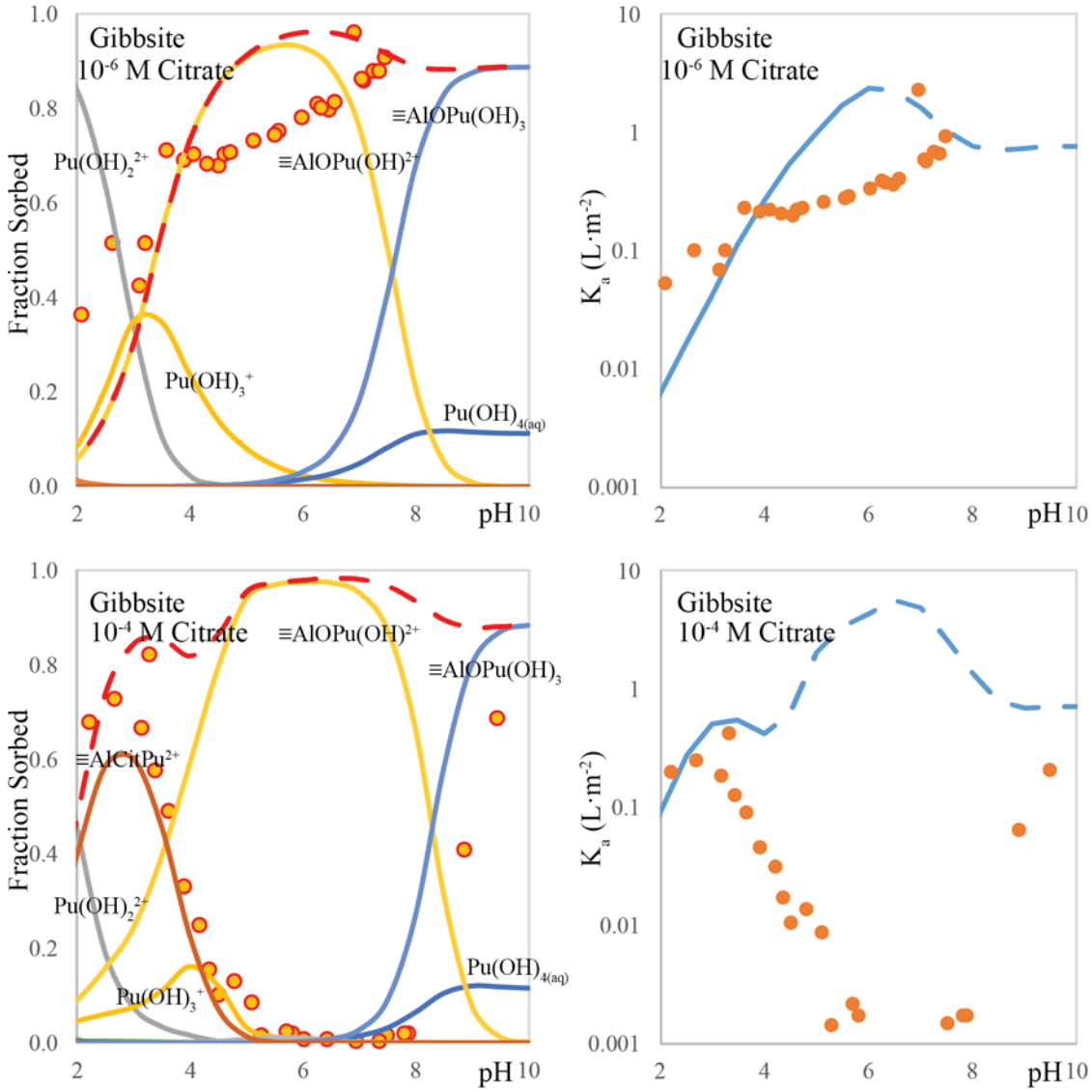

Figure C3. Pu (10^{-10} M) sorption to 5.5 g·L^{-1} gibbsite in the presence of 10^{-6} M (top) and 10^{-4} M (bottom) citrate. Pu-citrate complexation predicted using the reactions and constants by Metivier and Guillaumont.[70] Fraction sorbed (left) and surface area normalized distribution coefficent (right). Data given by circles, model fit by lines. The total sorbed fraction is given as a dashed red line.

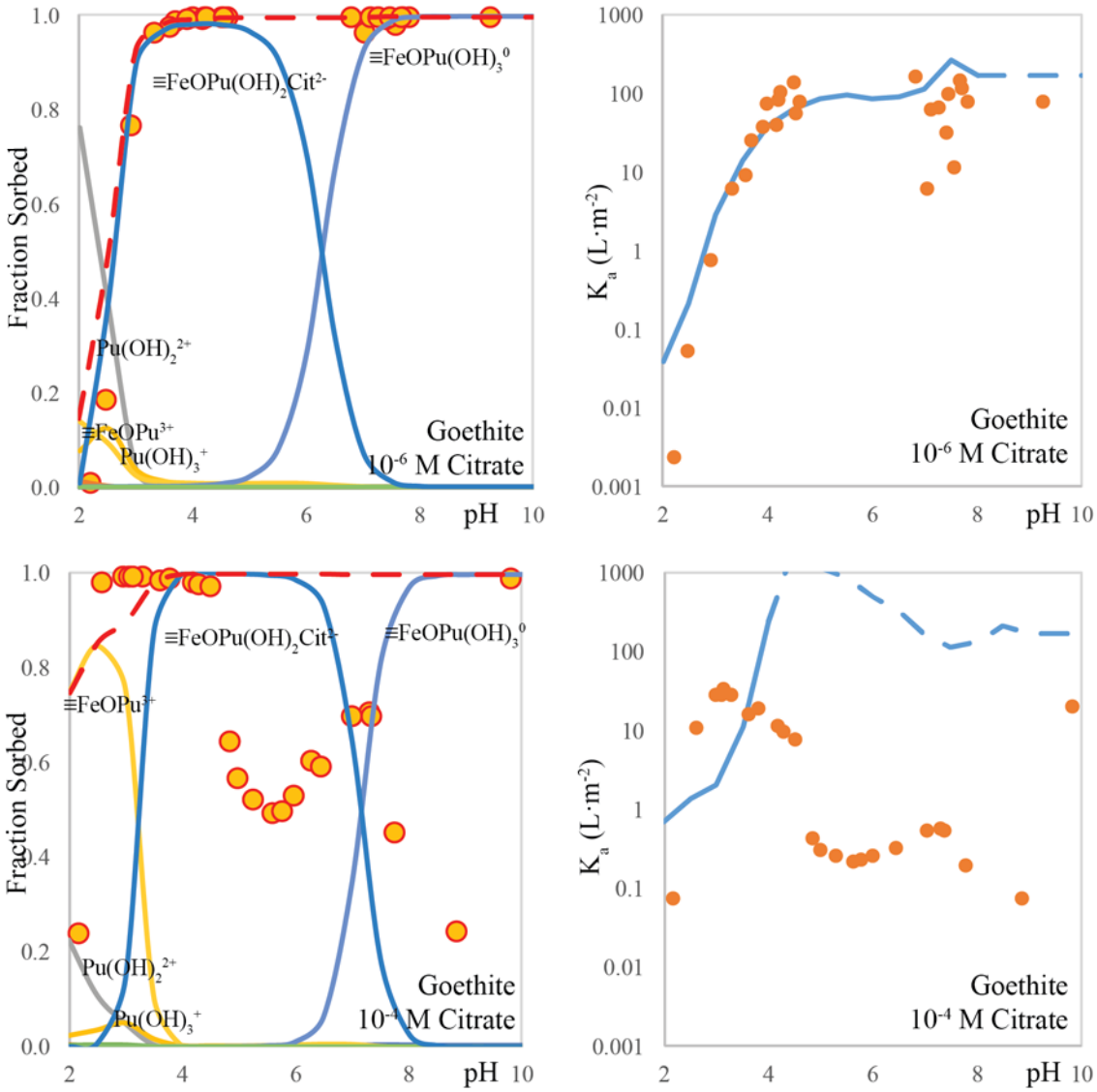

Figure C4. Pu (10^{-10} M) sorption to 0.11 g·L^{-1} goethite in the presence of 10^{-6} M (top) and 10^{-4} M (bottom) citrate. Pu-citrate complexation predicted using the reactions and constants by Metivier and Guillaumont.[70] Fraction sorbed (left) and surface area normalized distribution coefficent (right). Data given by circles, model fit by lines. The total sorbed fraction is given as a dashed red line.

Citrate Sorption to Analig-Pu02 Resin

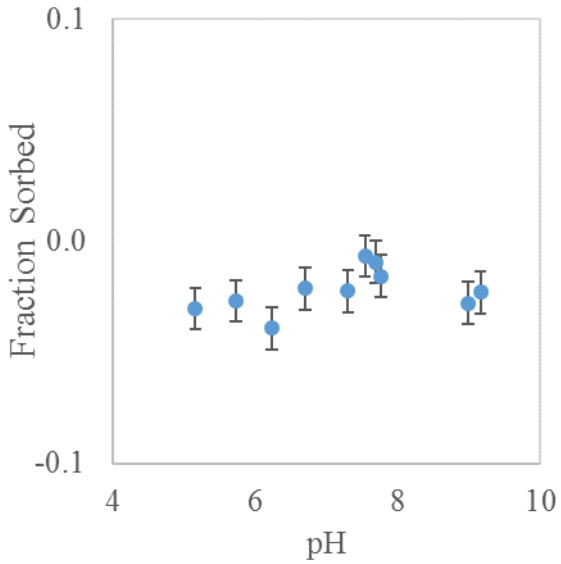

Figure C5. Fraction of total citrate sorbed to Analig-Pu02 resin in 10^{-4} M citrate competitive complexation experiments. Citrate sorption determined using ^{14}C citrate tracer. Error bars calculated from counting statistics.